University Of Southampton

Faculty of Natural & Environmental Sciences

School of Biological Sciences

Peroxisome Proliferator-activated Receptor gamma Inhibits Cell Growth and Negatively Regulates DNA methyltransferase Promoter Activity in SK-N-AS Neuroblastoma Cells

by

Chih-Hua Huang

Abstract

Neuroblastoma is the most common extra-cranial childhood solid tumour which arises from embryonic neural crest cells that fail to undergo a differentiation programme to form mature sympathetic neurones. Most children with advanced stage neuroblastoma have a 5-year event free survival rate of only 20%. However, the spontaneous differentiation of some early stage neuroblastoma into non-malignant gangliomas has prompted the search for agents that can induce neuroblastoma differentiation. Peroxisome proliferator-activated receptor gamma (PPARγ) is a member of the nuclear receptor superfamily of ligand-dependent transcription factors which play a major role in adipocyte differentiation and exhibits anticancer activity against a range of tumour cells *in vitro*. High levels of PPARγ have been shown to be associated with differentiated neuroblastoma and low levels of PPARγ with poorly differentiated tumours. Therefore, the aim of this project is to investigate whether PPARγ acts as a tumour suppressor gene in neuroblastoma. Our research shows that overexpression of PPARγ in the human neuroblastoma cell line *SK-N-AS* cells inhibited cell growth but had no effect on cell viability or the degree of differentiation, suggesting that PPARγ may modulate cell cycle progression in *SK-N-AS* neuroblastoma cells. Additionally, we show that PPARγ strongly represses the DNMT1 promoter activity. This suggests that PPARγ may in addition to regulating the cell cycle also modulate epigenetic processes within the cell.

Acknowledgements

Contents

List of Abbreviations

$15dPGJ_2$	15-deoxyΔ-$^{12,\,14}$ prostaglandin J_2
AChE	Acetylcholinesterase activity
AF-1	Activation function 1
AF-2	Activation function 2
AML	Acute myeloid leukemia
AP-1	Activator protein -1
aP2	Activating protein 2
APAF-1	Apoptotic protease-activating factor 1
ATAR	All-trans-retinoic acid
ATR	Ataxia telangiectasia and Rad3-related
BCA	Biocinchoninc acid
BCL-2	B cell lymphoma 2
BDNF	Brain-derived neurotrophic factor
BSA	Bovine serum albumin
CASP-8	Caspase-8
CBP	CREB binding protein
CDDP	cis-diamminedichloroplatinum (II)
CDK	Cyclin dependent kinase
DMEM	Dulbecco's Modified Eagle's Medium
DMNT1	DNA methyltransferase 1
DM	Double minute chromatin bodies
DMSO	Dimethyl sulphoxide
DR1	Direct repeat 1
DPE	Downstream promoter element
E2F	Elongation 2 factor
EDTA	Ethylenediaminetetraaceticacid

ER	Estrogens receptor
FA	Fatty acid
FATP-1	Fatty acid transport protein 1
FCS	Foetal calf serum
GADD45	Growth arrest and DNA-damage inducible
GPS2	G protein pathway suppressor 2
HAT	Histone acetyltransferase
HDAC	Histone deacetylase
HMS	Histone methyltransferase
HSR	Homogeneously staining regions
HSP	Heat shock proteins
LOH	Loss of heterozygosity
LPL	Lipoprotein
MAPK	Mitogen-activated protein kinase
MBD	Methyl-CpG-binding domain
MeCp2	Methyl CpG binding protein 2
MDM2	Murine double minute
mIBG	Meta-iodobenzylguanidine
MMP	Matrix metalloproteinases
MYCN	Myc myelocytomatosis viral related oncogene
NCoR	Nuclear receptor co-repressor
NB	Neuroblastoma
NR	Nuclear receptor
NSCLC	Non-small-cell lung cancer
Sp1	Specificity protein-1
SRC	Steroid receptor co-activator
TAF	Transcription associated factors
TGS	Tumour suppressor gene

TMS1	Target of methylation-induced silencing 1
TR	Thyroid hormone receptor
TRK	Trk receptor
TSA	Trichostatin A
PPAR	Peroxisome proliferator activated receptor
PPRE	Peroxisome proliferator response element
p/CAF	p300/CBP-associated factor
PSA	Prostate specific antigen
PIC	Preinitiation complex
PR	Protein restricted
RB	Retinoblastoma protein
RGZ	Rosiglitazone
RIPA	Radioimmunoprecipitation assay
VDR	Vitamin D receptor

Chapter 1

1.1. General Introduction

1.1.1 Cancer

Cancer causes the death of about 7.9 million people per year according to the most recent World Health Organization census (WHO Mortality Database, 2007). Cancer has different characteristics involving uncontrolled growth, failure of cell differentiation, metastasis and invasion of neighbouring tissues. Metastasis is the process by which cancer cells spread via the vasculature system to start tumours in other parts of the body, often involving the adrenal medulla, liver, brain or the bones (Lodish et al., 2003). Cancer is caused by genetic damage or mutations which affect the regulation of cell growth or apoptosis. Mutations in DNA can be inherited or acquired. Acquired mutations occur either spontaneously through errors in meiosis or DNA replication or through physical or chemical agents such as radiation, viruses, transposons and mutagenic chemicals. The major types of mutations/alterations include chromosomal rearrangements, deletions, insertions or point mutations. There are two classes of genes which when mutated can lead to cancer; these are called proto-oncogenes and tumour suppressor genes (King 2000). Proto-oncogenes are cellular genes, which mainly promote cell growth or cell survival. They can be activated by chromosome translocations, gene amplifications or point mutations which results in either overexpression or increased activity of the protein product (King 2000). For instance, the MYCN gene, which is involved in cell proliferation, has been found to be amplified up to 150 times in neuroblastoma (Ishola and Chung 2007, Maris et al 2007). Approximately 100 oncogenes have been identified to date (Rang et al., 2003) and these include genes such as Ras, Myc, ERK and tyrosine receptor kinases (TRK). On the other hand, the normal cell expresses proteins which inhibit the neoplastic properties of a cell by either restricting cell growth or being involved in DNA repair; these are the tumour suppressor genes and approximately 30 of these have been found (Rang et al., 2003). Loss of function of a tumour suppressor gene due either to a deletion or mutation can also lead to cancer. For example, p53 is a tumour suppressor gene, which plays a pivotal role in maintaining genome integrity and is inactivated in over 50% of cancers. DNA damage leads to the activation of p53 which acts as a transcription factor (King 2000). p53 can bind to the promoter region of specific genes, such as $p21^{CIP1}$ (cyclin-dependent kinase inhibitor 1) to induce cell cycle arrest. At the same time, p53 can also stimulate repair

of DNA damage, by activating genes such as growth arrest and DNA-damage inducible (GADD45) (King 2000). However, if DNA has been damaged, then p53 can also induce programmed cell death where it inhibits the anti-apoptotic factors, BCL2 and BAX resulting cell apoptosis which in turn leads to the accumulation of mutations, rearrangements and an increased risk of cancer.

1.1.2 Regulation of gene expression

Cancer is a disease of the genome that may be triggered by alterations/mutations in DNA which lead to the altered expression or activity of genes. In this section, we will focus on how transcriptional regulation of the gene occurs (Lodish et al., 2003).

1.1.2.1 Transcription factors and transcriptional regulation

We already know that the human body has around 30,000 genes (Pecorino 2005). These are encoded by our DNA. A gene can roughly be divided into two parts. One is the regulatory region and the other is the coding region. In this section, however, we focus on the regulatory region (or promoter region). The regulatory region is where RNA polymerase II, an enzyme that transcribes all protein coding genes and miRNA genes, binds and initiates transcription. A typical RNA polymerase II promoter region will contain a TA rich sequence called a TATA box. This is the sequence to which RNA polymerase binds via the transcription factor II D (TFIID) to initiate transcription. The TATA box, however, is present in only about 10 to 15% of human genes. Some genes lack a TATA box and instead have a downstream promoter element (DPE). The binding of the preinitiation complex (PIC) to either the TATA box or DPE elicits only a low level of transcription (Thomas et al., 2006). For higher levels of transcription, additional factors called transcription factors bind upstream of the PIC, stabilise binding and enhance transcription. The sequences to which these transcription factors bind are called upstream sequence regions or are referred to as response elements. Moreover, an additional element is often also present in a RNA polymerase II promoter. This is the enhancer element. It can regulate transcription at a distance and in a position- and orientation-independent manner. These different types of cis acting elements are however only important because of the transcription factors or DNA binding proteins that they bind.

Transcription factors are that bind to gene promoters and regulate transcription. They contain a set of independent protein modules or domains such as DNA-binding 12 domains, transcriptional activation domains, dimerisation domains and ligand-binding domains (Thomas et al., 2006). There are a number of different classes of DNA binding domains, including the helix-turn-helix motifs, the leucine zipper motif, the helix-loop-helix motif, and the zinc finger motif. These domains will be discussed further in section 1.3 (figure 1.1).
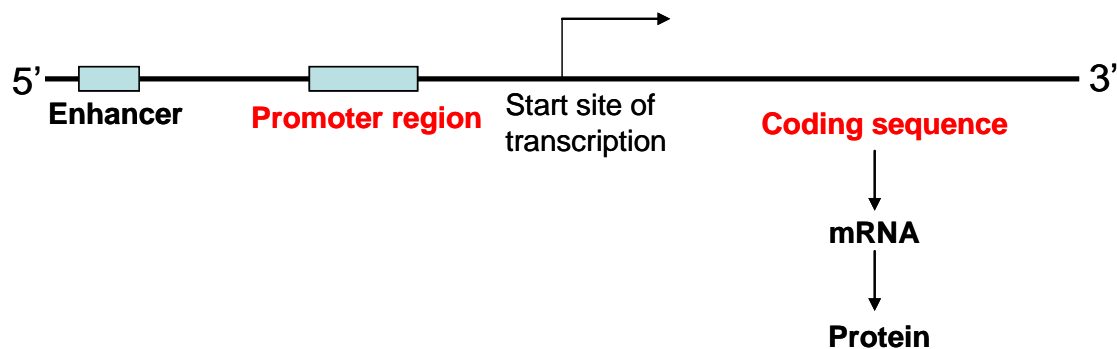
Figure 1.1. Two functional parts of the gene.

1.1.3 Epigenetics

Traditionally cancer has been seen as a genetic disease however there is now increasing evidence that cancer can be caused by both genetic and epigenetic alterations (Esteller 2002). Epigenetics is defined as processes that induce heritable changes in gene expression without altering the DNA sequence. The main epigenetic mechanisms are DNA methylation, histone modification and micro RNAs.

1.1.4 DNA Methylation

In 1948 the Hotchkiss group first identified 5-Methylcytosine (m^5C) in DNA; they called this DNA methylation. DNA methylation is an action in which a methyl group is added to 5'-cytosine of DNA. The majority of methylated cytosines are found as part of the dinucleotide CpG. CpGs are not randomly distributed throughout the genome but tend to cluster in regions at the 5' ends of genes called promoters in areas known as CpG islands. CpG islands are defined as a sequence longer than 200 base pairs with a GC content of over 50%, in a genome-wide average of about 40% (Takai and Jones 2002). In general hypomethylation is associated with transcriptional activation and hypermethylation with transcriptional silencing. DNA methylation inhibits transcription either by blocking transcription factor binding or through the binding of methyl CpG binding proteins which in turn recruits histone modifying enzymes to the DNA which induces a closing down of the chromatin structure. DNA methylation is essential for genomic imprinting, X chromosome inactivation and for establishing and maintaining tissue-specific patterns of gene expression (Bird 2002).

DNA methylation is brought about by the DNA methyl transferases of which there are three main types: DNA methyl transferase 1 (DNMT1) which is the maintenance methyl transferase responsible for copying patterns of methylation from the parental strand of DNA onto the newly synthesised strand during replication. DNMT3a and 3b are the *de novo* forms responsible for establishing DNA methylation patterns (Reik et al 2001). DNA methylation is largely established during development (Dean et al 2003) and essentially stably maintained throughout our life although there is some epigenetic drift in old age which has been linked to cancer (Mathers 2003) (figure 1.2).

A.
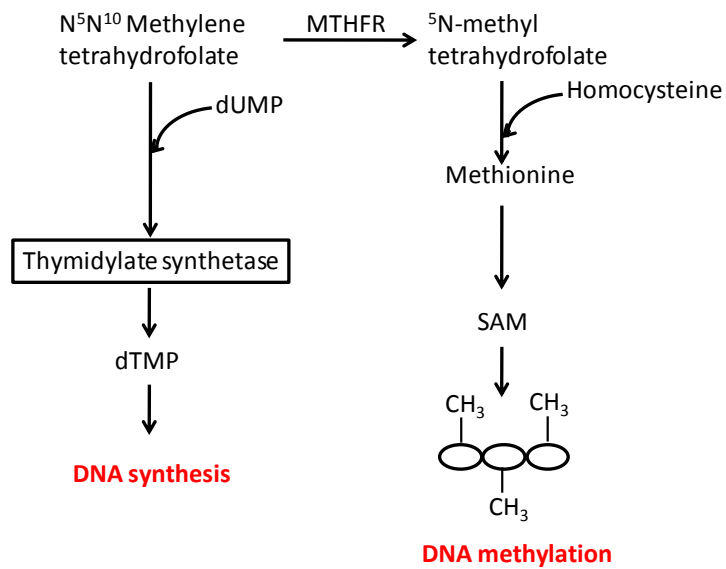
B.
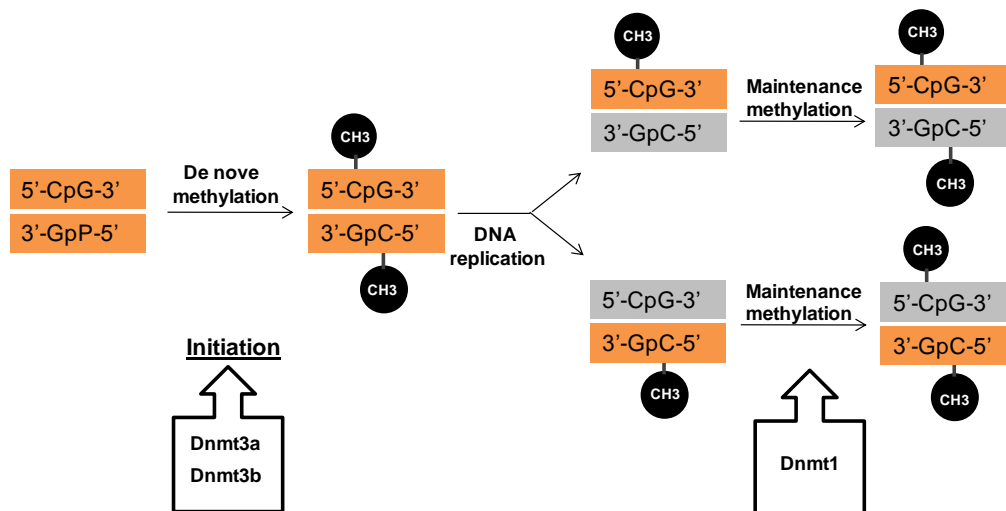
C.
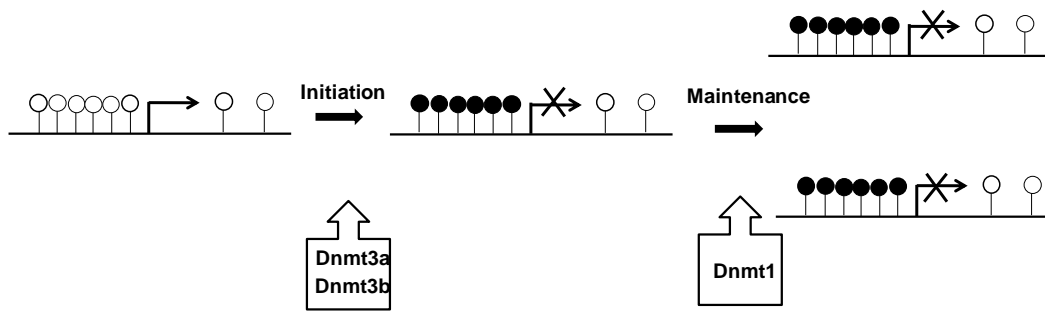
D.
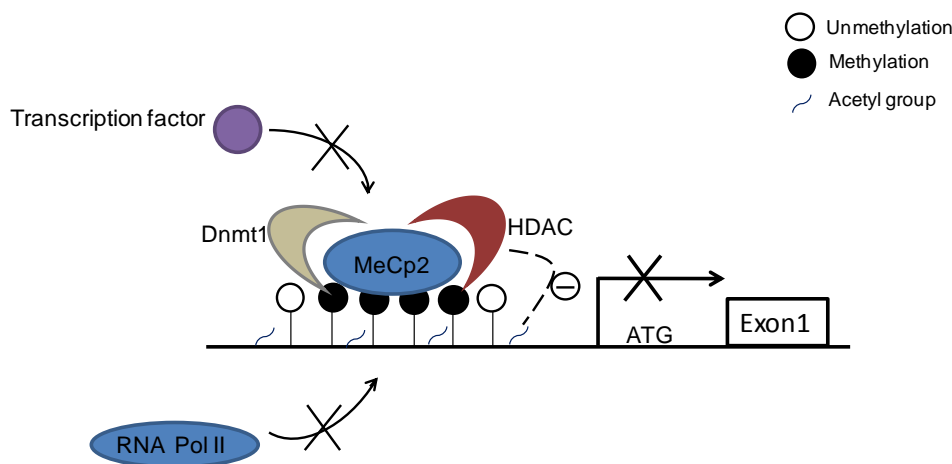
Figure 1.2. A. Mechanism of DNA methylation. The methyl group is donated by universal methyl donor S-adenosylmethionine (SAM), which is converted to S-adenosylhomocysteine (SAH). **B.** The family of DNMT can be divided into *de novo* and maintenance. The *de novo* enzymes are DNMT3a and DNMT3b which can create m^5CpG dinucleotides in unmethylated DNA and the maintance enzyme DNMT1 binds to the methyl groups to hemimethylated DNA during replication. **C.** Gene silencing can be caused by CpG methylation. The methyl group (CH_3) is linked to C-G di-nucleotide which usually exists in the promoter region of a gene. When the gene is methylated on the CpG island, it can affect the chromatin status of the gene and prevent the binding of regulatory factors. **D.** DNMT1 can recruit the protein methyl CpG binding protein 2 (MeCp2), which in turn can recruit histone deacetylases (HDACs) which remove acetylated groups from the lysine of the histones promoting transcription silencing.

1.1.5 Histone Modification

The DNA in our cells is wrapped around a series of positively charged proteins called histones which interact with the negatively charged DNA in a structure known as chromatin. The basic unit of chromatin is a nucleosome. In a nucleosome 146 base pairs of DNA is wrapped around a core of eight histone proteins; two molecules of histone 2A, two of histone 2B, two of histone H3 and two of histone H4. Each nucleosome is then folded upon itself to form a solenoid or 30nm fibre which is then further compacted and looped to form a 200nm fibre (Lodish et al., 2003). There is now substantial evidence which shows that post-translational modification of the histones plays a key role in regulating gene expression. Histone proteins have 2 domains-a globular domain and an amino terminal tail domain which is rich in lysine residues. Modification of the N-terminal tails of the histones by acetylation, methylation, ubiquitination or phosphorylation sets up the histone code which is deciphered (Abedin et al 2009) by the readers of the cells which in turn bring about gene activation or repression. The most studied histone modifications are histone acetylation and methylation. Histone acetylation is brought about by the recruitment of histone acetyl transferases (HATs) via activating transcription factors which then acetylate the lysines in N-terminal tails of the histones neutralising their positive charges leading to an opening-up of the chromatin structure and gene activation. In contrast inhibitory transcription factors recruit histone deacetylases (HDACs) which remove the acetyl groups from the histones restoring their positive charge leading to a closing down of the chromatin and gene repression (Kouzarides 2007). Histone methylation in contrast is associated with both gene activation and gene repression depending on which lysine residue within the histone tail is methylated. Methylation of H3K4 is associated with gene activation while methylation of H3K9 is associated with gene repression (Kouzarides 2007).

1.1.6 Epigenetics and Cancer

It has been demonstrated that the dysregulation of epigenetic processes is a major contributor to human disease, such as cancer in mammals (Plass 2002). A change in the epigenetic regulation of genes has been implicated as a causal mechanism in a number of cancers including lung (Li et al 2006), breast cancer and colon cancer as well as urological cancers (Krishnan et al 2007). Specifically increased cancer risk is associated with global hypomethylation of the genome with concurrent hypermethylation of the promoters of

tumour suppressor genes. Global hypomethylation can induce the activation of proto-oncogenes, loss of imprinting, chromosomal instability and reactivation of transposons, while promoter hypermethylation is associated with the inactivation of tumour suppressor genes involved in DNA repair, cell cycle control and apoptosis. The mechanism by which global hypomethylation is induced is unclear, but may reflect the global decline in DNA methylation associated with increasing age (Ehrlich 2002). It has been reported that a reduction in DNMT1 activity has been related to age (Lopatina et al 2002), which may lead to the increased expression of oncogenes, such as *c-Myc* and *c-N-ras*. Therefore, it appears that modulation of DNMT1 activity is a key regulatory step in the induction of tumorigenesis. This may be accompanied by methylation *de novo* of tumour suppressor genes (Lengauer 2003) by increased DNMT3a activity (Hermann et al 2004). Together these changes represent a shift in the regulation of gene control which, in turn, may predispose the genome to further changes in methylation which results ultimately in neoplasia.

1.1.7 Folic Acid, DNA Methylation and Cancer

Folate is one of the water-soluble B vitamins, needed for one-carbon transfer. However, mammals are unable to synthesis folic acid *de novo* and need to obtain it from their diet or from microbial breakdown in the gut. Folate is essential for synthesis of purine nucleotides and thymidylate (Duthie 1999) which are required for DNA synthesis and for DNA/histone methylation reactions. Folate deficiency therefore can lead to a decrease in intracellular S-adenosylmethionone (SAM, the universal methyl donor) and alterations in DNA methylation (figure 1.3). For instance, it is widely known that liver tumour development is promoted by methyl deficiency. Wainfain and Poirier reported that in rats fed a methyl-deficient diet (deficient in choline, folic acid and vitamin B2); global DNA hypomethylation was found which was induced over a very short period of time. The mRNA expression of proto-oncogenes, *c-myc*, *c-foc* and *c-Ha-ras*, increased but the level of these proto-oncogenes returned to normal when the rat was fed the control diet (Wainfan and Poirier 1992). A methyl group deficient diet has also been shown to unregulate DNMTs in rat liver (Steinmetz et al 1998, Wainfan et al 1989, Wainfan and Poirier 1992). Age and dietary folate have been reported to be determinants of genomic hypomethylation and p16[INK4a] hypermethylation in mouse colon (Keyes et al 2007). In contrast folate supplementation has been reported to be associated with a reduced risk of colorectal, lung, pancreatic, esophageal, stomach, cervix, breast, neuroblastoma and leukaemia (Choi and Mason 2002, Kim 1999b). Thus, together, these findings suggest a mechanism whereby folate intake may modulate the risk of developing cancer through the induction of altered DNA methylation leading to long-term stable changes in gene expression.
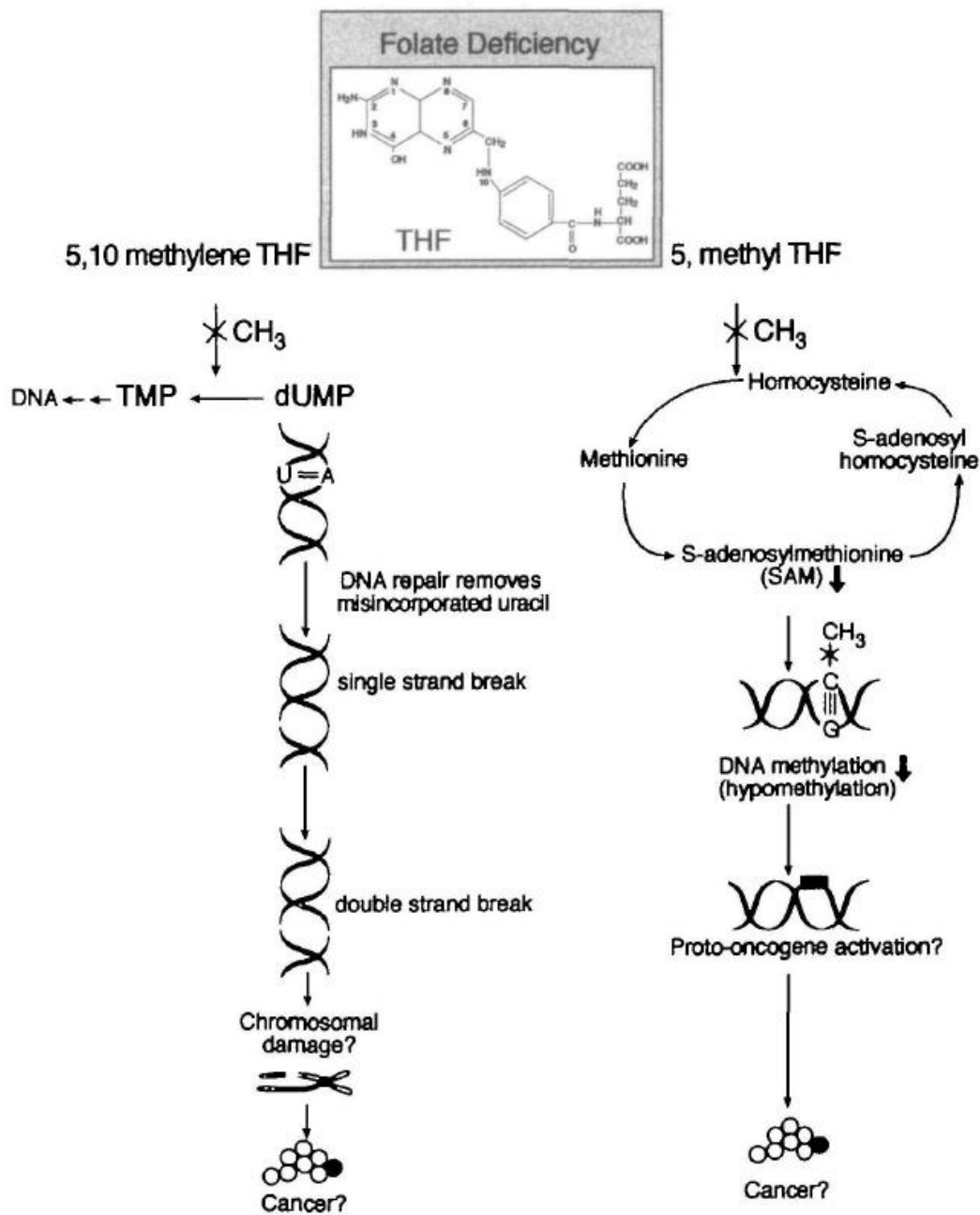
Figure 1.3. The mechanisms of folic acid deficiency and DNA instability (adapted from (Duthie 1999)).

1.2 Neuroblastoma

When sympathetic neuroblasts fail to undergo terminal differentiation, this may lead to neuroblastoma (Ishola and Chung 2007, Maris et al 2007). Neuroblastoma is the second most common cause of lethal cancer in children (Morgenstern et al 2004). Neuroblastoma cells are formed from neural crest cells. These cells are involved in the development of the peripheral nervous system. The neuroblastoma is a solid and malignant tumour which appears as a lump or mass in the abdomen or in the chest, neck or pelvis around the spinal cord (Schwartz et al 1974). Various image-based and surgery-based systems are used for assigning a disease stage (Maris et al 2007). The four clinical neuroblastoma stages as described by both the International Neuroblastoma Staging and the Shimada Classification systems (Shimada et al 1999) are 1, 2A, 2B, 3, 4 and 4S (Special)-Table 1.1

Table 1.1 Panel: INSS staging system

Stage	Definition
1	Localised tumour with complete resection with or without microscopic residual disease; typical ipsilateral lymph nodes negative for tumour microscopically.
2A	Localised tumour with incomplete resection; typical ipsilateral non-adherent lymph nodes negative for tumour microscopically.
2B	Localised tumour with incomplete resection; typical ipsilateral non-adherent lymph nodes positive for tumour. Extended contra-lateral lymph nodes should be negative microscopically.
3	Unrespectable unilateral tumour infiltrating across the middle with or without regional lymph node involvement; or localised unilateral tumour with contra lateral regional lymph node involvement; or midline tumour with bilateral extension by infiltration (unrespectable) or by lymph node involvement.
4a	Any primary tumour with dissemination to distant lymph nodes, bone, bone marrow, liver, skin, or other organs (except as defined by stage 4S)
4S	Localised primary tumour (as defined for stages 1, 2A or 2B), with dissemination limited to skin, liver, or bone marrow (limited to infants< one year age)

(Ishola and Chung 2007, Maris et al 2007).

In stage 1, the tumours are found within one area and can be removed by surgery. In stage 2A, the tumours are found within one area. They can or cannot be removed by surgery. In stage 2B, the tumours are frequently found in lymph nodes. In stage 3, the tumours probably cannot be removed by surgery and they may have spread to another part of the body. In stage 4, the tumours have spread to the skin or other parts of the body and also to distant lymph nodes. In stage 4S (special in stage 4), the tumour has spread to skin, liver and bone marrow and is almost only ever seen in children less than one year old. However, although stage 4S neuroblastoma patients have widespread dissemination of disease, they have a favourable prognosis and a high rate of spontaneous regression (Evans et al 1971). Generally, the patients require minimal treatment when they are in 4S stage neuroblastoma. For instance, the survival rate of a two year old child approaches around 90% (Nickerson et al 2000); however, there is a higher risk of death in neonates who have hepatic involvement resulting in respiratory, renal or gastrointestinal compromise. Most 4S patients usually need cytotoxic therapy to reduce the tumour burden (Evans et al 1981). Moreover, the biological features of most stage 4S tumours have a favourable histology and non-amplified MYCN gene (Goto et al 2001). However, it would be interesting to know how and why patients with 4S neuroblastoma who undergo spontaneous regression could be of potentially great benefit in opening up new therapy for the other stages of neuroblastoma.

1.2.1 Gene Aberrations in Neuroblastoma

There are several genetic abnormalities associated with neuroblastoma. Loss of heterozygosity (LOH) is due to a change from a heterozygous to a homozygous state as a result of mutations in the second normal allele (King et al., 2000). This occurs when homologous chromosomes already have one mutated allele which is passed on to the next generation However, when the normal gene from one of the allele chromosomes has lost its function, there is a high possibility that this will be related to an unfavourable prognosis and poor patient outcome in tumour patients (King, 2000). Over 70% of tumours have observed LOH on chromosome 1 which is usually a deletion at the 1p36 region (Brodeur et al 1981, Gilbert et al 1982). Deletions in the short arm of chromosome 1p are related to both MYCN amplification and advanced disease stage (Maris et al 2007).

1.2.2 Oncogene Amplification in Neuroblastoma

Normally, an increase in the gene dosage relies on genetic mechanism of DNA amplification. The normal developmental programme is associated with scheduled gene amplification (figure 1.4); for instance, the gene in the ovaries of the fruit fly or the actin gene present during myogenesis in the chicken, where gene amplification occurs normally. However, unscheduled amplification or sporadic amplification has been found to occur in solid tumours. Oncogene amplification is important in several solid tumours which could reflect in the genetic instability in solid tumour cells. There are two main types of DNA amplification: double minutes (DMs) or homogenously staining regions (HSR). DMs have a small chromatin body, and the paired chromosome-like structures lack a centromere. They represent a form of extra-chromosomal gene amplification. When DM chromatin occurs, DNA replication is seriously flawed in normal cells. This can result in the production of many single copies of genes in the chromosome. The DMs process is associated with increased oncogene expression and is associated with a poor prognosis, especially in solid tumours, involving brain tumours and neuroblastoma (Bigner et al 1990, Bigner and Vogelstein 1990). HSRs are chromosomal segments with various lengths which are stained after G-banding. These types of aberration are similar to the gene amplification or copy number gains that we already know about (Biedler and Spengler 1976, Cox et al 1965). The features of DM and HSR are very common in neuroblastoma. A good example of gene amplification in neuroblastoma is the oncogene-MYCN (myc myelocytomatosis viral related

oncogene). The sequence of MYCN is localised to DM and HSR and it is the first oncogene of clinical significance demonstrated to associate with neuroblastomas (Bigner et al 1990, Bigner and Vogelstein 1990). Moreover, it is also the first one to be associated with aggressively growing tumour phenotypes, while in 4S stage MYCN amplification is rarely seen. In neuroblastoma the MYCN gene is frequently amplified by about 140 fold and all copies of the amplified gene are transcriptional active, which could explain the reason why the expression of MYCN mRNA is found at a high level in many patients. Therefore, it has been demonstrated that amplification of MYCN is strongly related with tumorigenesis, with tumour progression and poor prognosis in patients of all ages, at all stages of neuroblastoma (Ambros et al 1995, Brodeur et al 1984, Perez et al 2000).
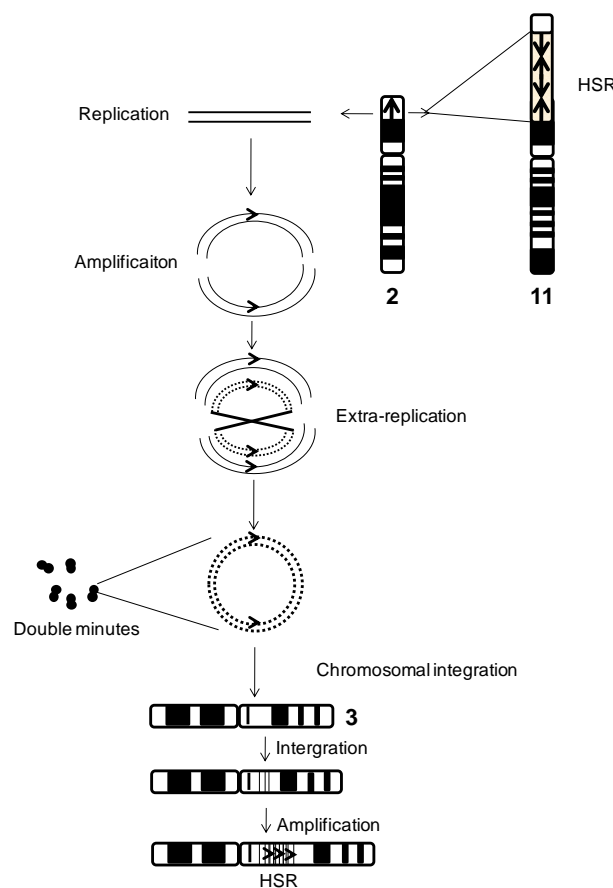
Figure 1.4. DNA amplification. DNA amplification is increased by repeating DNA replication. The recombination can cause tandem arrays of the amplification DNA. It can be excised by chromosome form to double minutes. The other chromosome can be integrated either into the other chromosome or double minute chromosome and it can become the homogenous staining region.

1.2.3 Neuronal Differentiation Markers in Neuroblastoma

The neurotrophin receptors (NTRK1, NTRK2, and NTRA3 encoded TrkA, TrkB and TrkC) and their ligands (NGF, BDNF and neurotrophin-3, respectively) are important factors which regulate cell survival, cell growth and differentiation of neural cells. The expression patterns of Trks affect the sympathetic nervous system. TrkA is a signalling receptor for the nerve growth factor (NGF). TrkB is a receptor for brain neurotropic nerve growth factor (BDNF) and neurotrophin 4 (NT4). TrkC is a receptor for Neurotrophin-3 (NT3) (Schramm et al 2005) (figure 1.5A). Schramm and colleagues (2005) have shown that TrkA plays a major role in increasing neuronal differentiation to form benign ganglioneuromas. Expression of TrkA is strongly correlated with favourable outcomes of neuroblastoma, as for instance the expression of TrkA is related to the differentiation state of the neuroblastoma and the normal copy number of MYCN. Moreover, low expression of TrkA is related with a high copy number of MYCN (Nakagawara et al 1993, Suzuki et al 1993). In contrast, the expression of TrkB which promotes neuroblast proliferation is correlated with the phenotype of invasion and high-risk disease (Nakagawara et al 1993, Suzuki et al 1993). Furthermore, it has also been found that TrkB is expressed on unfavourable and aggressive neuroblastoma (Nakagawara et al 1993, Suzuki et al 1993). Therefore, TrkA and TrkB have been used as neuronal differentiation markers in neuroblastoma (Schramm et al 2005) (figure 1.5B).

A.
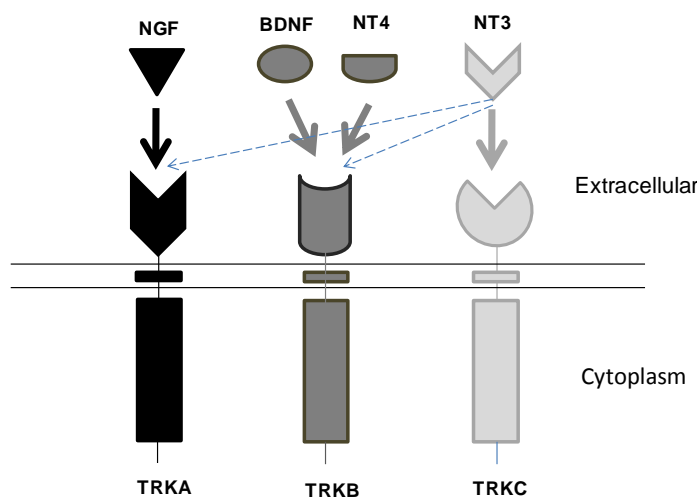
B.
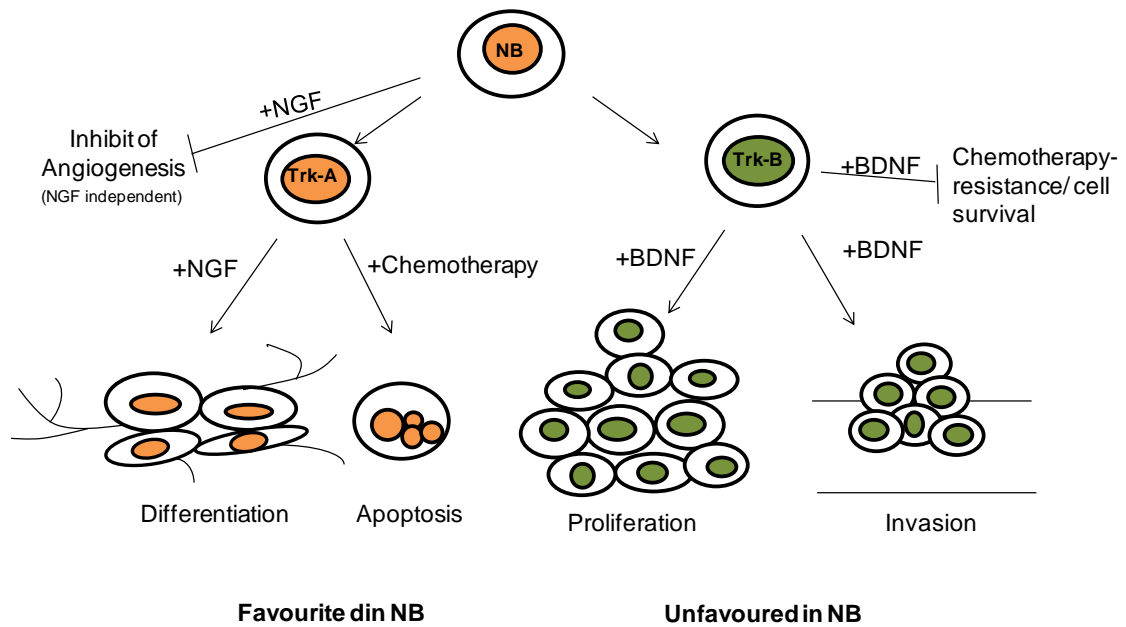
Figure 1.5. **A.** Trk receptors and their neutrophin ligands **B.** The roles of TrkA and TrkB in neuroblastoma cells. The signal of TrkA results in cell growth inhibition, differentiation and angiogenesis; TrkA with chemotherapy-induced cell apoptosis. In contrast, TrkB activation by BDNF leads to cell proliferation, invasion and chemotherapy resistance.

1.2.4 Neuroblastoma and Epigenetics

There is now evidence that epigenetics may play a role in neuroblastoma as well. Alaminos and his group has shown that the promoter regions of caspase-8 (CASP8) and tumour necrosis factor receptors DR4, DR5, DcR1 and DcR2 are hypermethylated and silenced in paediatric neuroblastoma (Alaminos et al 2004). Moreover, Grau's group in 2010 demonstrated that prognosis of a patient is not only based on patient's age at diagnosis, the tumour stage and MYCN amplification but also can now be classified according to the degree of methylation in neuroblastoma. They found that the patient's survival could be influenced by epigenetic aberrations: for example, relapse susceptibility is associated with hypermethylation of CASP8 and poor prognosis is associated with the hypermethylation with target of methylation-induced silencing (TMS1) and apoptotic protease activating factor 1 (APAF1) showed a high influence on overall survival of neuroblastoma. They suggested that this could be a good prognostic factor of disease progression for simultaneous analysis of hypermethylation of APAF1 and TMS1 (Grau et al 2010).

1.2.5 Micro RNA and Neuroblastoma

It has been shown that miRNAs can regulate the expression of both tumour suppressor genes and proto-oncogenes. In neuroblastoma it has been reported that miRNA-34a acts as a tumour suppressor gene. miRNA-34a expression increases during retinoic acid-induced differentiation of the *SK-N-BE* cell line, whereas E2F3 protein levels decrease. Thus, adding to the increasing role of miRNAs in cancer, miR-34a may act as a suppressor of neuroblastoma tumorgenesis (Welch et al 2007). Das and colleagues have also shown that all-*trans* retinoic acid (ATRA) up-regulates miR-152 which targets DNMT1 leading to a down regulation in DNMT1 expression and reducing cell invasiveness, anchorage-independent growth and contributing to the differentiated phenotype (Das et al 2010).

1.2.6 Conventional Chemotherapy Drugs and Epigenetic Therapy

1.2.6.1 Chemotherapy Drugs

Chemotherapy drugs are the most common way to treat cancer. Chemotherapy drugs are used as the first line in the treatment of localised disease; their aim is to stop proliferation and kill cancer cells (Roger et al., 2000). The function of chemotherapy drugs is to target DNA, RNA and protein to interrupt the process of cell division; however they are not cancer cell specific and also target normal dividing cells. Many chemotherapy drugs are used to treat neuroblastoma, including cisplatin (Pinkerton et al., 1994). These can increase the survival rate of patients with advanced neuroblastoma (Pinkerton et al., 1994). Chemotherapy is used in neuroblastoma along with other treatments such as surgery, radiotherapy and bone marrow transplantation (Morgenstern et al 2004).

1.2.6.2 The Mechanism of cisplatin and Etoposide

Cisplatin is one of the most widely used drugs for the treatment of solid tumours in adults and children. Cisplatin (cis-Diamminedichloroplatinum (II), CDDP) is an anticancer drug that has been used in the treatment of childhood and adult malignancies. Multi-drug therapy which includes cisplatin is an important component for treating childhood cancer, including medulloblastoma and neuroblastoma (Jordan and Carmo-Fonseca 2000, Zamble and Lippard 1995). Cisplatin binds to the guanine and adenine bases in the position of N7 and induces cross links within the DNA. However, cellular damage may be caused at a number of structural levels by cisplatin, although there is a general consensus in the field that genomic DNA is the primary site for cisplatin toxicity. This is because cisplatin has been shown to cause both intra- and interstrand crosslinking of DNA. The cisplatin adducts that are formed in the process both bend and unwind the DNA duplex, resulting in DNA lesions that inhibit cell cycle progression, leading to cell death by apoptosis. There have been a number of reports which suggest that cisplatin action involves the tumour suppressor p53. The DNA damage induced by cisplatin leads to the activation of p53 via ATR (ataxia telangiectasia and Rad3-related) kinase (Pabla et al., 2008). Moreover, once p53 has been activated, it also leads to the induction of BAX, Noxa and PUMA which can lead to cell apoptosis (King 2000) (Siddik 2003). Etoposide is also used to treat advanced neuroblastoma; this is a chemotherapy drug which inhibits topoisomerase II (D'Arpa and Liu 1989). Unfortunately, patients often

develop a resistance to etoposide, especially in recurrent disease. In human therapy, a combination of many drugs is often applied to reduce the possibility of resistance to chemotherapy drugs (D'Arpa and Liu 1989).

```
┌─────────────┐
│  Cisplatin  │
└─────────────┘
       │
       ▼
┌─────────────┐
│ DNA damage  │
└─────────────┘
       │
       ▼
   ┌───────┐
   │  ATR  │
   └───────┘
       │
       ▼
   ┌───────┐
   │ ChK2  │
   └───────┘
       │
       ▼
┌─────────────────┐
│ p53 activation  │
└─────────────────┘
```
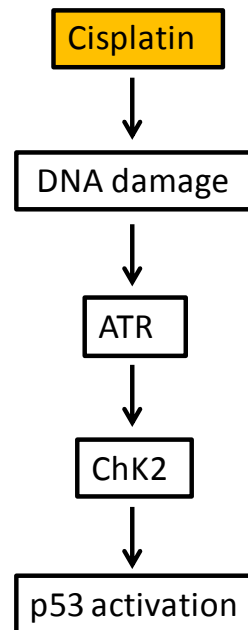
Figure 1.6. Treatment with cisplatin induced the response of DNA rapidly, which led to the activation of ATR and further phosphorylation. It activates Chk2. p53 can be activated by either ATR or Chk2.

1.2.6.3 DNA Methylation as a Chemoprevention Target

Epigenetic therapies that target DNA methylation and DNA methyltransferases have recently attracted significant interest for their use in cancer prevention. The DNA methylation inhibitors, such as 5-aza-2'-deoxycytidine, zebularine (Cheng et al 2004), antisense oligonucleotides to DNMT1 (MacLeod and Szyf 1995), and procainamide (Lin et al 2001) are capable of reversing aberrant promoter hypermethylation, leading to gene reactivation and restoration of cell growth control, apoptosis and DNA repair capacity (Bender et al 1998, Herman et al 1998, Murakami et al 1995, Zhu et al 2001). 5-aza-2'-deoxycytidine is a drug that targets the epigenome. It is a nucleoside analogue of cytosine. When 5-azacytidine is incorporated into DNA, it inhibits DNA methylation and reactivates silenced genes (Jones and Taylor 1980). The 5-aza-2'-deoxycytidine covalently binds to DNMTs and stops the activity of enzyme (Cross et al 1997, Jones et al 1998, Nan et al 1997). It has been used successfully in the treatment of acute myeloid leukaemia (AML) (Glover and Leyland-Jones 1987). Rasheed's (2007) group reported that treatment with the DNA methylation inhibitor, 5-aza-2'-deoxycytidine, can induce gene expression of p16[INK4a] which is often hypermethylated in neuroblastoma cells. Histone deacetylases (HDAC) have also been recently used as anti cancer agents. HDAC functions as a regulator for cell growth, differentiation, survival and angiogenesis (Bolden et al 2006). Inhibitors of HDACs such as Trichostatin A (TSA) have been used as treatment in various clinical trials in cancer patients (Rasheed et al 2007).

1.3 Nuclear Receptors

In order to develop safer and more efficient ways to treat neuroblastoma, scientists have been trying to understand the different intracellular pathways of proliferation, survival, and cell-cycle regulation and differentiation that are implicated in the pathogenesis of the disease (Ishola and Chung 2007). For instance, *in vitro* studies suggest that Retinoic acid (RA), which is a vitamin A derivative and a powerful inducer of cellular differentiation and growth inhibition in normal and cancer cells may be able to modulate neuroblastoma cell growth (Livera et al 2002). RA binds to the nuclear receptors RAR and RXR. Nuclear receptors are a super family of proteins which include receptors for classical steroid hormones which act as ligand-activated transcription factors and play an important role in normal physiological processes. Nuclear receptors (NRs) include RAR, RXR, PPARs, thyroid hormone receptor (TR), vitamin D receptor (VDR) and the steroid receptors, such as the estrogen receptor (ER). In total there are 48 known nuclear receptors in the human genome. NRs bind to a variety of hydrophobic ligands, such as steroid hormones, fatty acids, leukotrienes, prostaglandins, cholesterol derivatives and bile acids. Ligand binding induces a conformational change in the receptor allowing the receptor to activate a set of downstream target genes. Despite very encouraging results *in vitro* where retinoic aicd was able to very effectively inhibit neuroblastoma cell growth and induce cell differentiation, *in vivo* studies revealed that neither 13-*cis*-RA nor all-*trans*-RA had any therapeutic benefit for children with recurrent or refractory tumour in neuroblastoma (Adamson et al 2007, Finklestein et al 1992). Regardless of these observations, research into the benefits of RA still continues. For example, studies are ongoing investigating the combination of a synthetic retinoid with other pharmacological agents (Garattini et al 2007).

Given the early promise of retinoic acid, researchers then turned their attention to other nuclear receptors particularly the family of PPARs. Issemann and Green discovered PPARs in 1990 when they cloned it from mouse liver. Subsequently, PPARs has been found in Xenopus, rats and humans (Desvergne and Wahli 1999, Sher et al 1993). PPARγ and PPARβ/δ were identified first; followed by PPARα later on (Desvergne and Wahli 1999, Hihi et al 2002, Kliewer et al 1994). PPARs have a tissue-specific distribution (table 2) and can regulate gene expression (Tontonoz et al 1994). The PPARs are involved in a number of biological responses, such as adipogenesis, lipid homeostasis, immune function, cell

proliferation/apoptosis and carcinogenesis (Akiyama et al 2005, Burdick et al 2006, Desvergne and Wahli 1999, Lee et al 2003, Michalik et al 2004).

Table 1.2 Tissue expression of PPARs

	α	β/δ	γ
Adipose tissue		+	+
Colon			+
Liver	+		
Heart	+		
Muscle	++		
Vascular wall			+
Skin		+	
Brain		+	
Macrophages			+

Source: modified from Voutsadakis, 2007

1.3.1 PPARα (alpha)

PPARα is a 52 kDa protein which is encoded on chromosome 22q13.31 (Sher et al 1993), (Stienstra et al 2007). PPARα is expressed in metabolic tissues such as liver, heart, kidney, intestinal mucosa and skeletal muscles (Auboeuf et al 1997, Escher and Wahli 2000, Kliewer et al 1994, Mandard et al 2004, Schoonjans et al 1996) and is detected in brown fat and the immune system involving lung, placenta and smooth muscle tissue (table 2). It regulates fatty acid catabolism and inflammatory processes.

1.3.2 PPAR β/δ (beta/delta)

PPARβ is a 50 kDa protein which is encoded on chromosome 6p21.2 (Skogsberg et al 2000). It has been shown that PPARβ/δ is ubiquitously expressed at low levels in most tissues (Lemberger et al 1996, Mukherjee et al 1997) but it is expressed at high levels in placental and skeletal muscle (Mukherjee et al 1997). Recent data suggest that PPARβ/δ is a powerful metabolic regulator. It has been reported that PPARβ can regulate the expression of acyl-CoA synthetase 2 in the brain which is related to basic lipid metabolism (Basu-Modak et al 1999).

1.3.3 PPARγ (gamma)

Human PPARγ is located on chromosome 3 and at 3p25. There are three isoforms which are PPARγ1, PPARγ2 and PPARγ3; these three isoforms result from different promoter usage (Abdelrahman et al 2005, Fajas et al 1998, Greene et al 1995, Zhu et al 1995). PPARγ1 and PPARγ3 mRNA both encode the PPARγ1 protein, which is expressed in most tissues, whereas PPARγ2 mRNA encodes the PPARγ2 protein, which is specific to adipocytes and contains an additional 28 amino acids at the amino terminus (Abdelrahman et al 2005, Fajas et al 1998, Ricote et al 1998). PPARγ2 is expressed exclusively in adipose tissue and plays a pivotal role in adipocyte differentiation, lipid storage in the white adipose tissue, and energy dissipation in the brown adipose tissue (Barak et al 1999, Chawla et al 1994). PPARγ is critical for adipocyte differentiation; as it regulates the adipocyte-specific genes, such as adipocyte P2 (aP2) which is an intracellular lipid-binding protein, which controls lipid storage and metabolism (Heldin and Ostman 1996). It also plays a key role in controlling cell proliferation and cell cycle arrest during the differentiation process, as differentiation induced by PPARγ is associated with a loss of DNA binding for the growth-related E2F/DP transcription complex and exit from the cell cycle at G1 (Altiok et al 1997). Knockout PPARγ mice (deficient) have been shown to have a lack of adipose tissue, while PPARγ +/- mice show a decrease in adipose tissue (Kubota et al 1999, Miles et al 2000). In contrast, PPARγ1 is expressed in the colon, the immune system (e.g. monocytes and macrophages) and other tissues. PPARγ is involved in glucose metabolism through the improvement of insulin sensitivity and represents a potential therapeutic target of type 2 diabetes (Edelman 2003). Indeed, insulin-sensitising thiazolidinedione (TZD) drugs which are specific activators of PPARγ ligands are currently used very successfully to treat type II diabetes (Zhang et al 2004).

1.3.4 Mechanism of PPARs

The PPAR subtypes all function as ligand-activated transcription factors. In the classical model of PPAR activation, PPARs bind to DNA as heterodimers with the 9-*cis* retinoic acid receptor RXR. The PPAR/RXR heterodimer binds to DNA (Tugwood et al 1992) at peroxisome proliferator's response elements (PPREs) which were originally identified in the promoter of the acyl coenzyme A (acyl-CoA) oxidase gene. The PPRE comprises two half sites of the conserved sequence AGGTCA with a spacing of one nucleotide called DR-1 (<u>AGGTCA</u> X <u>AGGTCA</u>) (figure 1.7). However, there is emerging evidence that the optimal binding site differs subtly for each PPAR. This subtle difference in binding preference along with differences in tissue-specific expression may explain the different functions of the different PPARs (Palmer et al 1995).

Activation of transcription through the PPARγ/RXR dimer is blocked by associated co-repressor proteins, such as the nuclear receptor co-repressor (NCoR), histone deacetylases (HDAC), and G-protein pathway suppressor 2 (GPS2) (Xu et al 1999a). The addition of ligand causes dissociation of the corepressor proteins followed by the recruitment of coactivators, such as PPAR coactivator (PGC-1), the histone acetyltransferase p300, and the CREB binding protein (CBP). Formation of the PPAR activation complex leads to histone modification (e.g. through acetylation) and altered expression of genes involved in fatty acid metabolism, lipid homeostasis, and adipocyte differentiation (figure 1.8). However, there is also evidence that, as with other nuclear receptors, heat shock proteins (Hsp) may facilitate the folding of newly translated PPARs (Sumanasekera et al 2003). The association of PPAR with Hsps, and perhaps other proteins, may keep PPAR in the cytoplasm until the appropriate ligand binds the PPAR ligand binding domain, leading to protein dissociation and nuclear import of PPAR.
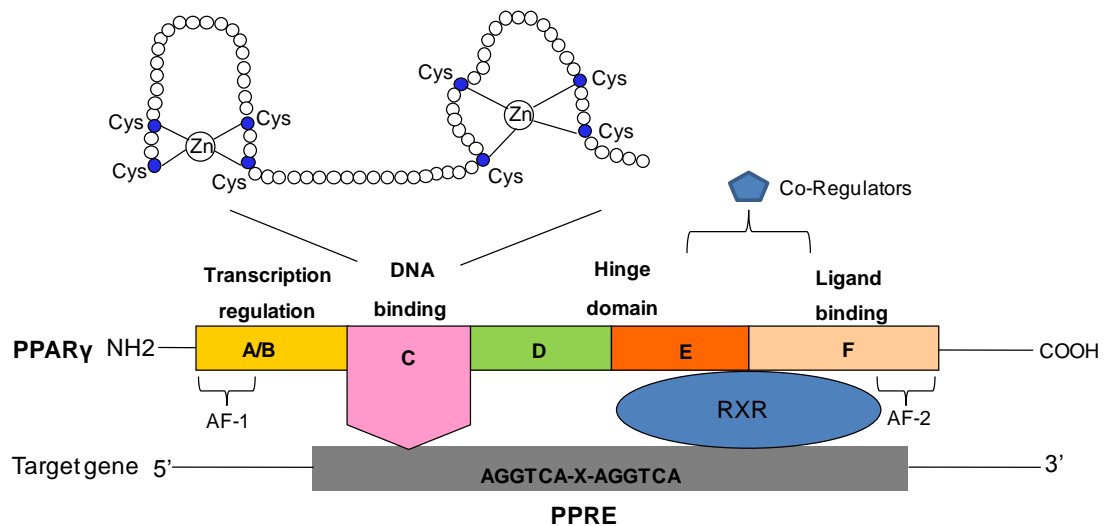
Figure 1.7. Schematic representation of functional domains of PPARγ. The N-terminal A/B region contains the putative ligand-independent transactivation domain (AF-1). The C region has two zinc fingers and contains the DNA binding domain The D domain is for co-factor docking. The E/F region contains the ligand binding domain (adapted from (Li et al 2006, Mansure et al 2009a)).

A.

Ligand-independent repression

Corepressor complex

mSIN3 · HDAC
RbAp48
HDAC1/2
SAP46 · SAP30 · p70
SAP18 · Sin3A · p32 · mi2
SMRT
PPARγ · RXR
TGACCT

Histone deacetylation

RNA Pol II

PPAR γ ligands binding

B.

Ligand-dependent transactivation

Coactivator dismissal

Coactivator association

Coactivator complex

CBP/p300 · P/CAF
P/CIP
SRC-1
PPARγ · RXR
TGACCT

Histone acetylation

RNA Pol II

Transcription

Chromatin remodoling

Regulation
Adipocyte differentiation
Lipid metabolism
Insulin sensitisation
Inflammatory
Atherosclerosis
Carcinogenesis

C.

Ligand-dependent repression

PPARγ

NF-κB
AP-1

RNA Pol II

Transcription

Figure 1.8. Model of PPARγ action. A. The PPARγ receptor and RXR form a heterodimer and bind the PPRE within the promoter of a gene. Without PPARγ ligand binding, the heterodimer complex recruits a multicomponent co-repressor complex. The silencing mediator for retinoid and thyroid hormone receptors (SMRT) interacts with the multicomponent corepressor complex through PPARγ. The corepressor includes SIN3 and HDAC. **B.** Upon ligand binding the corepressor complex is replaced by a coactivator complex which includes SRC, CBP/p300 and P/CAF, which leads to an opening up of the chromatin and gene transcription (Zhu et al 1996). **C.** PPARγ can also repress transcription by inhibiting the activities of other transcription factors, such as NFκB and AP-1 families (ligand-dependent transrepression) (Mansure et al 2009b).

1.3.5 The Ligands of PPAR

PPARγ is activated by ligands, which can be divided into two groups - natural ligands and exogenous ligands. There are numerous natural ligands which include fatty acids, eicosanoids, components of oxidised low-density lipoproteins and prostaglandins. Short chain fatty acids weakly activate PPARs, while polyunsaturated acids bind and activate PPARs more effectively (Xu et al 1999b). One of the most important natural ligands is prostaglandin J2 derivative (15dPGJ2).

1.3.5.1 15-deoxy-D12, 14-PGJ2 (15dPGJ2)

Prostaglandins (PG) are a group of lipids which are derived from fatty acids, primarily arachidonic acid. They are released from membrane phospholipids by the action of phospholipases. The PG contains 20 carbon atoms, including five carbon rings. The PG functions as a messenger molecule and it is produced by the cells which respond to a variety of extrinsic stimuli and regulate cellular growth, differentiation and homeostasis. Arachidonic acid is first converted to an unstable endoperoxide intermediate by cyclooxygenase to arachiphospholipids. In addition, arachiphospholipids are converted into one of several related products, such as PGD2, PEG2α, prostacyclin (PGI2), and thromboxane A2. However, it has been demonstrated that these products affect the second messengers through interactions between G protein-coupled receptors (Hirata et al 1994). The cyclooxygenase products including PGD2 exist in a variety of tissues and cells. These effect many biological

processes, such as platelet aggregation, relaxation of vascular and nonvascular smooth muscle and nerve cell function (Giles and Leff 1988). PGD2 can quickly undergo dehydration *in vivo* and *in vitro* to yield additional, biologically active PGs of the J2 series which bind with high affinity to PPARγ (Fitzpatrick and Wynalda 1983, Kikawa et al 1984).

1.3.5.2 Thiazolidinediones (TZDs)

The thiazolidinediones (TZD) are a class of anti-diabetic compounds with potent adipogenic activity that have been shown to have a high affinity for PPARγ. TZDs include pioglitazone, troglitazone and rosiglitazone. They have been used an oral anti-diabetic drug to improve insulin sensitivity in type 2 diabetes patients (Seufert et al 2004). Activation of PPARγ by TZDs results in a dramatic decrease in the concentration of serum glucose in patients who have diabetes. The mechanism by which PPARγ affects insulin sensitivity is unknown, but in rat adipose tissue TZDs appear to regulate the expression of target genes through PPARγ, such as lipoprotein lipase (LPL). This enzyme is made primarily in adipose tissue and in muscle. It plays a critical role in transporting fats and breaking down lipoproteins. When it is activated, adipocyte can facilitate the uptake of circulating fatty acid. It also controls glucose and lipid metabolism and energy balance; it directs fatty acid away from skeletal muscle by stimulating their uptake by the adipose tissue (Dulloo et al 2004).

1.3.6 PPARγ and Cancer

There is now much evidence that PPARγ is important in carcinogenesis, such as prostate, colon, breast, lung and various haematological cancers (Wang et al 2006b). Several PPARγ mutations have been found in a number of cancers. Four different mutations in the PPARγ gene have been found in colon cancer cells (Sarraf et al 1999). One of the mutations, in exon 3 where a frame shift occurs producing a protein which is inactive (Sarraf et al 1999). Furthermore, PPARγ mutations, both non-sense and mis-sense mutations, have also been found in the ligand binding domain; encoded for by exon 5, they affect ligand binding activity which in turn reduces the ability of PPARγ to activate its target genes (Sarraf et al 1999).

It has also been shown that the treatment with PPAR agonists inhibits proliferation of a variety of cancer cell lines and induces either apoptosis or cellular differentiation (Elstner et

al 1998, Rodway et al 2004b, Sarraf et al 1998, Wang et al 2006b). The mechanism of growth arrest generally involves modulation of the activity and expression of cyclins and cyclin-dependent kinase (CDKs), resulting in decreased phosphorylation of retinoblastoma protein and a lack of E2F mediated gene transcription. Recent reports have demonstrated that cyclin-dependent kinase inhibitor (CDKI) expression is up-regulated during cell differentiation both *in vitro* and *in vivo* (Chellappan et al 1998, Harper and Elledge 1996), suggesting that these CDKIs may play an universal role in exiting from the cell cycle and/or maintenance of the irreversible growth arrest. The CDK inhibitors, which include p21^{CIP1}, p18 and p27^{KIP1}, are induced by ligands of PPARγ and cause cell cycle arrest in adipocyte and colon cancer cells (Chen and Xu 2005, Morrison and Farmer 1999). PPARγ may play a key role in cell cycle arrest as agonists of PPARγ have been shown to induce the CDK inhibitors such as p18, p21^{CIP1} and p27^{KIP1} which are the inhibitors of CDK which block the cyclin/CDK complexes. As a result, the phosphorylation of retinoblastoma (RB) protein was inhibited. Therefore, E2F will not be released from the retinoblastoma protein, which will lead to cell cycle arrest (Chang and Szabo 2000, Han et al 2004, Lapillonne et al 2003, Wang et al 2006b, Yang et al 2005, Yoshizawa et al 2002, Yoshizumi et al 2004). Therefore, activation of PPARγ by ligands has now been shown to inhibit cell growth in many cancers. For instance, in pancreatic cancer, the PPARγ ligands, both glitazones and troglitazone, induce p21^{CIP1} expression which in turn affects cell cycle arrest (Elnemr et al 2000). In addition, after treating with troglitazone, the expression of p21^{CIP1}, p27^{KIP1} and p18 is induced, which suggests that CDKI leads to a increase in cell cycle arrest in human hepatoma cells (Koga et al 2001). Moreover, given their potency in cell culture systems, TZDs have been used more recently in several clinical trials treating human malignancies, prostate (Hisatake et al 2000, Mueller et al 2000), colon (Kulke et al 2002) and breast cancers (Burstein et al 2003).

1.3.7 Clinical Trials

PPARγ ligands (TZD) have been used for clinical trials in patients, involving liposarcoma, or colon or prostate carcinoma (Demetri et al 1999, Mueller et al 2000). It has been shown that, when used to treat high grade liposarcomas, troglitazone induces tumour cell differentiation *in vivo* (Demetri et al 1999). Differentiation was accompanied by the expression of adipocyte-specific genes, involving aP2, adipsin and PPARγ (Demetri et al 1999). In addition, it has been shown that in 41 patients (men) who are in phase Π of clinical trials in advanced prostate cancer and being treated with troglitazone (Mueller et al 2000), the expression of prostate-specific antigen (PSA) was decreased in 20% of the patients (Mueller et al 2000). PSA is a tumour marker to detect prostate cancer which is related to the size of the tumour. In conclusion, troglitazone can be used to minimise tumour progression *in vivo*. However, rosiglitazone (RGZ), another class of TZD, has not had the same outcome. RGZ did not bring about significant morphological changes or have an effect on the tumour progression (Debrock et al 2003, Smith et al 2004).

1.3.8 Troglitazone and Cisplatin

To improve the efficacy of TZDs a number of groups have examined the effects of combining TZDs with traditional anticancer agents. Reddy's (2008) group demonstrated that PPARγ ligands act synergistically with either platinum-based chemotherapeutic agent cisplatin or the taxane-platinum to inhibit cell proliferation in NSCLC cells both *in vitro* and *in vivo* (Reddy et al 2008). Moreover, Hamaguchi's group in 2010 has demonstrated that troglitazone, ciglitazone, RGZ and 15dPGJ2 act in a dose-dependent manner in mesothelioma cells (EHMES-10 and MSTO-211H cells), but when combined with cisplatin there was an additive inhibition on MPM cell growth when compared to treatment with an individual drug, alone (Hamaguchi et al 2010).

1.3.9 PPARγ and Neuroblastoma

There is agreement that PPARγ/ RXR signalling plays an important role in inhibiting cell proliferation and/or inducing apoptosis (Grommes et al 2004a). PPARγ is expressed in tumours of the nervous system, such as astrocytomas, glioblastomas and neuroblastomas (Han et al 2001b, Nwankwo and Robbins 2001, Strakova et al 2004). Moreover, Han et al. (2001b) found that in neuroblastoma tumours with a well-differentiated phenotype, high levels of PPARγ were expressed, whereas in undifferentiated tumours very low levels of PPARγ were found, suggesting that the level of PPARγ may be an important determinant of cell differentiation and a potential prognostic marker.

Activation of PPARγ by both natural and synthetic ligands has also been shown to induce cell cycle arrest, apoptosis and/or differentiation. Kim and colleagues (2003) have shown that the natural ligand 15dPGJ2 in both *SK-N-SH* and *SK-N-MC* cells inhibits cell growth. Following treatment with 15dPGJ2 in *SK-N-SH* and *SK-N-MC* cells, proapoptotic proteins are increased, involving caspase 3 and caspase 9. Rodway and colleagues (2004) have also shown that 15dPGJ2 can inhibit cell growth and induce apoptosis in *IMR-32* cells. They also found that lysophosphatidic acid attenuates the degree of the cytotoxic effects of PPARγ activation induced by 15dPGJ2 in neuroblastoma cells.

Synthetic ligands of PPARγ have also been shown to inhibit neuroblastoma cells *in vitro*. Valentiner et al. (2005) demonstrated that TZD, including ciglitazone, pioglitazone, troglitazone and RGZ, inhibited *in vitro* growth and viability of the human neuroblastoma cell lines (*SH-SY5Y*, *SK-N-SH*, *IMR-32*, *LAN-5*, *LAN-1*, *LS* and *Kelly*) in a dose-dependent manner, showing considerable effects only at high concentrations of ligand (10μM and 100μM). However in these studies and in other studies there is growing evidence that 15dPGJ2 and the TZD exert many of their anti cancer effects through a PPARγ independent pathway, so the exact contribution that PPARγ makes to growth inhibition in neuroblastoma cells is unclear.

1.4 The aims of our research

The main aim of this research is to determine whether PPARγ acts as a tumour suppressor gene in neuroblastoma cells and the mechanism of its action.

This will be tested by investigating

1. whether alterations in the level of PPARγ expression in neuroblastoma cells affects the level of cell growth, viability or differentiation.

2. whether agonists of PPARγ can be used alone or in combination with either conventional chemotherapy drugs or with methyl donors to inhibit neuroblastoma cell growth.

3. whether PPARγ affects the epigenetic status of the cells.

Chapter 2

Material and Methods

2.1 Materials

Chemicals were obtained from Sigma-Aldrich (Poole, Dorset UK) unless otherwise stated. Tissue culture plastics and cell culture medium were obtained from Invitrogen

2.2 Methods

2.2.1 Bacterial growth medium

2.2.1.1 Luria broth (LB) medium

LB medium was made by adding 1000ml of distilled water to 20g of LB. The solution was autoclaved under standard conditions. Finally, ampicillin was added to the LB medium to make a final concentration of 100µg/ml.

2.2.1.2 LB agar

A concentration of 1.5% (w/v) agar was added to the LB medium and autoclaved. Ampicillin was added to the LB agar to make a final concentration of 100µg/ml after the LB agar had cooled down to 55ºC.

2.2.2 Glycerol stocks

A single colony of bacteria was picked from an LB agar or LB^{amp} plate and inoculated into 10ml of LB or LB^{amp} medium and incubated in a shaking incubator at 37ºC overnight. 500µl of overnight culture was mixed at a ratio of 1:1 with sterile glycerol and vortexed gently to mix. Glycerol stocks were initially frozen in liquid nitrogen and subsequently stored at -80ºC until use.

2.2.3 Small scale isolation of plasmid DNA

A single colony of DH5α transformed with the required plasmid was incubated in 10ml LB^{amp} medium at 37ºC overnight in a shaking incubator. The overnight cultures were then centrifuged at 3000rpm for 10 minutes to harvest the cells. The cell pellet was then re-suspended in 100µl glucose-Tris buffer (1% glucose, 25mM Tris pH 8.0, 10mM ethylenediamine tetraacetic acid (EDTA)) and incubated at room temperature for 5 minutes. 200µl of cell lysis solution (0.2M NaOH, 1% sodium dodecyl sulphate (SDS)) was then added to the suspension, which was inverted twice and placed on ice for 5 minutes. 150µl of neutralisation solution (3M Potassium acetate, 11.5% glacial acetic acid) were added to the preparation, which was inverted and placed on ice for a further 15 minutes. The samples were centrifuged at 12000 rpm for 15 minutes. The supernatant was collected and an equal volume of 1:1 phenol: chloroform was added, mixed and centrifuged at 12000 rpm for -5 minutes. The top aqueous layer was then transferred to a fresh tube and treated with 10 units of RNase A for an hour at 37ºC. An equal volume of 1:1 phenol: chloroform was added, mixed and centrifuged. The top layer was then transferred to a clean tube, mixed with sodium acetate (3M pH 5.2) and two volumes of ethanol and placed in a -20ºC freezer for 30 minutes to precipitate the plasmid DNA. The precipitated plasmid DNA was pelleted by centrifugation at 12000 rpm for 10 minutes, air-dried and re-suspended in 40µl of sterile water.

2.2.4 Large scale isolation of plasmid DNA

10ml of LB^{amp} were inoculated with a single colony of DH5α containing the required vector and grown in a shaker incubator at 37ºC for 6 hours. These precultures were used to inoculate 500ml volumes of LB^{amp} which had been pre-warmed in a shaking incubator at 37ºC prior to the addition. These 500ml LB^{amp} cultures were incubated in a shaking incubator at 37ºC overnight. Overnight cultures were centrifuged at 4000 rpm for 20 minutes at 4ºC in Sorvall RC-3B centrifuge (Kendro Laboratory Products Limited, Bishop's Stortford, and Hertforshire, UK). The pellets were re-suspended in 4ml Sucrose-Tris buffer (730mM sucrose, 50mM Tris-HCL (pH 8.0) containing 188,000 Units of lysozyme). The suspensions were placed on ice for 15 minutes, then 500mM EDTA pH 8.0 was added to make the final concentration of 10mM and the suspensions were returned to ice for a further 15 minutes. Three volumes of Triton buffer (150mM Tris-HCl pH 8, 187.5mM EDTA, 3% (v/v) Triton X-100) were added and the samples were mixed and incubated on ice for 30 minutes until lysis occurred.

Samples were centrifuged at 18000 rpm for 1.5 hours at 4ºC in a Beckman J2-21 centrifuge (Beckman Coulter Inc., Fullerton, Califorma) and the supernatant (lysate) was collected. The supernatant was made up to 500mM NaCl (final concentration) extracted with an equal volume of 1:1 phenol: chloroform and centrifuged at 3000 rpm for 10 minutes. The top layer was decanted to a fresh tube and an equal volume of chloroform was added to make a 1:1 mix. The preparation was mixed vigorously with the chloroform and centrifuged at 3000 rpm for 10 minutes. The top layer was collected, to which 10% polyethylene glycol (PEG) was added and dissolved at 37ºC. Once the PEG had dissolved the solution was stored at 4ºC overnight. Next day the preparation was centrifuged at 12000 rpm for 20 minutes at 4ºC to obtain a pellet. The pellet was re-suspended in 500µl 0.1M Tris-HCl (pH 8) and treated with 10 units RNase A for an hour at 37ºC. 500µl PEG buffer (33.4mM PEG 6000, 1M NaCl, 1mM EDTA, 10mM Tris pH 8) was added to the preparation, which was placed on ice for an hour. A pellet was obtained by centrifugation at 12000 rpm for 15 minutes and re-suspended in 400µl Tris-NaCl (10mM Tris-HCl (pH 8), 500mM NaCl). This solution was treated with a further 10 units of RNase A for 2 hours at 37ºC and extracted twice with an equal volume of 1:1 phenol: chloroform. The DNA was then ethanol-precipitated, centrifuged at 12000 rpm for 10 minutes, air-dried in a tissue culture hood and dissolved in 100µl tissue-culture sterile water. Plasmid DNA was visualized on 1% agarose gel. Its optical density was measured at 260 nm using a spectrophotometer to determine its concentration.

2.2.5 Preparation of competent cells and transformation

On day one, a glycerol stock of DH5α *Escherichia coli* cells was streaked out on to an LB plate without antibiotics. The plate was left overnight at 37ºC. 10ml of LB medium was inoculated with a single colony of DH5α *Escherichia coli* cells and incubated in a shaking incubator at 37ºC overnight. 100µl of overnight culture was added to 10ml of fresh LB. Cells were grown at 37ºC for 2~3 hours until their OD 600 reached 0.4 and they were in the exponential phase of growth. Cells were centrifuged at 3000 rpm for 10 minutes, the supernatant discarded and the pellet placed on ice. The pellet was re-suspended in 5ml of sterile ice-cold 100mM $CaCl_2$ and placed on ice for 30 minutes. Plasmid DNA (50ng) was mixed with 100µl of competent cells, which were left on ice for 30 minutes. Cells were heat-shocked at 42ºC for 1.5 minutes and returned to ice for a further 30 minutes. Cells were inoculated by mixing with 400µl of LB and incubating with shaking at 37ºC for 30 minutes.

Cells were pelleted at 3000 rpm for 5minutes and re-suspended in 100µl LB, before being plated out on LB^{amp} agar and incubated in a warm room overnight at 37ºC.

2.2.6 Plasmid DNA

pcDNA 3.1 is a mammalian expression plasmid from Invitrogen. Human pSG5-PPARγ1 is a mammalian expression plasmid. PPREx3-TK-Luc, PPARγ dominant negative and rat DNMT1-Luc are the reporter expression plasmid (Table 2.1).

Table 2.1.

Construct Name	Source	Details of plasmid or construct
pcDNA 3.1	Invitrogen	Ampicillin and Neomycin resistance genes for selection, expression of gene controlled by CMV promoter
pSG5-PPARγ1	Kind gift from Dr. R.Evans (Salk Institute, San Diego)	This is an expression vector carrying the full length cDNA of PPARγ (Elbrecht et al, 1996)
PPARγ dominant negative	Kind gift from Professor V.K. Chatterjee (University of Cambridge U.K.)	PPARγ mutant with preserved ligand and DNA binding properties, increased corepressor recruitment
PPREx3-TK-Luc	Kind gift from Professor Ronald Evans (University of California, San Diego)	Luciferase reporter gene under transcriptional control of a triple repeat PPAR response element (PPRE)
Rat DNMT1-Luc	Kind gift from Amal Alenad (University of Southampton, U.K.)	Luciferase reporter gene under transcriptional control. Ampicillin resistance gene for selection; this is useful both in *vitro* and in *vivo*

2.2.7 Restriction enzyme digestion

Restriction enzyme digestion was carried out by incubating plasmid DNA (500ng) with 0.5 units of restriction enzyme in a 1X restriction enzyme digestion buffer. The reaction was incubated at 37ºC for an hour and the results analysed by gel electrophoresis.

2.2.8 Agarose gel electrophoresis

For separating DNA fragments around 0.1~10 kb, a 1% agarose gel was used. 1g of agarose was mixed with 100ml of 1X TAE buffer and heated in a microwave until the solution becomes clear, and it was then cooled down in water bath at 50~55ºC for 10 minutes. At the same time, the gel casting tray was prepared by sealing the end of the gel chamber with the masking tape. 5µl of ethidium bromide (from a stock solution of 10mg/ml) was added to the cooled gel and then poured into the gel tray. When set, the comb and tape was removed and the gel placed into the gel tank. 1X TAE buffer was poured into the gel tank to submerge the gel to 2~5 mm depth. The DNA to be analysed was mixed with loading buffer and then loaded into the wells and run alongside a DNA ladder (Fisher BioReagents DNA ladder #Cat: BP2571-100). Electrophoresis was carried out at 100 volts (V) for an hour and the DNA visualised using a UV light box or gel imaging system.

2.2.9 Conventional polymerase chain reaction

2.2.9.1 p14^{ARF} for promoter region

The p14^{ARF} promoter region was amplified using conventional PCR. The primers used to amplify the p14^{ARF} promoter region were (forward 5'-GCCTCGAGTGGGCTAGACACAAAGGACTCG-3' and reverse 5'-GCAAGCTTGCACCCGCCTTCCCTGAGC-3'). 5µl genomic DNA (250ng) was mixed with 5µl 10X PCR buffer, 7 or 3.5µl 25mM magnesium chloride, 10µl Q-solution, 1.5µl 10mM dNTP mix, 0.5µl forward primer (10µM) and 0.5µl reverse primer (10µM). Water was added to make a total volume with 50µl (table 2.2). The PCR reaction was then incubated in Omnigene PCR thermocycler (Hybaid, Ashford, UK) for 45 cycles with 0.5µl Hot start Taq polymerase (Qiagen, UK). The PCR reaction was shown in Table 2.2. PCR products were run on a 1% agarose gel and visualised by UV light.

Table 2.2 (a). PCR condition of p14^{ARF}

Gene	Denature		Annealing		Extension		No. of Cycles
	Temp. (ºC)	Time (sec)	Temp. (ºC)	Time (sec)	Temp. (ºC)	Time (sec)	
p14^{ARF}	95	30	57.7~67.6	60	72	60	40

Table 2.2 (b). The condition with different amount of MgCl2

	Genomic DNA	dNTP	p14^{ARF} (10mM) (r)	p14^{ARF} (10mM) (f)	10X buffer	Q-solution	MgCl2 (25mM)	Taq	H2O
Reaction 1	0.4	1.5	0.5	0.5	5	10	**7**	0.5	24.6
Reaction 2	0.4	1.5	0.5	0.5	5	10	**3.5**	0.5	28.1

Table 2.2. **PCR conditions**. **2.2a** The tables show the denaturing, annealing and extension temperatures and times for the PCR of p14^{ARF} promoter region. The PCR product was analysed on a 1% agarose gel after 40 cycles. **2.2b**. This shows the components of the PCR reaction when different concentrations of MgCl2was used in order to optimise the PCR conditions.

2.3.1 RNA extraction

Total RNA was extracted using TRIZOL® reagent (Gibco Life Technologies TM, Paisley, Scotland). The cell pellet was washed with PBS and then lysed by gentle pipetting up and down in 1ml of TRI REAGENT®. The cells were lysed at room temperature for 10 minutes before the addition of 200µl of chloroform. The TRI REAGENT®-chloroform mix was mixed vigorously and incubated at room temperature for 5 minutes and centrifuged at 12000 rpm for 15 minutes at 4ºC. The aqueous layer was isolated and RNA was precipitated with 500µl of isopropyl alcohol. The RNA precipitate was collected by centrifugation at 12000 rpm for 10 minutes. The RNA pellet was air-dried and re-suspended in 20µl of autoclaved, 0.1% (v/v) diethyl pyrocarbonate (DEPC)-treated water and stored at -80ºC. The RNA concentrations (µg/µl) were determined by measuring its optical density at 260 nm.

2.3.2 Preparation of cDNA for real-time RT-PCR

Total cellular RNA was used to synthesise cDNA. In order to ensure removal of any possible potentially contaminated DNA, the RNA was treated with a DNase I (Promaga, Cat No. M198A). Firstly, 1µg RNA was added to 1µl DNase I and 10x DNase I reaction buffer, and added nuclease-free water to 100µl and then put the mixture in the 50µl tube in the PCR machine at 37ºC for 30 minutes (DNA digestion) and 65 ºC for 10 minutes (stop reaction). Then, the RNA concentrations were determined by measuring its optical density at 260 nm. The RNA was then ready to be transcribed to the cDNA.

1µg RNA (DNA-free) was added to 1µl of 10mM dNTP which includes dATP, dTTP, dCTP and dGTP (Promega, Chilworth, UK), and then the mixture was combined with 1µl random hexamers with 90 OD units in 0.1% (v/v) DEPC water (Amersham Pharmacia Biotech Limited, Little Chalfont, UK), and followed by 0.1% (v/v) DEPC water to a total volume of 10µl. Following this, this mixture was incubated at 70ºC for 10 minutes and then cooled on ice. To this mix, 2µl of 5X Reverse transcriptase buffer, 1 unit of Moloney-Murine Leukemia Virus (M-MLV) reverse transcriptase and 0.1% (v/v) DEPC water were added to make a total volume of 20µl. The final mixture was incubated at room temperature for 10 minutes to ensure elongation of the random hexamers and subsequently at 37ºC for 50 minutes. It was then heated to 80~94ºC to denature the M-MLV reverse transcriptase and stored at -80ºC before use.

2.3.3 Measurement of mRNA expression by real-time RT-PCR

Measurement of the levels of specific mRNA transcripts was carried out using the primers listed (Supplemental Table 2). Total RNA was isolated from *SK-N-AS* cells. For quantitative RT-PCR reactions, cDNA (5µl) was mixed with 12.5µl of SYBR Green JumpStart Taq Ready Mix (Sigma) and 1µl of each primer (10µM) in a total volume of 25µl. PCR was carried out in a real-time PCR cycler® (Bio-Rad). Reactions were performed at 95ºC for 10 minutes, 40 cycles of 95ºC for 10 seconds, 53ºC to 60ºC for one minute, 95ºC for one minute, 72ºC for one minute and then finally 72ºC for 10 minutes (each primer set has been described in table 2). Quantisation of targets in each sample was accomplished by measuring the cycle number (Ct) using the relative expression method. Samples were analysed in duplicate and

the expression of the individual transcripts was normalised to the housekeeping gene (cyclophilin).

Table 2.3 RT-PCR primers

Gene	Forward primers Reverse primers	Denature		Annealing		Extension		No. of Cycles
		Temp. (ºC)	Time (sec)	Temp. (ºC)	Time (sec)	Temp. (ºC)	Time (sec)	
PPARγ	5'-TGCAGATTACAAGTATGAC- 5'-TCGATATCACTGGAGATC-3'	95	30	53	60	72	60	40
p14^{ARF}	5'-TCTAGGGCAGCAGCC-3' 5'-GGCGCAGTTGGGCTCCGC-3'	95	10	60	60	72	60	40
p16^{INKα}	QIAGEN QT00062090	95	10	54.1~60.2	45	72	60	40
p21^{CIP}	5'-ACCTGGAGACTCTCAGGGT-3' 5'-GCTTCCTCTTGGAGAAGATCA-3'	95	10	54.1~60.2	45	72	60	40
Rat DNMT1	QIAGEN QT00493577	95	10	55	45	72	60	40
Cyclop-hilin	5'-TTGGGTCGCGTCTGCTTCGA-3' 5'-GCCAGGACCTGTATGCTTCA-3'	95	10	60	60	72	60	40

2.3.4 Preparation of siRNA

2.3.4.1 Ligation of the siRNA insert

The siRNA was designed as reported previously (Gan et al., 2008). The sequence of the sense strand of PPARγ siRNA was 5'-GCCCTTCACTACTGTTGAC-3'. The detail of this double strand insert was shown in figure 3.7B. The 2 strands were annealed by mixing 2µl of each oligonucleotide (1ug/ul) with 46µl of annealing buffer (100mM, K-acetate, 30mM, HEPES-KOH, PH 7.4, 2mM, Mg-acetate) and then incubated at 90°C for 3 minutes, followed by 37°C for an hour in the PCR machine. Then the product was ready for the next step for ligation with the pSilencer vector (digested with EcoR I and Apa I) or stored at -20°C until required.

2.3.4.2 Digestion of pSilencer 1.0-U6

Apa I and EcoR I restriction enzymes were used to cut the pSilencer 1.0-U6 vector and create a directional cloning site. Following digestion, the linearised vector was purified after gel electrophoresis on a 1% agarose gel using QIAquick Gel Extraction Kit (Qiagen, UK). Following this, the purified vector was diluted to 0.1μg/μl following which is ready for ligation or transformation for the negative control.

2.3.4.3 Digested pSilencer vector with ligated insert for ligation

The double-stranded siRNA insert was brought to a concentration of 8ng/μl for the ligation. Firstly, 1μl of the insert (8ng) was added to 1μl of the linearised vector (100ng), 1μl 10X T4 DNA Ligase Buffer, 1μl T4 DNA Ligase (T4 DNA ligase) and 5μl Nuclease-Free Water for a 10μl ligation reaction. The ligation reaction was then incubated at room temperature overnight. A negative control ligation should be performed with linearised vector alone and no insert. Finally the pSilencer vector with insert was ready for transformation on to competent cells (DH5α).

2.3.5 Preparation of PPARγ ligands

2.3.5.1 15-deoxy 12, 14 prostaglandin J2

15-dexoy Δ 12, 14 prostaglandin J_2 (11-oxoprosta-5Z, 12E, 14Z-tetraen-1-oic acid) was obtained from Cayman Chemicals (Alexis Corporation, Bingham, UK) supplied in methyl acetate. Solvent was removed by evaporation under N_2 and 15dPGJ$_2$ was re-suspended in 100μl dimethyl sulfoxide (DMSO). It was diluted at a ratio of 1: 10 with DMSO before use. 15dPGJ$_2$ could be used at a concentration of 10μM.

2.3.5.2 Rosiglitazone

Rosiglitazone was obtained from Cayman chemicals (Alexis Corporation, Bingham, UK) as a white solid. Rosiglitazone was dissolved in DMSO to give a stock solution of 100mM, which was stored at -20ºC.

2.3.6 Cell culture

The human neuroblastoma cell lines *SK-N-AS* were maintained in Dulbecco's Modified Eagle's Medium (DMEM) containing 10% (v/v) fetal calf serum (FCS) and 100mM glutamine, supplemented with 0.1mg/ml penicillin/streptomycin. Cells were incubated in a humidified atmosphere containing 5% (v/v) CO_2. *SK-N-AS* cells are derived from the bone marrow of a female patient with neuroblastoma and consist of a single polygonal shaped cell (expression during human neuroblastoma-differentiation, cell growth and differentiation). The cells are non-MYCN amplified, S-type, and derived from a bone marrow metastasis. The cells do not express the oncogene MYCN or the anti-apoptotic protein BCL2 but appear to express NF-kappa-B constitutively (Gatsinzi and Iverfeldt 2011) The cells were passaged by incubation with 1X Trypsin-EDTA (500 units Trypsin, 0.53mM EDTA) in the 37ºC incubator for 5~10 minutes until the cells detached from the plate. At this stage, the cells can then be passaged for a new generation. The cells then can be passaged for a new generation

2.3.7 Freezing cells in liquid nitrogen and resuscitation of frozen cells

After trypsin-EDTA treatment, cells were centrifuged at 1500 rpm for 5 minutes and the culture medium was carefully removed. Cells were re-suspended in 1ml of freezing culture medium (10% v/v DMSO in complete medium) and stored on dry ice at -70ºC and frozen overnight at -80ºC before being transferred to liquid nitrogen stores. For resuscitation, cells were rapidly thawed and diluted in 6ml of complete culture medium. The cells were then pelleted at 1000 rpm for 3 minutes and the culture medium decanted off. Cells were then re-suspended in 6ml of fresh complete medium, transferred to a tissue culture flask and incubated at 37 ºC in a humidified atmosphere containing 5% (v/v) CO_2.

2.3.8 Cell growth and cell count determination

SK-N-AS cells were seeded at $1x10^5$ cells/ml in a 6-well plate and incubated overnight to facilitate attachment. Cells were collected by centrifugation and re-suspended in 25µl PBS and 25µl 0.4% trypan blue. Four counts were made per treatment per day and an average calculated. Cell death (trypan blue positive cells due to loss of membrane integrity) was expressed as a percentage of trypan blue negative cells. The *SK-N-AS* cells were counted by hemocytometer and trypan blue was used for detecting dead cells. Cell growth was measured

by counting total cell number (white viable cells) per day and cell viability expressed as the number of trypan blue negative cells and divided by the total cell number (trypan blue white and Blue included).

To investigate the effect of PPARγ on the growth, differentiation and viability of neuroblastoma cells, *SK-N-AS* cells were transfected with either an empty expression vector or an expression vector containing the full length cDNA clone of human PPARγ. To confirm that the levels of PPARγ mRNA and protein were increased in the cells transfected with the expression vector containing the full-length clone of PPARγ, RNA and protein were extracted from *SK-N-AS* cells transfected with either the PPARγ expression vector or empty expression vector 24, 48 and 72 hours after transfection. Cells were transfected with metafectene has previously been shown to induce very high transfection efficiency in these cells (A Dawson unpublished data). This was confirmed by testing different ratios of metafectene/ plasmid DNA. The results showed very high transfection efficiency in *SK-N-AS* cells.

2.3.9 Light microscopy

SK-N-AS cells were observed using a camera linked to a Leica DM IL microscope (X40 objective lens) (Leica Microsystems GmbH, Ernst-Leitz-Strasses 17-37 and 35578 Wetzlar).

2.4 Metafectene transfection of *SK-N-AS* cultured cells

2.4.1 6-well plate with metafectene

This was tested with the best transfected efficiency which was 1µg DNA with 4µl metafectene reagent in *SK-N-AS* cells (as can be seen in figure 3.1AB). However, cells were plated at 1×10^5 cells per well in 6-well dishes in complete medium and allowed to attach overnight. Two tubes were set up per sample: tube A containing 1µg of reporter plasmid DNA and 100µl serum-free DMEM medium; and tube B containing 4µl Metafectene® (Biontex) and 100µl serum-free DMEM medium. The contents of tube A were added drop-wise to the contents of tube B to form a translucent precipitate (table 2.4). The precipitate was transferred to the cell culture medium and gently agitated, and then incubated for 30 minutes at room temperature. Afterwards, 1ml serum-free DMEM was added to 6-well plates and the

contents of tube A and B were combined. The cells were incubated at 37ºC for three hours when the medium containing the precipitate was removed. The cells were washed and 2ml fresh complete medium was added to the cells. The cells were incubated at 37ºC for 24, 48 and 72 hours.

2.4.2 12-well plate with metafectene

Cells were plated at 2.5×10^4 cells per well in 12-well dishes in complete medium and allowed to attach overnight. Two tubes were set up per sample: tube A containing 300ng of reporter plasmid DNA and 25µl serum-free DMEM medium; and tube B containing 1µl Metafectene® (Biontex) and 25µl serum-free DMEM medium. The contents of tube A were added drop-wise to the contents of tube B to form a translucent precipitate (table 2.4). The precipitate was transferred to the cell culture medium and gently agitated, and then incubated for 30 minutes at room temperature. Afterwards, 1ml serum-free DMEM was added to 12-well plates and the contents from tubes A and B were combined. The cells were incubated at 37ºC for three hours when the medium containing the precipitate was removed. The cells were washed and 500µl fresh complete medium was added to the cells. The cells were incubated at 37ºC for 24, 48 and 72 hours.

Table 2.4

	Cell number	Tube A		Tube B	
		DNA (ng)	DMEM (serum free)	Metafectene (µl)	DMEM (serum free)
6-well	1×10^5	1000	100	4	100
12-well	2.5×10^4	300	25	1	25

Table 2.4. Shows the different ratios of cell numbers, DNA and metafectene for 6-well and 12-well plates.

2.5 Protein assay

Cell extracts were assayed for protein content using the bicinchoninc acid (BCA) protein assay kit (Pierce, Rockford, Illinois). A standard curve was produced from a series of diluted albumin standards which were prepared from a 2mg/ml stock of bovine serum albumin (BSA) (in 0.09% saline and 0.05% sodium azide) using lysis buffer as the dilution. The working range of the assay was 20~2000µg/ml. 25µl of each standard or unknown sample was pipetted into a microplate well and then mixed thoroughly with 200µl of the working pipette in a microplate of 50 parts BCATM Reagent A and 1 part of BCATM Reagent B (50: 1, Reagent A: B). The plate was covered and incubated at 37ºC for 30 minutes, cooled to room temperature and then the absorbance of the samples was measured at 570 nm on a plate reader.

2.6 Western blot

Cells were lysed in modified radio-immune precipitation assay (RIPA) buffer (50mM Tris-HCl, pH 7.4, 150 mM NaCl, 1mM EDTA and 1% NP-40). The protein concentration of each sample was determined by BCA^{TM} protein assay kit from Pierce (Lot No. HE103661); 50µg of protein was electrophoresed on 12% SDS-polyacryamide gel using a Bio-Rad minigel apparatus. Proteins from this gel were transferred to a PVDF membrane from Amersham Bioscience (Hybond-P membrane, Lot No. RPN303F) and blocked overnight at 4°C with 10% dried milk powder and 0.02% Tween 20 in PBS. Membranes were incubated at room temperature for anhour at room temperature in 10% dried milk powder in phosphate-buffered saline and a 1:1000 dilution of PPARγ (Sc-7196) and alpha-actin (A2668) and washed in phosphate-buffered saline plus 0.2% Tween 20. Membranes were then incubated in phosphate-buffered saline plus 0.2% Tween 20 containing 10% dried milk powder with a 1:10000 dilution of goat anti-rabbit antibody coupled to horseradish peroxidase for one hour. Immunoreactive bands were then visualised using SuperSignal®.

Table 2.5.

Name	Description
10% Resolving Gel	4.2ml 4X resolving solution 5ml H$_2$O 3.3ml Acrylamide 30%

	100µl of APS write out (100mg/1ml)
	10µl TMED (mixed in last)
Resolving Solution	50ml of 1.5 M Tris pH 8.8
	2ml of 10% SDS
	l H$_2$O to make 200ml in total
Running Buffer (10X)	144g Glycine (250mM)
	242g Tris-Base (25mM)
	80g SDS (electrophoresis grade) 0.1% (w/v)
	H$_2$O to make up 8L in total
Blotting Solution	10g Marvel milk
	100ml TBS-0.1% Tween (400ml TBS+0.4ml Tween 20)
Stacking Gel	2.5ml stacking solution 2X
	850µl Acrylamide
	1.7ml H$_2$O
	50µl APS
	5µl TEMED (mixed in lastlast to mix in)
Stacking Solution	25ml 1 M Tris-Base pH 6.8
	2 ml 10% SDS
	H$_2$O to make up 200 ml in total
Transfer Buffer	200 ml Running buffer 1X
	50 ml Absolute Methanol
TBS-Tween (pH 7.4)	1.21g Tris-Base
	4g NaCl
	500ml dH$_2$O
	500µl Tween 20

2.7 Luciferase reporter assay

Luciferase activity in transfected cells was measured using the dual luciferase assay from Promega (Promega, Chilworth, UK). In brief, the cells were lysed in passive 1X lysis buffer (100µl/per well) and freeze-thawed twice. Cell debris was pelleted and the supernatant was transferred to a fresh tube. 5µl of the supernatant for each sample was first mixed with luciferase assay reagent Π (LAR$^\Pi$) and the firefly luminescence of the sample measured. For each sample, the firefly was measured three times in a TD-20/20 luminometer (Turner Designs, Sunnyval, California) and an average luminescence was calculated.

2.8 Statistics

For all quantification analysis, at least three independent experiments were performed. The significance of differences for paired data was determined using Student's t-test. P-values less than 0.05 were considered significant.

Chapter 3

3.1 Introduction

Neuroblastoma is thought to arise from embryonic neural crest cells which fail to undergo differentiation. The long-term survival of neuroblastoma is very poor as most children present with disseminated disease. It is well known, however, that spontaneous regression can occur in patients who are less than one year old (Berthold et al 2003) and hence much recent research has focused on understanding the differentiation pathway in neuroblastoma and identifying agents that induce neuroblastoma differentiation. One potential target is PPARγ, which has been shown to play a key role in cellular differentiation in a number of tissues, including adipocytes and monocytes (Barak et al 1999, Chawla et al 1994). Moreover, Han's group (2001) has shown that levels of PPARγ protein inversely correlate with the stage of neuroblastoma; high levels of PPARγ protein are found in both primary stage neuroblastoma and well-differentiated phenotypes (Han et al 2001c), while low levels are found in high stage undifferentiated neuroblastoma. Moreover, both endogenous and synthetic ligands of PPARγ have been shown to inhibit cell growth and/or induce differentiation or apoptosis in a wide variety of cancer cell lines, including prostate, colon, breast, lung and various hematological cancers (Panigrahy et al 2003, Wang et al 2006a). Clinical trials of the synthetic TZD ligand are also ongoing in prostate cancer patients; however, several recent studies have shown that many of the effects induced by both endogenous ligands, such as 15dPGJ2 and synthetic ligands like TZDs occur through pathways independent of PPARγ (Cerbone et al 2007). Therefore, the precise role of PPARγ in mediating the anti cancer effects of these ligands is unclear at present and whether the level of PPARγ present in neuroblastoma cells may play a role in determining the differentiation status of the cells. In order then to determine what role PPARγ plays in neuroblastoma growth and differentiation and whether high levels of PPARγ expression contribute to the well differentiated phenotype of neuroblastoma cells, we have investigated the effects of i) over-expressing PPARγ and ii) reducing the level of PPARγ in the human neuroblastoma cell line *SK-N-AS* on cell growth, differentiation and viability.

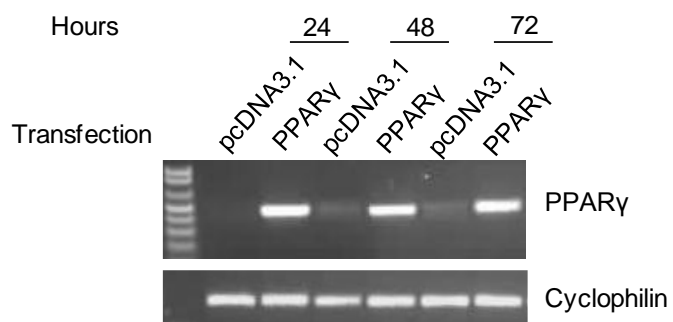# 3.2 Results

3.2.1 PPARγ overexpression in *SK-N-AS* cells

To investigate the effect of PPARγ on the growth, differentiation and viability of neuroblastoma cells, *SK-N-AS* cells were transfected with either an empty expression vector or an expression vector containing the full length cDNA clone of human PPARγ. To confirm that the levels of PPARγ mRNA and protein were increased in the cells transfected with the expression vector containing the full length clone of PPARγ, RNA and protein were extracted from *SK-N-AS* cells transfected with either the PPARγ expression vector or empty expression vector 24, 48 and 72 hours after transfection.

The detail of the experiments are that, firstly, RNA was collected, reverse transcribed into cDNA and analysed using real-time PCR. To ensure equal amounts of RNA were analysed in each sample, cDNA samples were initially analysed using the housekeeping gene cyclophilin. We found that the level of PPARγ mRNA was significantly increased in the cells which were transfected with the PPARγ expression vector compared to cells transfected with the empty expression vector (figure 3.1AB). Moreover, in order to determine that the increase in PPARγ mRNA corresponded to an increase in PPARγ protein expression, a western blot was carried out using an antibody specific for PPARγ (figure 3.1B). This showed that in cells transfected with the PPARγ expression vector there was a significant increase in PPARγ protein expression compared to cells transfected with the empty expression vector.
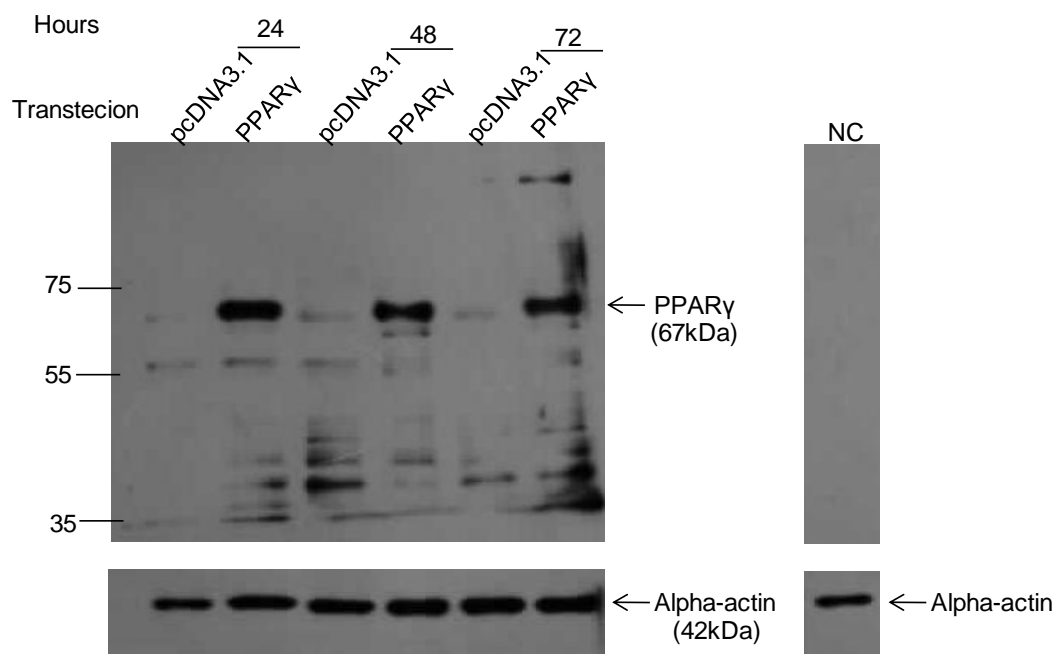
Having shown that PPARγ mRNA and protein expression were increased in the PPARγ transfected cells, we also investigated whether the level of PPARγ activity was increased in the cells transfected with the PPARγ expression vector. For this, *SK-N-AS* cells were co-transfected with a PPARγ reporter plasmid containing a PPRE element upstream of the TK promoter which drives expression of the luciferase reporter gene together with either the PPARγ expression vector or the empty expression vector. Cells were then treated with or without the PPARγ ligand 15dPGJ2. The results of the transfection showed that there was a higher level of luciferase activity in the cells transfected with the PPARγ expression vector than in control cells, and that upon 15dPGJ2 treatment, although PPRE activity increased in both control and PPARγ transfected cells, the level of PPRE activity was far higher in the PPARγ transfected cells compared to controls (figure 3.1C). As an additional control, cells were also transfected with an expression vector containing a dominant negative PPARγ

cDNA. The PPARγ dominant negative plasmid, which is an artificial PPARγ mutant receptor (mutated at L468A/E471A on PPARγ), has the ability to bind to the PPRE promoter region and bind the co-repressor, but in the presence of ligand does not exchange the co-repressor complex for a co-activator complex (Gurnell et al 2000). Transfection of the PPARγ DN plasmid reduced the level of PPRE luciferase activity in the transfected cells with or without ligand. Thus, these experiments demonstrate that transfection of cells with the PPARγ expression vector results in a significant increase in PPARγ expression and that the over-expressed protein is active and able to bind to its response element and activate gene expression.

A.

Hours

<u>24</u>   <u>48</u>   <u>72</u>

Transfection

PPARγ

Cyclophilin

B.   <u>Western blot</u>

Hours

<u>24</u>   <u>48</u>   <u>72</u>

Transtecion

NC

75 —

55 —

35 —

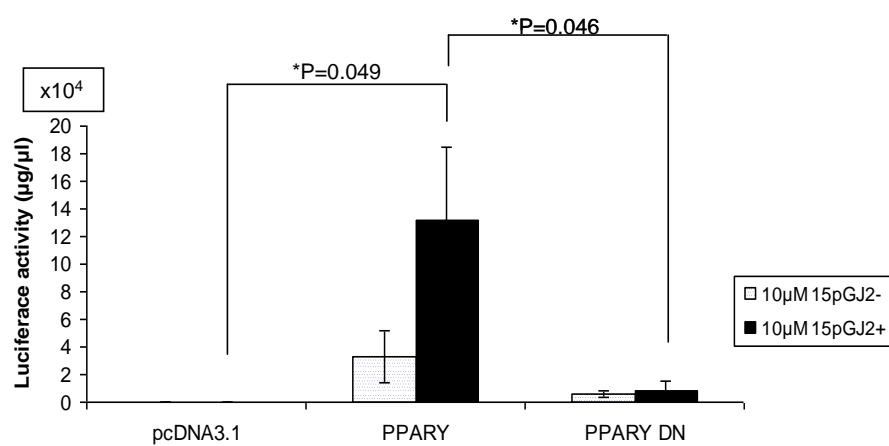← PPARγ
(67kDa)

← Alpha-actin
(42kDa)

← Alpha-actin

C.

**Figure 3.1. Expression PPARγ in *SK-N-AS* cells over periods of 24, 48 and 72 hours. A.** *SK-N-AS* cells were plated out in 6-well dishes at 1×10^5 cells per well and were transfected either with the empty expression vector or with the PPARγ expression vector. Reverse transcriptase PCR was used to detect the expression of PPARγ, and cyclophilin mRNA. Samples were run on a 1% agarose gel. The experiment was carried out in duplicate. **B.** Western blot analysis of PPARγ protein expression in PPARγ transfected cells compared to control transfected cells. Western blotting was performed using a human PPARγ-specific antibody. Alpha actin was used as a loading control. The negative control lacked the primary antibody (PPARγ). **C.** PPARγ activity is increased in PPARγ transfected cells. *SK-N-AS* cells were transfected with either the PPARγ expression vector or an empty expression vector together with the PPRE reporter plasmid in the presence or absence of 10μM 15dPGJ2. Luciferase activity was measured after 24 hours and normalised with protein concentration (1μg/μl). Statistics were calculated using student's *t*-test. The experiment represents three independent experiments ± s.d.

3.2.2 PPARγ promotes cell growth inhibition but did not affect cell viability

Having shown that the PPARγ cells were expressing active protein, and at a higher level than control cells, we next investigated the effect of increased levels of PPARγ on the growth, viability and differentiation of neuroblastoma cells. To determine whether over-expression of PPARγ has an effect on cell growth and cell viability in *SK-N-AS* cells, the cells were transfected with either the PPARγ expression vector or control vector and cell growth assessed after 24, 48 and 72 hours. After 24 hours, there was a small decrease in cell numbers in the PPARγ transfected cells compared to controls but this was not significant. However, by 48 hours, there was a significant decrease in cell numbers in the PPARγ transfected cells compared to controls (figure 3.2A). Interestingly, however, there was no corresponding decrease in cell viability over the same period (figure 3.2B) suggesting that over-expression of PPARγ affects cell growth by inducing growth arrest as opposed to affecting cell viability.
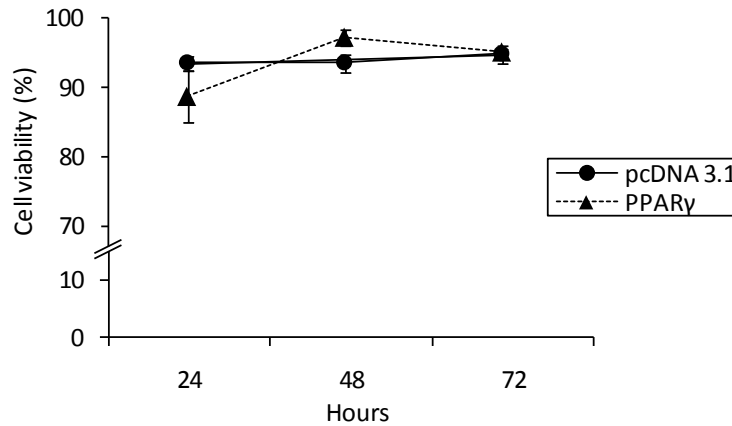
A.
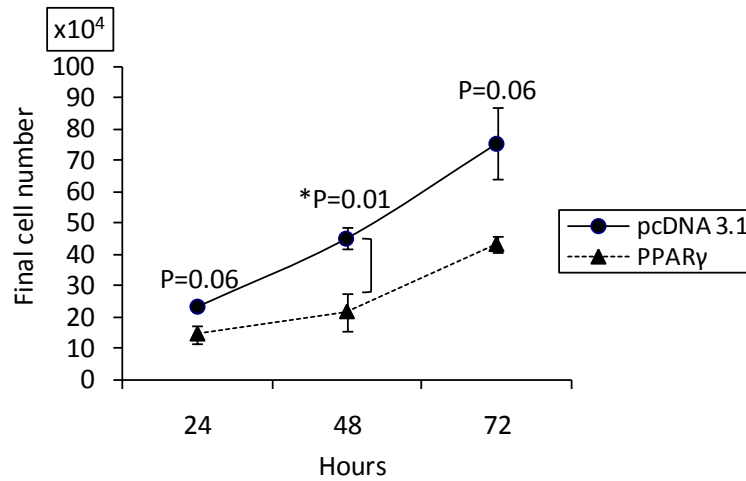
B.

Figure 3.2. The activation of PPARγ leads to growth inhibition. *SK-N-AS* cells were plated out in 6-well dishes at 1×10^5 cells per well and transfected with either the empty expression vector or PPARγ expression vector. **A.** Growth curves of vector-transfected and PPARγ-transfected cells were determined using a haemocytometer (*P=0.01). Cell growth was measured by counting the total number of white viable cells per day. The values represent the average of three independent experiments. **B.** Cell viability was calculated by dividing the trypan blue negative cells by the total number of cells The values produced are the mean ± s.d. of triplicate points from a representative experiment (n=3), which was repeated three times with similar results.

3.2.3 Increasing the expression of PPARγ has no effect on *SK-N-AS* cell morphology

Ligand-activated PPARγ plays a crucial role in adipocyte and monocyte/macrophage differentiation (Han et al 2001b). Moreover, ligand-activated PPARγ (using 10µM 15dPGJ2) induces cell differentiation in *LA-N-5* neuroblastoma cells after 10 days. To determine whether increasing levels of PPARγ may induce cell differentiation in *SK-N-AS* cells, transfected cells carrying the PPARγ plasmid were compared to the empty plasmid controls. However, the examination of cells at 24, 48 and 72 hours after transfection showed no obvious morphological difference in *SK-N-AS* cells (figure 3.3).
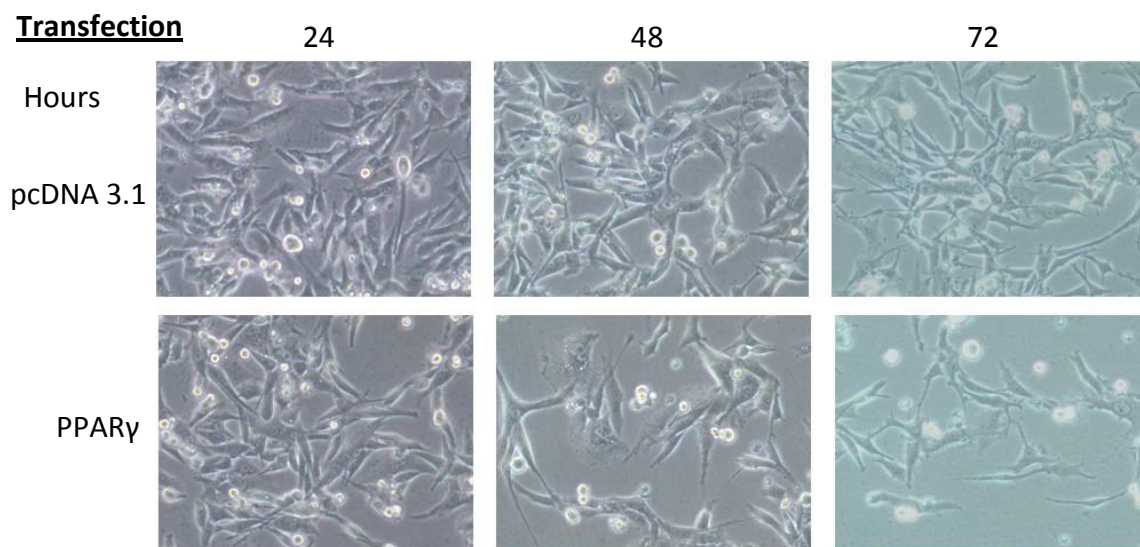
Figure 3.3. Effect of PPARγ overexpression on the morphological differentiation of *SK-N-AS* cells. Cells were plated out in 6-well dishes with 1×10^5 cells per well in complete medium and allowed to attach overnight, then transfected with a PPARγ or empty expression vector (1µg). These images are obtained at a magnification of 200X.

3.2.4 Overexpression of PPARγ increases expression of p14^{ARF}

Given that our experiments have shown that the overexpression of PPARγ decreased cell growth but did not affect cell viability in *SK-N-AS* cells, we next investigated whether the decrease in cell growth was accompanied by the induction of the cell cycle inhibitors p14^{ARF}, p16$^{INK4\alpha}$ and p21^{CIP1}.

Using primers specific for p14^{ARF}, we found that p14^{ARF} expression was reduced in PPARγ cells 24 hours after transfection compared to control cells; however by 48 (*P=0.03) and 72 hours after transfection there was a large increase in p14^{ARF} expression in the PPARγ transfected cells compared to the controls. Interestingly, the induction of p14^{ARF} at 48 and 72 hours coincides with the time points at which a significant decrease in cell growth was seen (figure 3.4). Because of time constraints, however, we were only be able to conduct this experiment twice (n=2). In the future, it would be useful to repeat this experiment in triplicate.
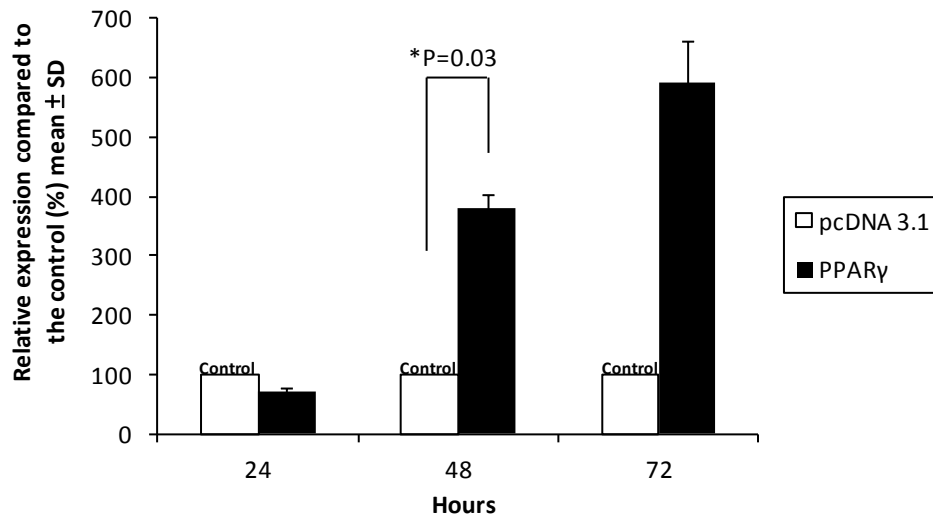
Figure 3.4. Induction of p14^{ARF} in PPARγ overexpressing cells. The expression of p14^{ARF} was detected using real-time PCR. *SK-N-AS* cells were plated out in 6-well dishes at 1×10^{5} cells per well and were transfected either with empty expression vector or with PPARγ expression vector. Real-time PCR analysis was used to detect the expression of PPARγ (n=2), with cyclophilin as an internal control. There was a significant increase after 48 hours (*P=0.03). Results are from two independent experiments done in duplicate.

3.2.5 Cloning p14^{ARF} promoter region in pGEM easy plasmid

Having shown that p14^{ARF} is induced in cells overexpressing PRARγ, we wanted to determine whether PPARγ can directly induce p14^{ARF} transcription. In p14^{ARF}, the PPRE sequence AAAATAAGGGGAATAGGGGAGC was found to be present -459 base pair upstream of the transcription start site. To determine whether PPARγ can directly bind and regulate the p14^{ARF} promoter, we attempted to clone the promoter region of p14^{ARF} into the reporter vector pGL3-basic via the TA cloning vector pGEM easy plasmid. The choice of p14^{ARF} promoter primers 5'-GCCTCGAGTGGGCTAGACACAAAGGACTCG-3' and reverse 5'-GCAAGCTTGCACCCGCCTTCCCTGAGC-3' was done using the Beacon software. The expected PCR product should be 809 base pair fragment. Using human genomic DNA as template for PCR, we repeatedly obtained a fragment of >1000 base pair despite optimisation through the use of altered Mg^{2+} concentrations and the addition of DMSO (figure 3.5C). However, it may be the case that because the primers are not specific enough, they may anneal to the wrong location on the demonic DNA. Therefore, if there had been more time available to conduct this experiment, it would have been useful to design another primer to done p14^{ARF} promoter regions.

A.
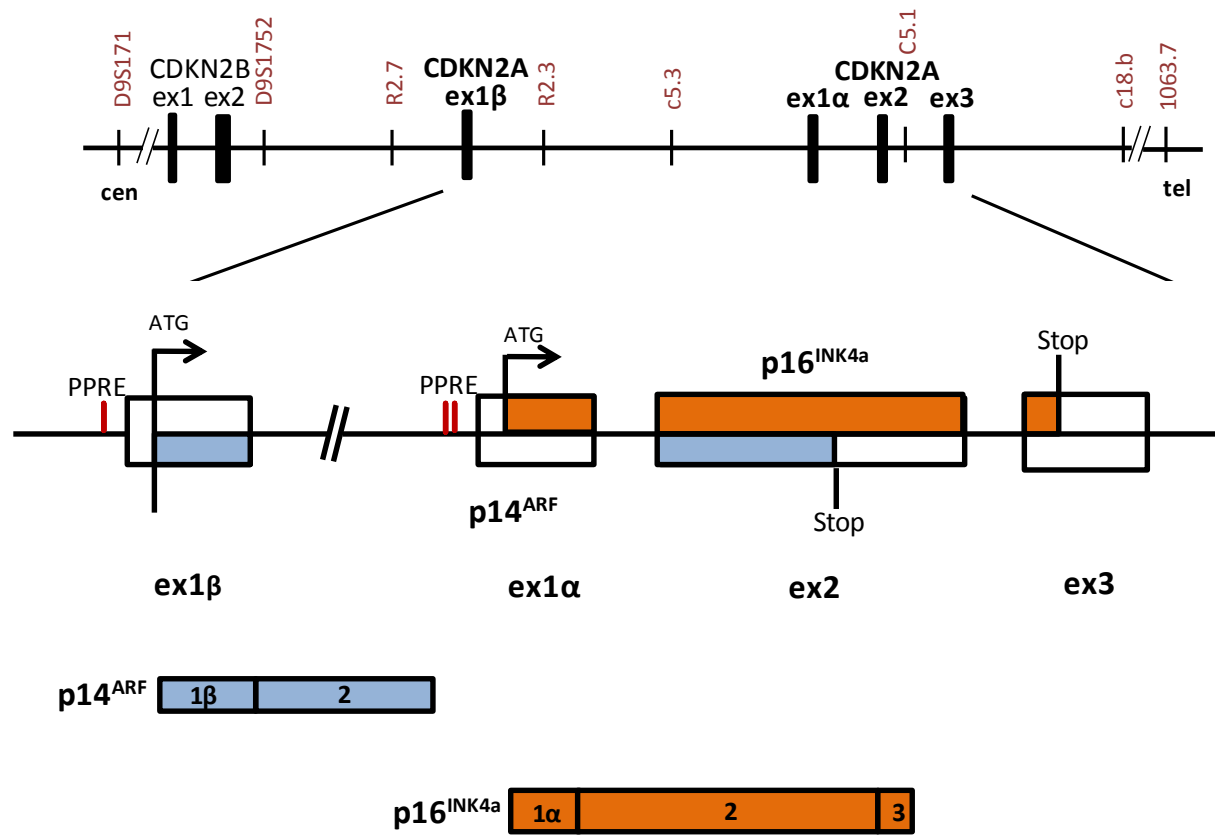
B.
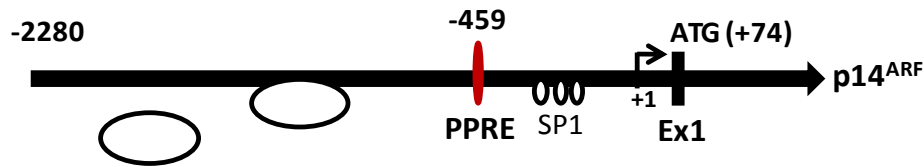
p14^ARF (Genbank AF082338)

```
                      Forward
AACCGAAAATAAAAATGGGCTAGACACAAAGGACTCGGTGCTTGTCCCAGCCAGGCGCCCTCGGCGACGC
GGGCAGCTGGGAGGGGAATGGGCGCCCGGACCCAGCTGGGACCCCCGGGTGCGACTCCACCTACCTAGTC
CGGCGCCAGGCCGGGTCGACAGCTCCGGCAGCGCCAGCGCCGCGCCGTGTCCAGATGTCGCGTCAGAGGC
GTGCAGCGGTTTAGTTTAATTTCGCTTGTTTTCCAAATCTAGAAGAGGAGCGGAGCGGCTTTTAGTTCAA
AACTGACATTCAGCCTCCTGATTGGCGGATAGAGCAATGAGATGACCTCGCTTTCCTTTCTTCCTTTTTC

                                                          Putative PPRE
ATTTTTAAATAATCTAGTTTGAAGAATGGAAGACTTTCGACGAGGGGAGCCAGGAATAAAATAAGGGGAA
        -459
TAGGGGAGCGGGGACGCGAGCAGCACCAGAATCCGCGGGAGCGCGGCTGTTCCTGGTAGGGCCGTGTCAG
GTGACGGATGTAGCTAGGGGGCGAGCTGCCTGGAGTTGCGTTCCAGGCGTCCGGCCCCTGGGCCGTCACC
GCGGGGCGCCCGCGCTGAGGGTGGGAAGATGGTGGTGGGGGTGGGGGCGCACACAGGGCGGGAAAGTGGC
GGTAGGCGGGAGGGAGAGGAACGCGGGCCCTGAGCCGCCCGCGCGCGCGCCTCCCTACGGGCGCCTCCGG


CAGCCCTTCCCGCGTGCGCAGGGCTCAGAGCCGTTCCGAGATCTTGGAGGTCCGGGTGGGAGTGGGGGTG

                          Reverse
GGGTGGGGGTGGGGGTGAAGGTGGGGGGCGGGCGCGCTCAGGGAAGGCGGGTGCGCGCCTGCGGGGCGGA

                                  +1 Transcription start site
GATGGGCAGGGGGCGGTGCGTGGGTCCCAGTCTGCAGTTAAGGGGGCAGGAGTGGCGCTGCTCACCTCTG
GGTGCCAAAGGGCGGCGCAGCGGCTGCCGAGCTC
```
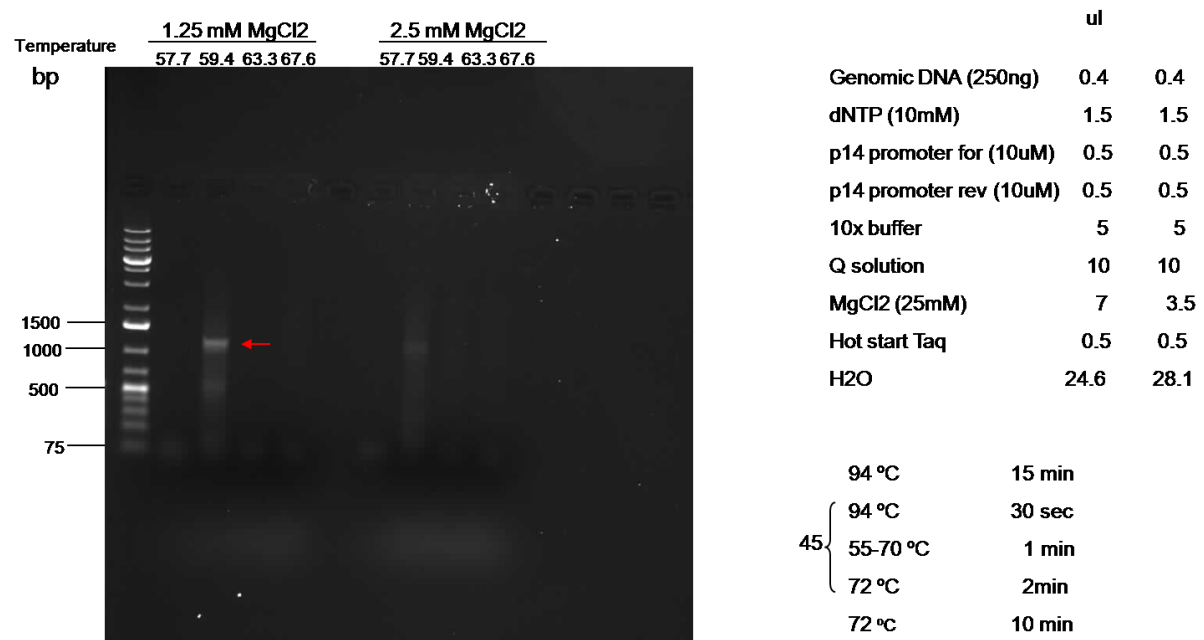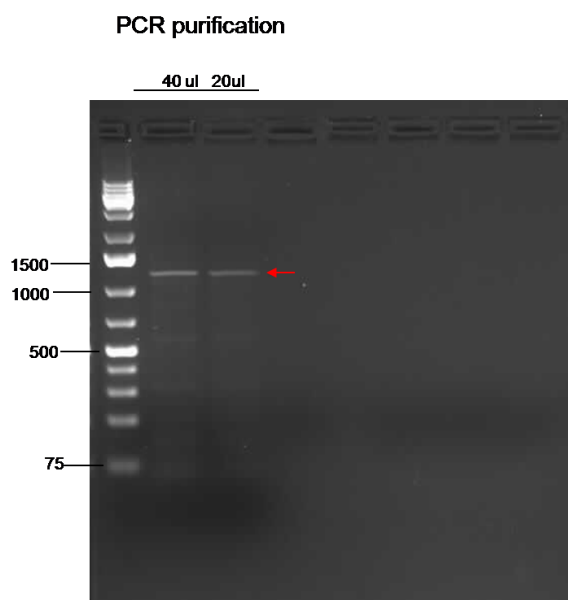
C.

	ul	
Genomic DNA (250ng)	0.4	0.4
dNTP (10mM)	1.5	1.5
p14 promoter for (10uM)	0.5	0.5
p14 promoter rev (10uM)	0.5	0.5
10x buffer	5	5
Q solution	10	10
MgCl2 (25mM)	7	3.5
Hot start Taq	0.5	0.5
H2O	24.6	28.1

	94 °C	15 min
	94 °C	30 sec
45	55-70 °C	1 min
	72 °C	2min
	72 °C	10 min

D.

Figure 3.5. The promoter region of p14^{ARF}. A. Schematic diagram showing the genomic location of p14^{ARF}/p16$^{INK4\alpha}$. **B.** Location of the putative PPRE within the promoter of p14^{ARF}. **C.** Amplification of the promoter region of p14^{ARF} using different concentrations of MgCl$_2$ and different annealing temperatures. **D.** Purified p14^{ARF} promoter region product (the size is around 1200 base pair).

3.2.6 Determining whether the expression of p16$^{INK4\alpha}$ and p21^{CIP1} (mRNA level) can be increased by overexpression of PPARγ in *SK-N-AS* cells

It has been demonstrated that PPARγ can directly regulate the cell cycle inhibitor p16$^{INK4\alpha}$ in fibroblasts via a PPRE site AGTGTGAAGGAGACAGGACAGTA (Gan et al, 2008). We also investigated whether the cell cycle inhibitor p21^{CIP1} contained a putative PPRE site using MatInspector (http://www.genomatix.de/en/index.html). This predicted a PPARγ binding site within the p21^{CIP1} promoter sequence at CCAGAGTGGGTCAGCGGTGAGCC (figure 3.6B). Given that both p16$^{INK4\alpha}$ and p21^{CIP1} contain potential PPRE sequences within the promoter regions of these genes, and are potentially regulated by PPARγ, we next investigated whether the overexpression of PPARγ in *SK-N-AS* cells led to an increase in the expression (mRNA) of these cell cycle inhibitors. Then, we can determine whether PPARγ directly or indirectly regulates the genes by using site directed mutagenesis and transient transfection assays.

To determine whether the expression (mRNA level) of p16$^{INK4\alpha}$ or p21^{CIP1} is influenced by PPARγ, cDNA was made from RNA extracted from *SK-N-AS* cells (overexpression PPARγ in *SK-N-AS* cells) and amplified with primers specific to p16$^{INK4\alpha}$ and p21^{CIP1} (QIagen). A range of annealing temperatures (54.1, 56.4 and 60.2°C) was used to initially determine the best conditions for amplification. cDNA was made from RNA extracted from cells grown either in 10% serum or in serum-free medium to induce growth arrest (Pecorino 2005) which can be a positive control of p16$^{INK4\alpha}$ and p21^{CIP1}. This is because without serum included in the culture medium, the cell cycle inhibitor, such as p16$^{INK4\alpha}$ or p21^{CIP1}, may be increased (Pecorino 2005). However, multiple PCR products were consistently seen at all three temperatures tried (figure A.B).
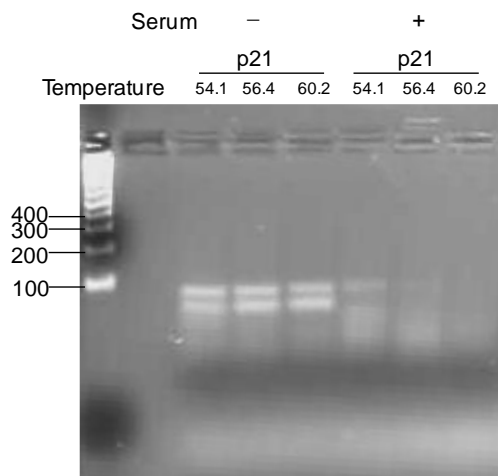
A.

B.
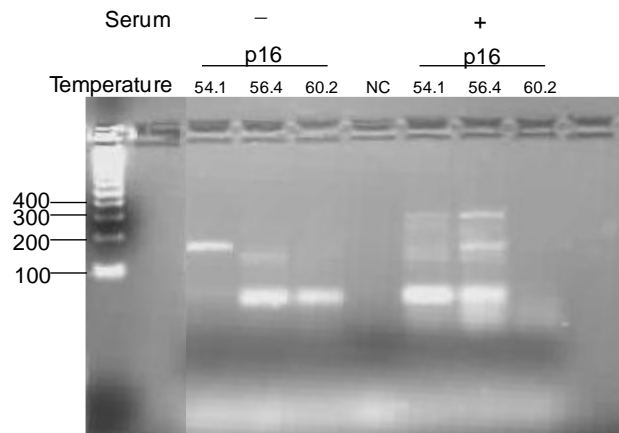
Figure 3.6. Detecting the mRNA expression of p16$^{INK4\alpha}$ and p21^{CIP1} from *SK-N-AS* cells. **A/B.** Total RNA was isolated from *SK-N-AS* cells grown either in serum (FCS) or without serum for 24 hours. The RNA was then reverse-transcribed into cDNA and amplified with specific primers for p16$^{INK4\alpha}$ and p21^{CIP1}, using a range of different annealing temperatures. . For p16$^{INK4\alpha}$ a 92 base pair PCR product was expected and for p21^{CIP1} a 79 base pair product.

.

3.2.7 Production of a PPARγ siRNA constructs to knock down PPARγ expression

siRNAs have been proven to be extremely useful for reducing the expression of target genes and analysing gene function. To complement the overexpression studies, we also sought to decrease the level of PPARγ in neuroblastoma cells to determine the effect on cell growth, differentiation and cell viability. To construct a PPARγ siRNA construct, the vector pSilencer (figure 3.7C) was digested with EcoRI and ApaI and purified (figure 3.7DEF). The siRNA insert sequence to reduce PPARγ expression was based upon the sequence previously published in Gan et al. (2008); this is shown in figure 3.7B. This was produced as two oligonucleotides which were annealed to give the stem loop structure and EcoRI and ApaI cohesive ends. Cloning of this into the pSilencer vector will result in the loss of the Hind III site between the EcoRI and ApaI regions (see figure 3.7C). We then aimed to transfect this construct into neuroblastoma cells to assess the effect on PPARγ expression, cell proliferation, cell viability and differentiation. However, after ligation of the annealed oligonucleotide with the cut pSilencer vector and transformation, 20 colonies were picked and the plasmid DNA purified. If the insert has been cloned, then the recombinant plasmid should not be digested by Hind III (figure 3.7DE). However, the results showed that the plasmids in each case were cut by HindIII, suggesting that the siRNA sequence had not been cloned into the pSilencer plasmid (figure 3.7F).

A.

PPARγ protein translation region

+1 <u>translation start site</u>

```
GTGTGAATTACAGCAAACCCCTATTCCATGCTGTTATGGGTGAAACTCTGGGAGATTCTCCTATTGACCCAGAAAGCGATTCC
TTCACTGATACACTGTCTGCAAACATATCACAAGAAATGACCATGGTTGACACAGAGATGCCATTCTGGCCCACCAACTTTGG
```
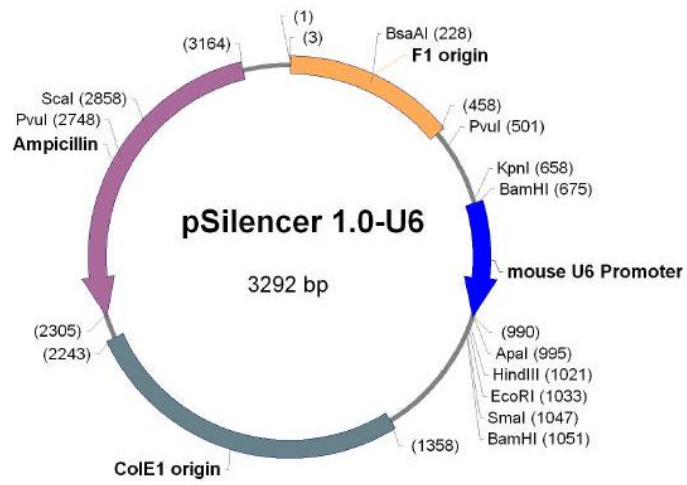
siRNA target site

```
GATCAGCTCCGTGGATCTCTCCGTAATGGAAGACCACTCCCACTCCTTTGATATCAAGCCCTTCACTACTGTTGACTTCTCCA
GCATTTCTACTCCACATTACGAAGACATTCCATTCACAAGAACAGATCCAGTGGTTGCAGATTACAAGTATGACCTGAAACTT
CAAGAGTACCAAAGTGCAATCAAAGTGGAGCCTGCATCTCCACCTTATTATTCTGAGAAGACTCAGCTCTACAATAAGCCTCA
TGAAGAGCCTTCCAACTCCCTCATGGCAATTGAATGTCGTGTCTGTGGAGATAAAGCTTCTGGATTTCACTATGGAGTTCATG
CTTGTGAAGGATGCAAGGGTTTCTTCCGGAGAACAATCAGATTGAAGCTTATCTATGACAGATGTGATCTTAACTGTCGGATC
CACAAAAAAAGTAGAAATAAATGTCAGTACTGTCGGTTTCAGAAATGCCTTGCAGTGGGGATGTCTCATAATGCCATCAGGTT
TGGGCGGATGCCACAGGCCGAGAAGGAGAAGCTGTTGGCGGAGATCTCCAGTGATATCGACCAGCTGAATCCAGAGTCCGCTG
ACCTCCGGGCCCTGGCAAAACATTTGTATGACTCATACATAAAGTCCTTCCCGCTGACCAAAGCAAAGGCGAGGGCGATCTTG
ACAGGAAAGACAACAGACAAATCACCATTCGTTATCTATGACATGAATTCCTTAATGATGGGAGAAGATAAAATCAAGTTCAA
ACACATCACCCCCCTGCAGGAGCAGAGCAAAGAGGTGGCCATCCGCATCTTTCAGGGCTGCCAGTTTCGCTCCGTGGAGGCTG
TGCAGGAGATCACAGAGTATGCCAAAAGCATTCCTGGTTTTGTAAATCTTGACTTGAACGACCAAGTAACTCTCCTCAAATAT
GGAGTCCACGAGATCATTTACACAATGCTGGCCTCCTTGATGAATAAAGATGGGGTTCTCATATCCGAGGGCCAAGGCTTCAT
GACAAGGGAGTTTCTAAAGAGCCTGCGAAAGCCTTTTGGTGACTTTATGGAGCCCAAGTTTGAGTTTGCTGTGAAGTTCAATG
CACTGGAATTAGATGACAGCGACTTGGCAATATTTATTGCTGTCATTATTCTCAGTGGAGACCGCCCAGGTTTGCTGAATGTG
AAGCCCATTGAAGACATTCAAGACAACCTGCTACAAGCCCTGGAGCTCCAGCTGAAGCTGAACCACCCTGAGTCCTCACAGCT
GTTTGCCAAGCTGCTCCAGAAAATGACAGACCTCAGACAGATTGTCACGGAACACGTGCAGCTACTGCAGGTGATCAAGAAGA
CGGAGACAGACATGAGTCTTCACCCGCTCCTGCAGGAGATCTACAAGGACTTGTACTAGCAG
```
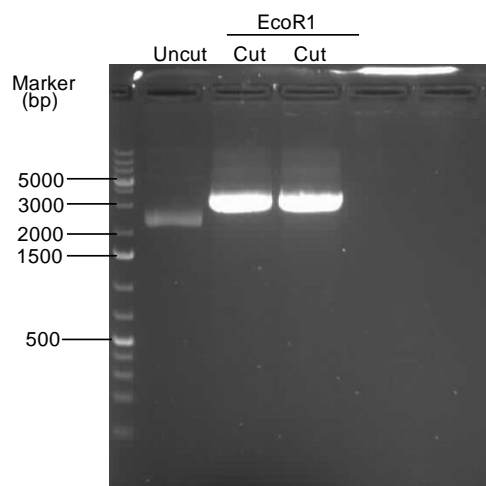
<u>translation stop codon</u>

B.

```
ApaI              Sense                  Loop            Antisense              EcoRI
   5'-GCCCTTCACTACTGTTGACTTCAAGAGAGTCAACAGTAGTGAAGGGCTTTTTT-3'
   3'-CCGGCGGGAAGTGATGACAACTGAAGTTCTCTCAGTTGTCATCACTTCCCGAAAAAATTAA-5'
```
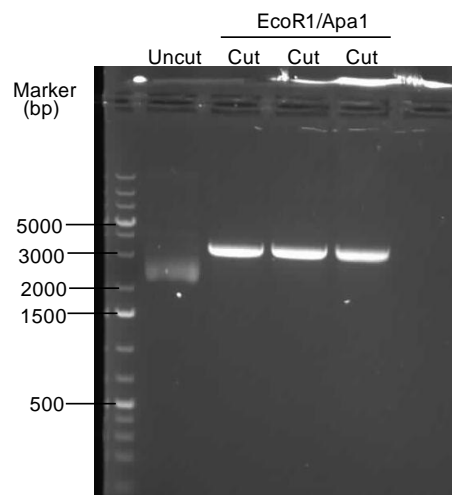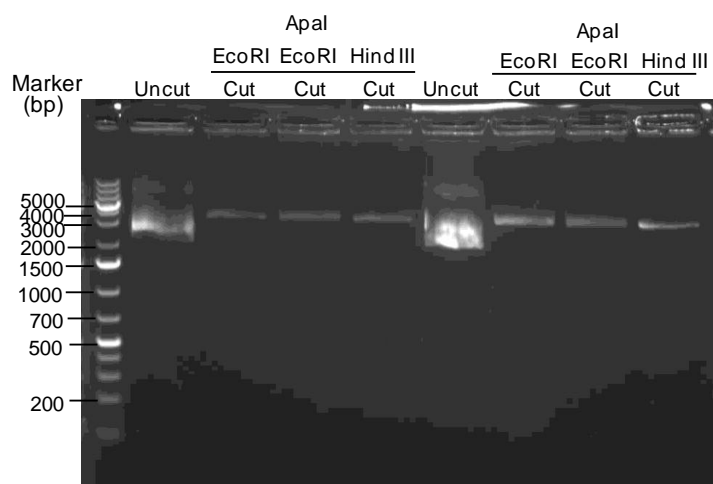
C.

D.

E.

F.

Figure 3.7. **Cloning the PPARγ siRNA oligonucleotide into the pSilencer plasmid. A.** The position of PPARγ siRNA target sequence is shown. **B.** Annealed primer pairs were chosen for production of the PPARγ siRNA; overhangs are included for ease of cloning. **C.** The map of the pSilencer TM 1.0-U6 siRNA expression vector (Ambion). **D/E.** The pSilencer plasmid was cut with EcoRI. EcoR1-digested pSilencer plasmid was further digested with ApaI. The cut plasmid DNA was extracted from the gel ready to clone into the pSilencer plasmid. **F.** Restriction eneyme digests analysis of resulting clones. This shows analysis of two clones. These plasmids were digested with HindIII to check whether the insert has been cloned into the pSilencer plasmid. Neither sample 1 nor sample 2 carries the PPARγ siRNA.

3.3 Discussion

PPARγ is a key regulator of adipogenic differentiation and glucose homeostasis (Picard and Auwerx 2002). Agonists of PPARγ have also been shown to be able to induce the differentiation of a wide range of cancer cell lines; however, in many cases the induction of growth arrest/differentiation was mediated through a PPARγ independent pathway. To assess what role PPARγ plays in the induction of cell cycle arrest and differentiation in neuroblastoma cells, *SK-N-AS* cells were transfected with an expression vector containing a full length cDNA of PPARγ. Cells were transfected with metafectene which Andrew Dawson, in the lab had previously shown to give a transfection efficiency of around 75% in these cells. To ensure equivalent transfection levels in the cells transfected with the control or PPARγ vector, a vector with a marker gene such as GFP could also have been used. We found that transfection of the PPARγ expression vector into neuroblastoma cells led to an increase in PPARγ, mRNA and protein, and increased PPARγ activity compared to cells transfected with the empty vector. Having established that the PPARγ transfected cells contain more active PPARγ protein, we next investigated the effect on cell growth, differentiation and cell viability. In order to ensure that the transfection of the PPARγ expression vector resulted in higher PPARγ expression, real time PCR and western blot were used to detect both mRNA and protein level.

Overexpression of PPARγ in *SK-N-AS* cells led to a decrease in cell growth. There was no effect however on cell viability, suggesting that PPARγ induces a decrease in cell growth not through a decrease in cell viability but through a reduction in the rate of cell growth. There was also no corresponding increase in the morphological differentiation of the cells, suggesting that PPARγ primarily affects the growth of the *SK-N-AS* cells (figure 3.2). Consistent with this we did observe an increase in the expression of the cell cycle inhibitor p14^{ARF}. Interestingly, the induction of p14^{ARF} in the PPARγ-transfected cells was not observed until 48 and 72 hours after transfection (figure 3.4). Indeed a decrease in p14^{ARF} expression was observed 24 hours after transfection. The increase in p14^{ARF} expression at 48 and 72 hours did however coincide with the decrease observed in cell growth. It is very interesting that the expression of p14^{ARF} was increased at 48 and 72 hours.

Interestingly, bioinformatics analysis of the p14^{ARF} promoter showed that, like p21^{CIP1} and p16$^{INK4\alpha}$, there is a potential PPRE within the p14^{ARF} promoter, leading to the possibility that PPARγ may directly regulate p14^{ARF} expression. If PPARγ did directly regulate p14^{ARF}

expression, one might perhaps expect an increase in p14^{ARF} expression at an earlier point in time. It may be, however, that the effect of fresh medium and serum after the transfection overrides the effect of PPARγ regulation, resulting in an initial decrease in p14^{ARF} after transfection.

To determine whether PPRAγ had a direct effect on p14^{ARF} transcription the primers promoter, part of the failure to detect a suitably sized PCR product may have resulted from the formation of primer dimers making it difficult to distinguish the potential amplicon from primer dimers. The problem could be circumvented by designing primers further apart in order to give a larger product. Multiple PCR products were consistently seen at all three temperatures (figure 3.6AB). However, it may be a possibility that the primers were designed by Qiagen, thus giving rise to an amplicon of a very small size. As result, this would make it increasingly difficult to distinguish the amplicon from potential primer dimers. Unfortunately, because of the difficulty in cloning the promoter region of p14^{ARF} we were unable to test this; but we could do nested PCR. Nested PCR is a strategy whereby two pairs of PCR primers are used for a single locus. The first PCR primer's product can be used for the second PCR primer's product. If the first PCR product is correct, the second PCR product can prove that the PCR product overall has more specificity than expected. Moreover, it has demonstrated that the endogenous expression of p21^{CIP1} is high in *SK-N-SH* cells (Mergui et al., 2010) and in our lab, we already have this cell line. For example, Takita et al. (1998) showed that a TGW cell line, which is a human neuroblastoma cell line, can be used as a positive control for p16^{INK4α}. These results suggest that these two cell lines (*SK-N-SH* and TGW) can potentially be used as positive controls for future experiments.

It has however been demonstrated that PPARγ can directly regulate the cell cycle inhibitor p16^{INK4α} in fibroblasts (Gan et al 2008). Expression of p16^{INK4α} is induced by activation of PPARγ (Gan et al 2008). p16^{INK4α} and p14^{ARF} are transcribed from the same gene cyclin-dependent kinase inhibitor 2A (CDKN2A). The p16^{INK4a} transcript contains exon 1α/exon 2/3 while the p14^{ARF} transcript contains exon 1β and exon 2 of chromosome 9, but p21^{CIP1} and p14^{ARF} are transcribed from and controlled by different promoter regions (Quelle et al 1995). Interestingly, p16^{INK4α} is not expressed in 60% of neuroblastoma cell lines (Takita et al 1998) and genetic alterations involving the 9p21 chromosomal region (encoding the p16^{INK4α} gene) are common in human cancers, with loss of LOH being correlated with poor prognosis. More importantly, expression of exogenous p16^{INK4α} in neuroblastoma cells dramatically delays the

cell cycle; and interestingly, treating these cells with 5-aza-2-deoxycytidine which is a DNMT1 inhibitor, resulted in increased expression of p16$^{\text{INK4}\alpha}$ and reduced cell proliferation, suggesting that p16$^{\text{INK4}\alpha}$ expression is regulated by methylation in neuroblastoma cells (Takita et al 1998).

Chapter 4

4.1 Introduction

Cancer occurs as a result of uncontrolled cell proliferation, a failure to differentiation, and/or through the development of resistance to apoptosis. Many different approaches to the treatment of cancer have been tried, involving chemotherapy, radiotherapy and hormone therapy. These agents inhibit DNA replication and/or induce apoptosis or necrosis. For instance small cell lung cancer and leukaemia can respond very quickly to chemotherapy drugs (cisplatin and etoposide) which induce apoptosis (Kurup and Hanna 2004). However, drug resistance may occur, caused for instance by deregulation of the apoptotic pathways (Viktorsson et al 2005). Resistance to standard chemotherapy results in a very poor prognosis, such that complete or partial multi- and high-dose treatments that previously gave about a 44% survival rate, result in a drop to below 23% in relapsed neuroblastoma patients (Chan et al 1997).

The observation however that stage 4S neuroblastoma undergoes spontaneous regression due to the differentiation or apoptosis of the cells has led to considerable interest in finding agents that induce neuroblastoma differentiation or apoptosis *in vivo* (Brodeur 2003, Ponthan et al 2003a, Ponthan et al 2003b). Ligands of PPARγ, which have been shown to induce differentiation/apoptosis in a number of cancer cell lines *in vitro,* have been recently used in a series of clinical trials to treat liposarcoma, colon and prostate cancers (Demetri et al 1999, Mueller et al 2000), with variable success. PPARγ ligands have also been shown to induce growth arrest and/or differentiation or apoptosis in neuroblastoma cells in culture, although the exact response appears to be dependent on the genotype of the neuroblastoma cells and the concentration of ligand used, although for different neuroblastoma cells, different concentrations are required to elicit the same response (Cerbone et al 2007).

The aim therefore of this chapter was to test the effect of different concentrations of PPARγ ligands on the growth, differentiation and viability of *SK-N-AS* cells and to determine whether PPARγ ligands may, in combination with conventional chemotherapy agents or methylating agents, have a greater effect on growth inhibition than either treatment alone.

4.2 Results

4.2.1 The effects of rosiglitazone, a synthetic PPARγ agonist on neuroblastoma cells *in vitro*

In order to determine the effect of RGZ, a synthetic PPARγ agonist on the growth and viability of *SK-N-AS cells*, the cells were treated with increasing concentrations of the PPARγ ligand RGZ (5~100μM) and the effect on cell growth determined over a 72 hours time period. The results showed that after 24 hours there was no difference in cell number in cells treated with 5 or 50μM RGZ, but at 100μM, the total cell number was decreased by 23% (figure 4.1A). After 48 hours of treatment, no difference in cell number was seen at any concentrations of RGZ used, while after 72 hours a decrease in cell number was seen at 5, 50 and 100μM RGZ. At the highest concentration (100μM), the final cell number was reduced to 64% (P=0.001) of the control level after 72 hours.

In terms of cell viability, after 24 hours of treatment no effect on cell viability was seen apart from in samples treated with 100μM RGZ where a small decrease in cell viability was seen. After 48 hours, there was no difference in cell viability at any concentration of RGZ, while after 72 hours a decrease in cell viability was observed only at the highest concentration of RGZ, where cell viability was decreased by 15% (figure 4.1B).
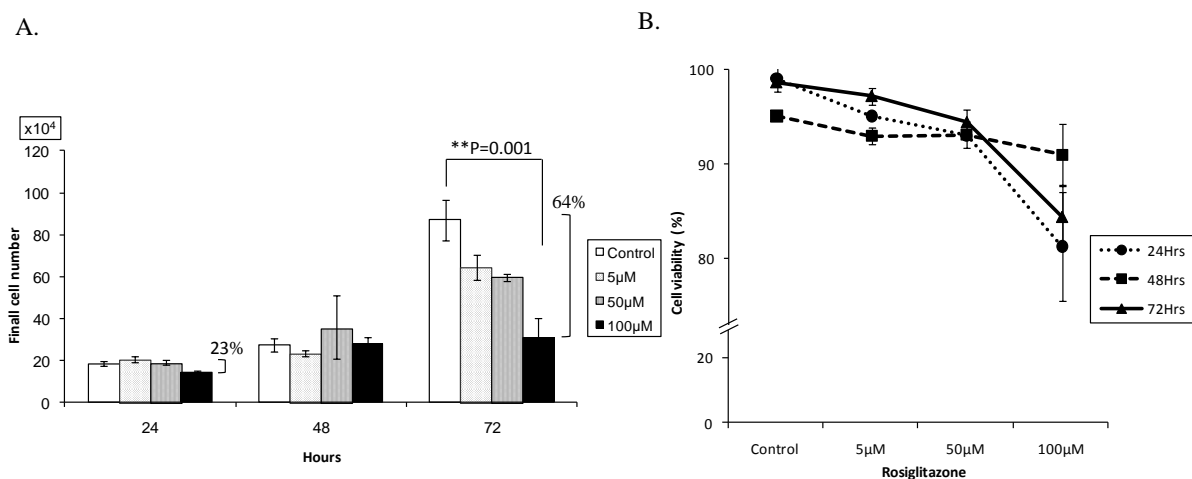
A.

B.

Figure 4.1. Time- and dose-dependent effect of rosiglitazone on *SK-N-AS* cell growth and viability. A/B. *SK-N-AS* cells were plated out in 6-well dishes at 1×10^5 cells per well and treated with either a vehicle control (DMSO) or increasing concentrations of RGZ (5~100μM) and the effects on cell growth **(A)** and cell viability **(B)** were measured over 24, 48 and 72 hours. Trypan blue was used to distinguish between live (white) and dead (blue) cells. Data are expressed as mean ± s.d. of two independent experiments. Denotes a significance of **P< 0.001 compared with the untreated cells.

4.2.2 The effect of combining rosiglitazone and conventional chemotherapy agents on *SK-N-AS* cells

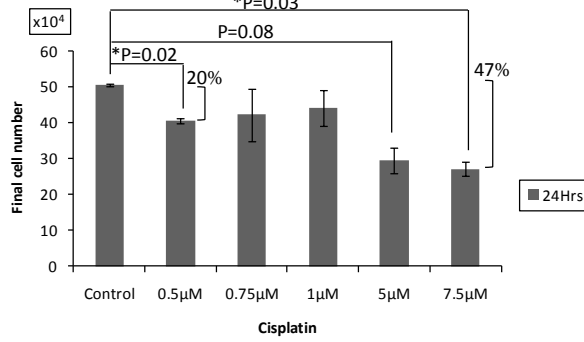## 4.2.2.1 The effect of cisplatin and etoposide on *SK-N-AS* cells

In order to determine whether treating neuroblastoma cells with a combination of PPARγ agonists and conventional chemotherapy agents might improve potency and allow a reduction in the concentration of conventional agents, we initially studied the effect of increasing concentrations of cisplatin and etoposide on neuroblastoma cells.

SK-N-AS cells were treated with either 0, 0.5, 0.75, 1.5 or 7.5µM cisplatin or 0, 0.1, 0.25, 0.5, 1, 1.5 and 2µM etoposide for 24 and 72 hours, and the effect on cell growth and viability analysed. These concentrations of cisplatin and etoposide had previously been shown to induce growth arrest and cell death in a range of cancer cell lines. After 24 hours, there was a trend towards decreased cell growth at all concentrations used, with a significant decrease in cell numbers at 7.5µM (P=0.03) of cisplatin (figure 4.2A). However, no significant decrease in cell viability was seen at these concentrations. After 72 hours, there was again a trend towards decreased cell growth at all concentrations of cisplatin used, with a significant decrease in cell growth at 7.5µM (P=0.08) cisplatin. However, no significant decrease in cell viability at any of the concentrations was observed (figure 4.2B).

The addition of increasing concentrations of etoposide to *SK-N-AS* cells showed no change in cell growth after 24 hours of treatment with any of the concentrations of etoposide used (figure 4.2C). After 72 hours, however, a significant decrease in cell growth was seen at 1.5µM (P=0.05) etoposide. There was however very little effect on cell viability at any concentration or at any time point (figure 4.2D).
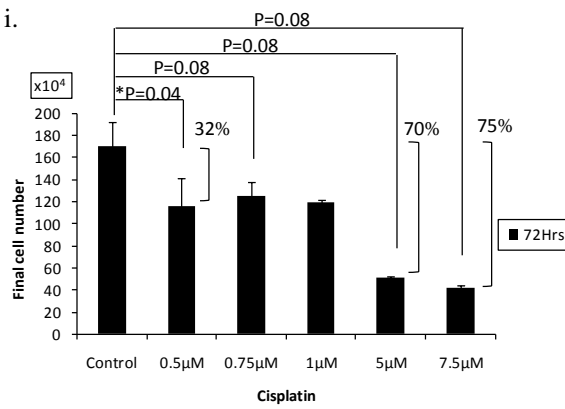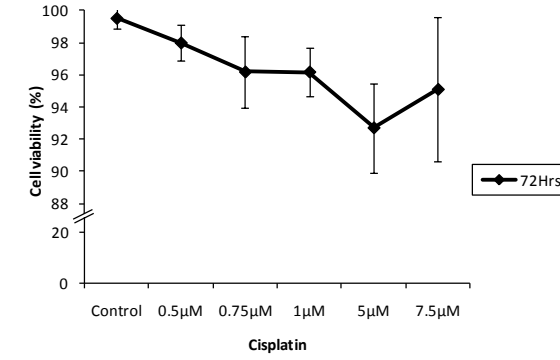
A.

i. **Cisplatin**   ii.
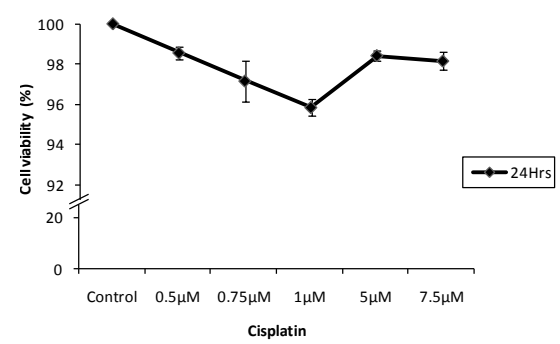
B.

i.   ii.

C.
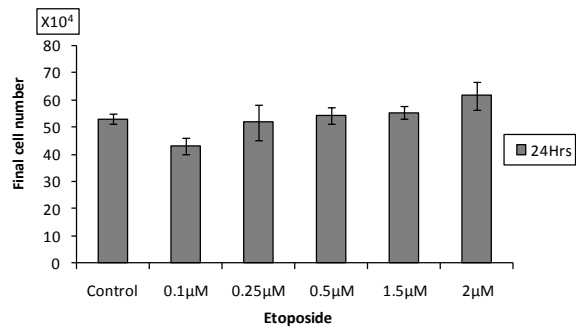
i. **Etoposide**   ii.
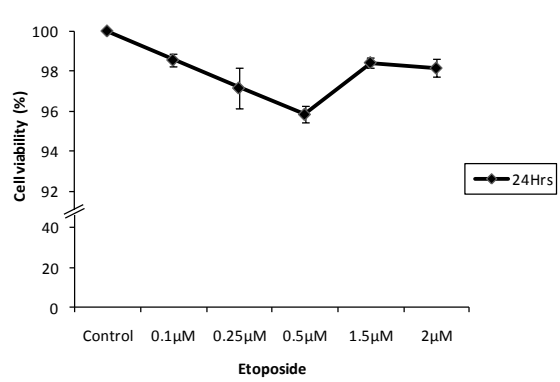
D.
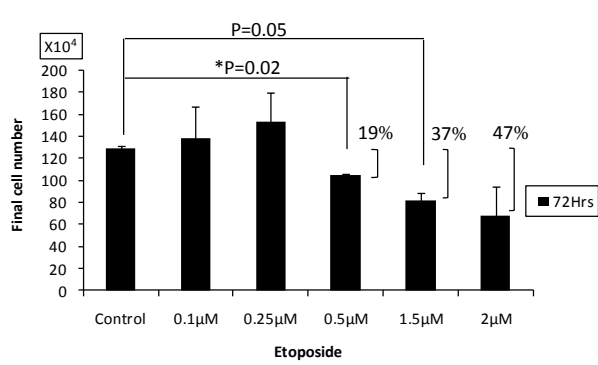
i.   ii.
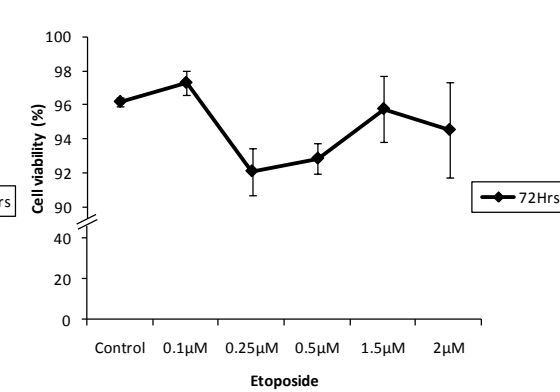
Figure 4.2. The effect of chemotherapy drugs, cisplatin and etoposide, on the cell growth and cell viability of *SK-N-AS* cells. *SK-N-AS* cells were plated out in 6-well dishes at $1\text{x}10^5$ cells and treated with either a vehicle control (DMSO) or increasing concentrations of cisplatin (0.5~7.5μM) and etoposide (0.1~2μM), and the effect on cell growth. **(A/C)** and cell viability **(B/D)** was measured over 24 and 72 hours. Values represent the mean of four experiments ± s.d. A Student's *t*-test was used to analyse the data; * P <0.05 when compared with the untreated cells.

4.2.2.2 Interaction of rosiglitazone and conventional chemotherapy agents leads to an increase in growth inhibition in *SK-N-AS* cells

Conventional chemotherapy drugs interfere with DNA replication and affect not only cancer cells but also rapidly dividing normal cells, giving rise to a range of side effects (Rang, 2003). Therefore, we combined cisplatin and etoposide with RGZ to determine whether the combination of agents might improve potency and allow a lower concentration of drugs to be used. *SK-N-AS* cells were treated with 100µM RGZ, the concentration at which we had consistently seen a reduction in cell growth, together with 1 or 5µM cisplatin (these concentrations of cisplatin had been shown previously to induce a small decrease in cell growth for 72 hours) and the effect on cell growth and viability measured. We found that as observed previously the addition of 1 and 5µM cisplatin alone decreased cell growth (figure 4.3). Similarly, in the presence of 100µM RGZ alone, there was also a decrease in cell numbers (figure 4.3). When a combination of RGZ and cisplatin (1µM) was used there was a 29% decrease in cell numbers compared to when cisplatin was used at this concentration alone; however at 5µM cisplatin, no additive effect of RGZ was seen. Neither cisplatin alone or in combination with RGZ had any effect on cell viability (figure 4.3A).

When etoposide (0.5, 1.5 and 2µM) was combined with 100µM RGZ, there were a 34% (0.5µM etoposide + RGZ), a 43% (1.5µM etoposide + RGZ) and a 2% (2µM etoposide + RGZ) decrease in cell number compared to cells treated with etoposide alone. The combination of etoposide at all concentrations used and RGZ also induced a decrease in cell viability compared to cells treated with etoposide alone (figure 4.3B).
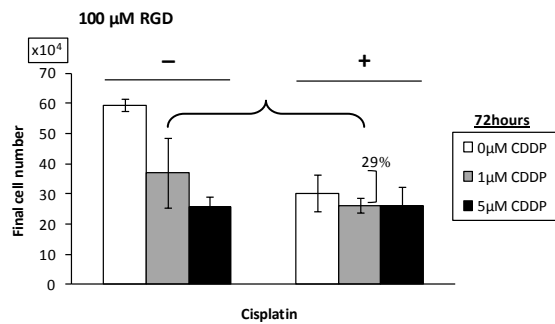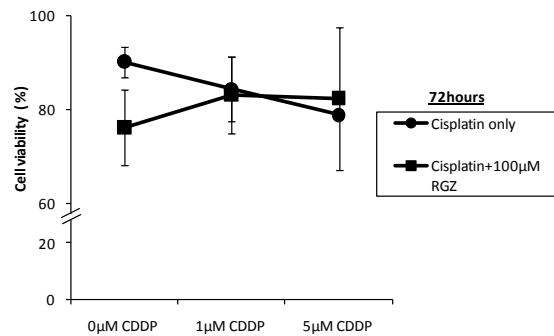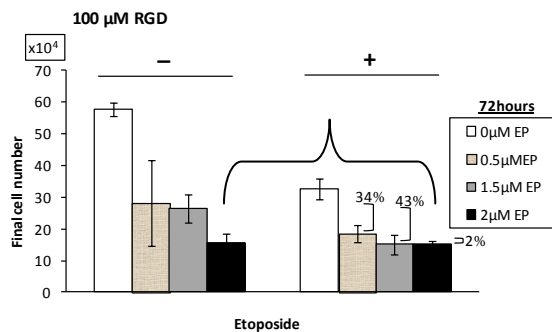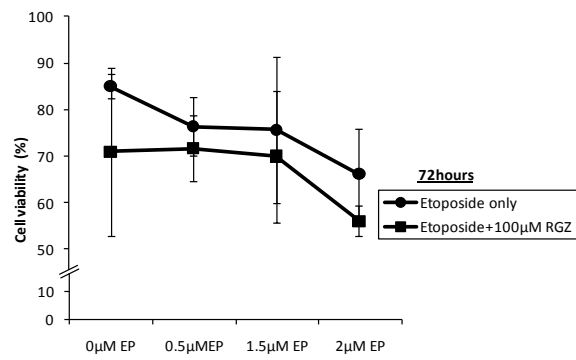
Figure 4.3. The effect of cisplatin and etoposide with rosiglitazone on *SK-N-AS* cell growth over 72 hours. A/B (i). *SK-N-AS* cells were plated out in 6-well dishes seeded with 1×10^5 cells and treated with either a vehicle control (DMSO) or 100μM RGZ together with either cisplatin or etoposide at the concentrations indicated. The effect on cell growth was measured over 72 hours. Values represent the mean ± s.d. of two independent experiments. **A/B (ii).** The graph shows the average percentage of *SK-N-AS* cell viability, as observed by trypan blue exclusion, of two independent experiments. Statistical analysis was carried out by Student's *t*-test to identify significant differences between samples.

4.2.3 PPARγ ligands and DNA methylating agents

Aberrant DNA methylation has been associated with the initiation and progression of cancer (Plass 2002). Folate is a methyl donor which has been shown to play a very important role in the body, as it is essential for DNA synthesis and DNA methylation (Rang, 2003). It has been demonstrated that the concentration of folate is normally 1 to 10ng/ml in plasma physiologically (Hernandez-Blazquez et al 2000). Low folate supply has been shown in many papers to be associated with carcinomas, such as cervical, lung, essophagal, pancreatic (Choi and Mason 2000) and breast (Zhang et al 1999). Maternal folic acid intake has also been reported to decrease the risk of several childhood cancers (Kim 1999a), including neuroblastoma (French et al 2003b). The recent fortification of flour with folic acid in the USA for the prevention of neural tube defects has also been associated with a reduction in neuroblastoma by 60% (French et al 2003b). However, the relationship between folic acid intake and cancer risk is complex as high levels of folic acid have been also associated with an increased risk of colon and breast cancer (Lu and Low 2002).

To determine therefore whether altering the methylation status of the cells might affect the response of neuroblastoma cells to PPARγ ligands, we treated *SK-N-AS* cells initially with increasing concentrations of folic acid and then in combination with either RGZ or conventional chemotherapy agents.

SK-N-AS cells were treated with increasing concentrations of folic acid (1, 5 and 50μM) and the effect on cell growth and viability was analysed. The results showed there was an unsignificant trend towards decreased cell growth in the folic acid-treated cells 24 hours after treatment. However, after 48 or 72 hours, no effect was seen. There was no effect on cell viability at either 24, 48 or 72 hours after folic acid treatment (figure 4.4AB).

A.

B.
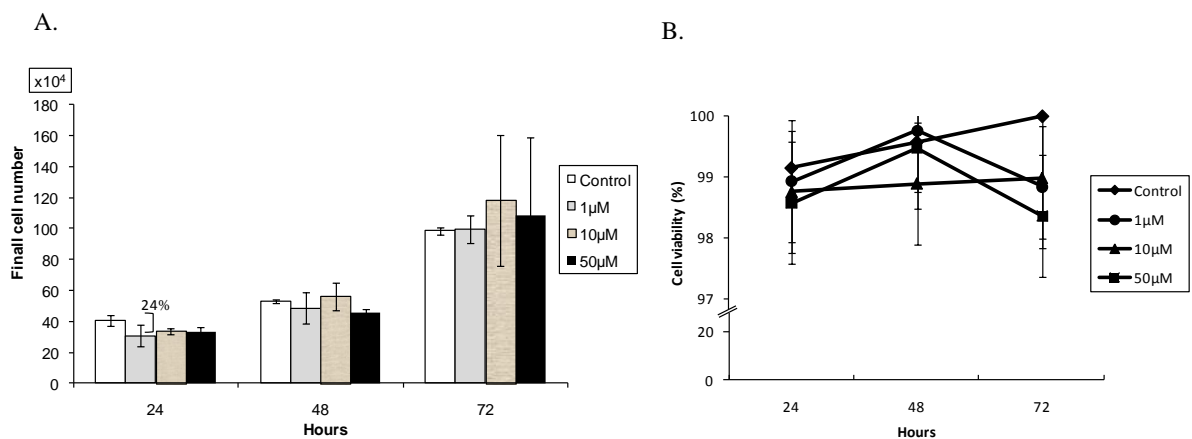
Figure 4.4. Graph showing the cell numbers after treating with different concentrations of folic acid over 24, 48 and 72 hours. *SK-N-AS* cells were plated out in 6-well dishes at $1x10^5$ cells and treated with either a vehicle control (DMSO) or increasing concentrations of folic acid (1~50μM) and the effects on cell growth and cell viability were measured over 72 hours. Trypan blue was used to distinguish between live and dead cells. The values represent the mean ± s. d. of two independent experiments.

4.2.4 Rosiglitazone and folic acid does not have a significant effect on cell growth in *SK-N-AS* cells

Rosiglitazone reduces neuroblastoma cell proliferation, while folic acid modifies the methylation status of genes (French et al 2003b); therefore, we would like to know whether combining RGZ and folic acid affected the response of the cells to RGZ. The results showed that in the presence of 1μM folic acid combined with 50μM RGZ, cell numbers decreased by 7% although this was not statistically significant, and by 21% with folic acid and RGZ (100μM) compared to cells treated with RGZ alone after 24 hours. No effect of folic acid on RGZ treatment was seen at other points in time (figure 4.5).
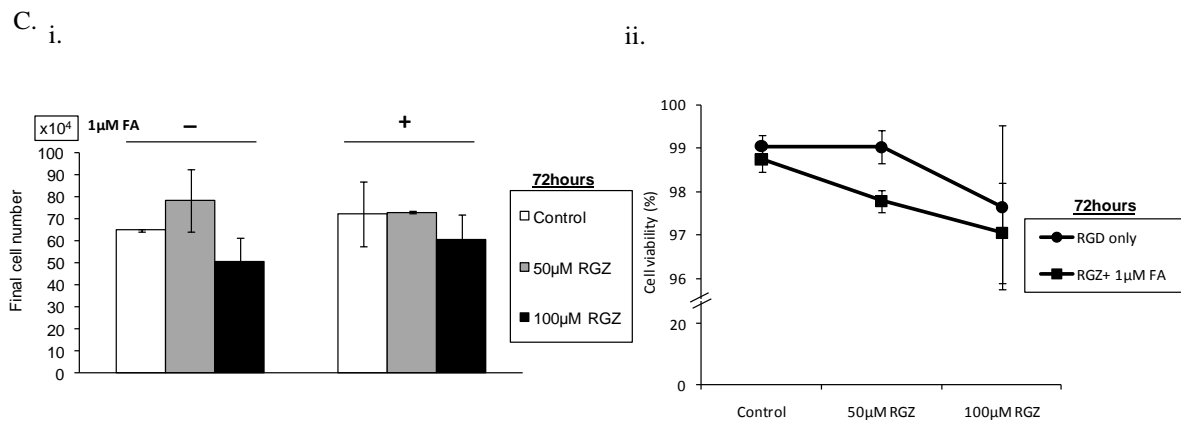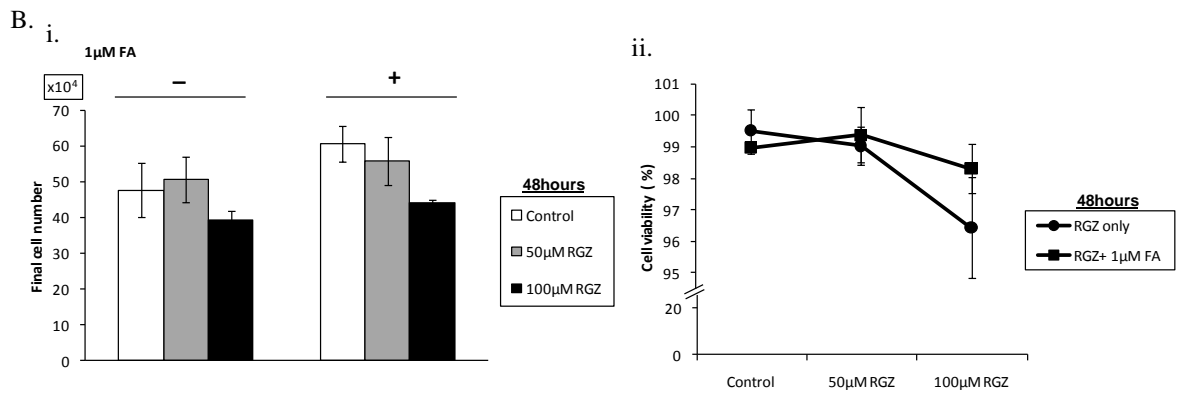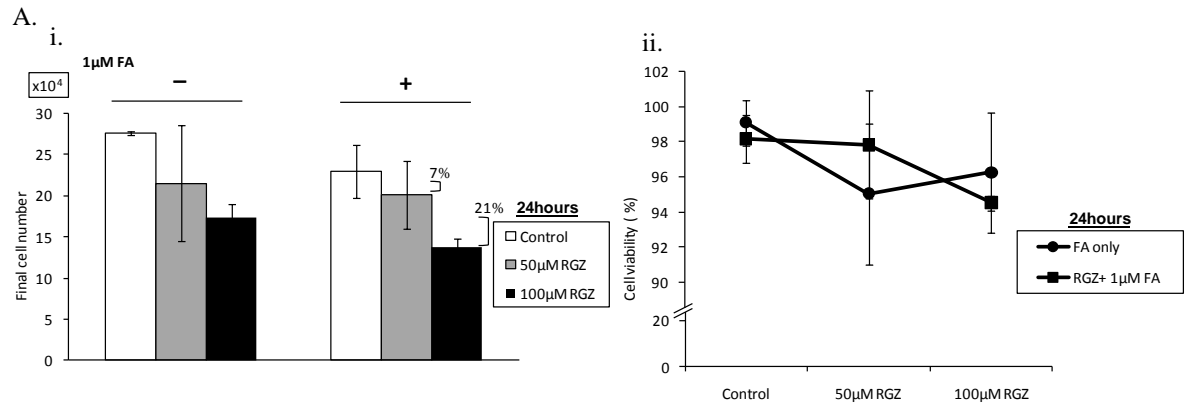
Figure 4.5. The effect of folic acid and rosiglitazone on *SK-N-AS* cells. A(i) B(i) C(i). *SK-N-AS* cells were plated out in 6-well dishes at 1×10^5 cells and treated with either a vehicle control (DMSO) or increasing concentrations of RGZ (50~100μM) with 1μM folic acid, and the effect on cell growth and cell viability was measured over 48 hours. Values represent the mean ± s.d of two independent experiments. Statistical analysis was carried out by Student's *t*-test to identify significant differences between samples.

4.2.5 The effects of cisplatin and folic acid on neuroblastoma cells

To determine whether the response of cells to cisplatin would be altered by the presence of folic acid, cisplatin (1µM and 5µM) was combined with folic acid and the effect on cell growth and viability assessed. However, the results show there is not a significant affect on either cell growth or cell viability after combining 1µM folic acid and 1µM or 5µM cisplatin over 24, 48 and 72 hours, respectively (figure 4.6ABC).

A.
　i.

1μM FA

24hours

Control
1μM CDDP
5μM CDDP

ii.

24hours

CDDP only
CDDP+ 1μM FA

B.
　i.

1μM FA

48hours

Control
1μM CDDP
5μM CDDP

ii.

48hours

CDDP only
CDDP+ 1μM FA

C.
　i.

1μM FA

72hours

Control
1μM CDDP
5μM CDDP

ii.

72hours

CDDP only
CDDP+ 1μM FA
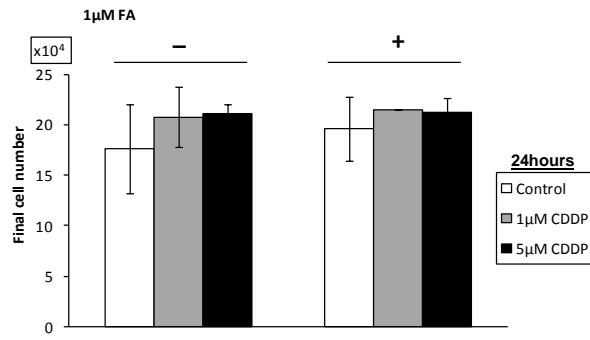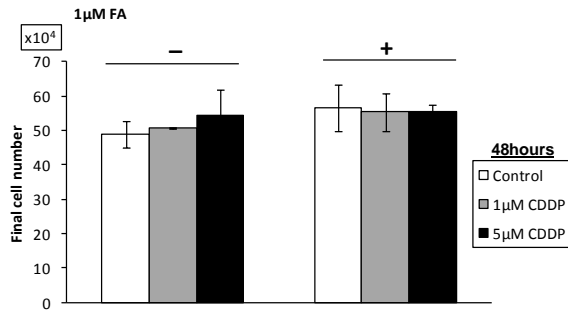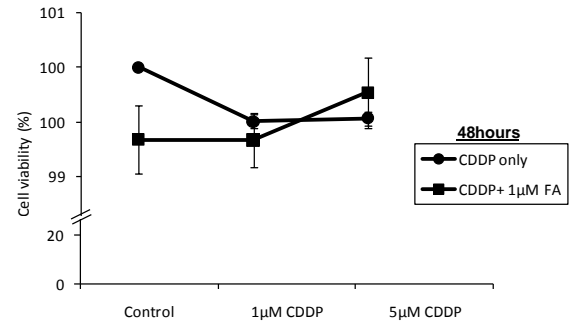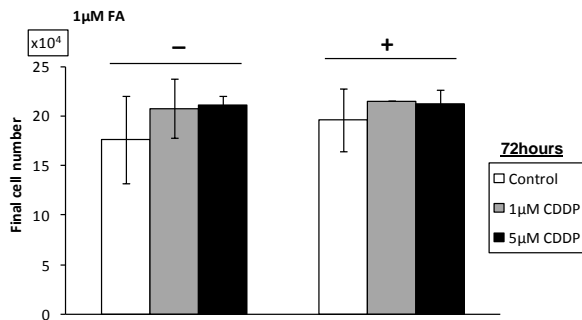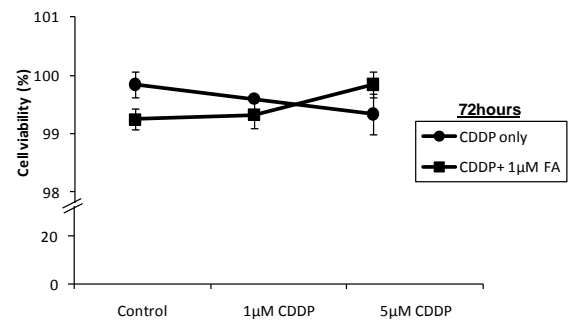
Figure 4.6. Graph showing the *SK-N-AS* cell numbers after treating with folic acid as a control, and folic acid and cisplatin in combination over 24, 48 and 72 hours. A(i) B(i) C(i). *SK-N-AS* cells were plated out in 6-well dishes at 1×10^5 cell and treated with either a vehicle control (DMSO) or increasing concentrations of cisplatin (1~5μM) with 1μM folic acid and the effects on cell growth and cell viability were measured over 24 hours. Trypan blue was used to distinguish between live and dead cells using a haemocytometer (n=2). The experiment was replicated twice independently. The values produced are the mean ± s.d. Cells were counted four times. **A(ii) B(ii) C(ii).** The graph shows the average percentage of *SK-N-AS* cell viability, as observed by trypan blue exclusion, of two independent experiments. Cells were counted four times at each concentration and averaged in each experiment. Error bars signify one standard deviation from the mean. Statistical analysis was carried out by student's *t*-test to identify significant differences between samples.

4.3 Discussion

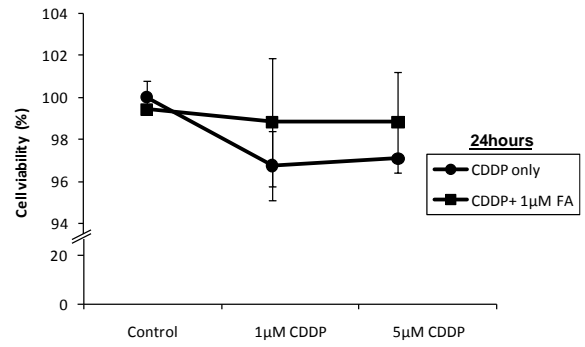There is now strong evidence that PPARγ ligands can inhibit neuroblastoma cell growth (Krieger-Hinck et al 2010, Valentiner et al 2005). In our group, Rodway and colleagues (2004) showed that PPARα agonist WY-14643 had no effect on the cell growth of the *IMR-32* neuroblastoma cell line, whereas 15dPGJ2, a PPARγ ligand, inhibited cell growth in the same neuroblastoma cells by inducing a G2/M arrest and autophagy. This was mediated only partly through a PPARγ dependent pathway. In the laboratory, Andrew Dawson (unpublished data) further showed that RGZ and ciglitazone also inhibited the growth of a number of neuroblastoma cell lines including *IMR-32*, *SK-N-AS* and *Kelly* cells, although the concentration required to induce 50% growth inhibition differed widely depending on the cell line, with 5μM RGZ required to induce 50% growth inhibition in *IMR-32* and *Kelly* cells and 100μM in *SK-N-AS* cells. Cellai and colleagues (2006) have also demonstrated that RGZ can significantly inhibit cell adhesion and invasiveness of *SK-N-AS* cells, but not in *SH-SY5Y* human neuroblastoma cells. They showed that 10μM and 20μM RGZ decreased cell adhesion over a 24-hour period of time in *SK-N-AS* cells and that this was through a PPARγ independent pathway. Similar effects have been reported in adrenal (Ferruzzi et al 2005) and pancreatic (Farrow et al 2003, Galli et al 2004) tumour cells where RGZ inhibits the matrix metalloproteinases (MMPs) activity in PPARγ in an independent manner.

In our experiments, we saw that 100μM RGZ significantly inhibited *SK-N-AS* cell growth over 72 hours, but did not affect cell viability (figure 3.1). We also combined RGZ with conventional chemotherapy drugs to determine if the potency of these agents could be improved and whether, by combining these agents, lower concentrations of the chemotherapy agents could be used, which have considerable side effects. Before combining RGZ with cisplatin and etoposide, we initially treated *SK-N-AS* cells with increasing concentrations of cisplatin and etoposide alone. We found that, as expected, both cisplatin and etoposide inhibited the growth of *SK-N-AS* cells. However, we did not detect any effect on cell viability of either cisplatin or etoposide, at any of the concentrations used. Both cisplatin and etoposide have been reported to induce cell death in neuroblastoma cells (Day et al 2009, Lindskog et al 2004) at concentrations similar to those used here. However, it may be that higher concentration of drug was required to see the cytotoxic effects of these drugs, so it would have been interesting to repeat the dose response curves for cisplatin and etoposide using higher concentrations of each drug, as well as using an alternative method of measuring

cell death. We did find, however, that combining both cisplatin at 1µM or etoposide at 0.5 and 1.5µM in the presence of RGZ increased the level of growth inhibition compared to cells treated with cisplatin or etoposide alone; although at the highest concentrations of cisplatin (5µM) and etoposide (2µM), no additive effect with RGZ was observed. It would be interesting to test the combination of PPARγ ligands with cisplatin and etoposide further and determine whether, *in vivo,* the sensitivity to cisplatin or etoposide had improved by using these agents in combination with RGZ. Combinations of fenretinide (4-HPR) and all-*trans*-retinoic acid with cisplatin have also been reported to enhance sensitivity to cisplatin in cancer cells (Formelli and Cleris 2000).

Loreto et al. (2007) have also shown that PPARβ/δ agonists oleic acid and GW0742 induce either cell cycle arrest in the G1 phase and increase neuronal differentiation in *SH-N-5YSY* cells which is a human neuroblastoma cell line, inducing p16$^{INK4\alpha}$ levels and decreasing cyclin D1 levels (Di Loreto et al 2007). Di Loreto and colleagues suggest that both PPARγ and PPARβ/δ ligands inhibit cell proliferation (Di Loreto et al 2007). It is possible to use dual agonists to affect tumour progression and recurrence (Di Loreto et al 2007).

We also examined the effect of folic acid on neuroblastoma cells and assessed whether folic acid in combination with either conventional chemotherapy agents or RGZ affected the response of neuroblastoma cells to these agents. Methylation is known to play a key role in cancer initiation and progression and it has been found that folic acid in the diet is associated with a decline in the risk of neuroblastoma (French et al 2003a). In addition, recent studies have implicated the enhanced expression of DNMT1 with resistance to chemotherapy drugs (Qiu et al 2002a). We found however those different concentrations of folic acid (1, 10 and 50µM) had no effect on either cell proliferation or cell viability. Neither did the combination of folic acid with either RGZ or cisplatin affect or alter the response of cells to these agents. However, to be sure that the addition of folic acid to the cells was affecting the methylation status or one-carbon metabolism within the cells, it would have been better to have confirmed that treatment with folic acid was increasing intracellular concentrations of folic acid, levels of DNA methylation and SAM/SAH ratios. In addition, it would be interesting to determine the effect of folate depletion or the effects of using anti-methylating agents such as the inhibitors of DNMT1 or 5-aza-2'-deoxycytidine (Baylin 2004).

In conclusion, even though chemotherapy drugs have been used a great deal with cancer cells, the levels of drug resistance and differences in cell types result in different responses to those

drugs. These results, however, suggest that using a combination of agents to both improve effect of cell proliferation and differentation and combat drug resistance may prove more promising.

Chapter 5

5.1 Introduction

More and more research has shown that DNA methylation is correlated with cancer and has an effect on the initiation and progression of cancer (Szyf et al 1984). In cancer cells, there is a dramatic change in DNA methylation status and in many cancer cells global DNA hypomethylation has been observed. DNA hypomethylation unmasks transponsons which cause chromosomal rearrangements and chromosomal instability. In addition to global hypomethylation in cancer cells, there is also gene-specific hypermethylation of tumour suppressor genes, which is one mechanism for loss of gene function. Such aberrant DNA methylation is strongly associated with aggressive cancers and poor outcome for cancer patients. DNA methylation patterns have also been shown to change during the process of aging, which may be a key contributor. For instance, it has been found that in somatic cells, ageing facilitates an increase in gene promoter methylation. Therefore, the methylation changes in ageing may be the first steps in early carcinogenesis (Gilbert 2009).

Alterations in the expression of the enzymes that bring about DNA methylation have also been observed in cancer cells. Increased expression of the maintenance DNA methyl transferase I (DNMT1) has been shown to be strongly correlated with poor tumour differentiation and frequent DNA hypermethylation in multiple CpG islands in malignant cancers (Ehrlich 2002). DNMT1 expression is known to be regulated by a number of factors including activator protein 1 (AP-1), E2F1 and Sp1/Sp3 (Yoder et al 1996). Interestingly we found a putative PPRE sequence within the promoter of rat DNMT1 (unpublished data from Alenad). The potential ability of PPARγ to regulate DNMT1 expression is very interesting as this might have implications for cancer progression and also contribute to the anti cancer effects of PPARγ and its ligands. Therefore, the aim of this chapter was to investigate the regulation of DNMT1 expression by PPARγ.

5.2 Results

5.2.1 Putative PPARγ binding sites in the rat and human DNMT1 promoter regions

To determine whether the human DNMT1 promoter region also contained a potential PPRE sequence, the rat and human promoter regions of DNMT1 were aligned and the sequence analysed using MatInspector (http://www.genomatix.de/en/index.html). Both the rat and human DNMT1 promoter regions were found to contain potential PPRE sequences (figure 5.1).

```
                        Forward
rat_      G--------TCCTAGAAT------TCACTGTATAGACTTGGCTAGCCTCAAATAGTGATC 1291
human_    GGAATGTAGTGGTACAATCATGGCTCACTGCA-ACCTCTGCCTCTCCGGTTCAAGTGATC 1354
          *        *  ** ***     ****** * *   ** ** **      *******

rat_      TGTCTGCCTCTGCCTCAGTGCAAG---GGATTAAAGGCATGCGCCACTGCTGC---CTGG 1345
human_    TTCCTGCCTCAACCTCTGGAGTAGTTTGGACTATGGGCACATGCCACAACGACTAGCTAA 1414
          *  ******* **** *   **   *** ** ****   ***** * *    **

rat_      GTTTTTTTTTTTTTTTTTTTTTTTTGGTTCTTTTTTTTGGAGCTGGGGACCGAACCCAG 1405
human_    TTTTTGTTTTTCTTTTTTTCTTTCTTTCTTTCTTTTTTTTTTTTTTTTTGAGATGCAG 1474
           **** ***** ******* *** **  **  *** ***     *       *  ***

rat_      GGCCT-TGCGCTTCCTAGGTAAGCGCTCTACCACTGAGCTAAA-----TCCCCAACCCTT 1459
human_    TTTCTCTATGTTACCTAGGCTGGTCTAAAACTCCTGGGCTCAAGCGATCCTCCCACCCTG 1534
           ** *  * * * ******   *     **  *** *** **   * ** *****

rat_      TTTTTCTT---TTTTAAAAAGACTGTTTTTAGACCAGGCTGAACACACAGATCCTCCCAC 1516
human_    GCCTCCCAAAGTGCTGGGATGACAGGCGTGAG-CCACGTGGTGCTTAAAAAGGCAACAA 1593
             * *    *   *   * *** *   * ** *** ***   *  * * *      **

                                               #PPARγ binding site
rat_      TTCTGCCCCCAGAGTGCTGGGATTAAAAA---CATGGCGCCACAGACTCCACCA---CCT 1570
human_    AAAACCCCCCACA-CACTGGGTATAGAAGTGGCATGGGCCTCTATACACTGTGAGATTCT 1652
           ****** *  *****  ** **      *****  *   * ** *    *    **

rat_      CTGCCCGACTCAAAAGATCACTTTTTTTAAAAAAAATTGT---GTTTGTGCATGTGAGT- 1626
human_    TGGTACTAGCTACAAATTCTGTGTATACTCAAGATTTTCTAGAGTAGGTGCAATTACCCC 1712
            *  *   * ***  ** ** * *** **   ** *** *  ** ***** *

                                #PPARγ binding site
rat_      GCGGTGCCCATAGAGAC-CAGAAG--AGGGCGTAG-GATCCCCTGGAAGTGGAACTACAA 1682
human_    GTTTTACAGATGAGGACACAGAGGCTGAGCCGTAGTGACCCACCTAAGGTCGTATAGCCA 1772
          *   *   **   ***  *** *     * ***** ** ** *   * ** *    * *

rat_      G-----GGCTTGGAGT--GCCTGGATGTGGGTGCCCTGTGAAAGGGGAGTACTACCTGCT 1735
human_    GCAAATAGATGGAGGTTGGATTGGAACTGAGGACTTTACTCAAGGG--CTCTCACAAACC 1830
          *      * * *  **  *    * *   *  *     *****    *   **   *

rat_      CTCAAGGGCT-------GATCCACCTCT-TCAGGC---AAGGGGGAGGTGAGTG---GCT 1781
human_    CTTGGGGGCTTCTCGCTGCTTTATCCCCATCACACCTGAAAGAATGAATGAATGAATGCC 1890
          **    *****       * *  * * *  ***   *   ** *    *** **    **

rat_      CCAGTCACAGTGC------------------------GGACGAGCCCACTCCAGC-CA 1814
human_    TCGGGCACCGTGCCCACCTCCCAGCAAACCGTGGGAGCTTGGACGAGCCCACTGCTCCGCG 1950
           * * *** ****                        ************ *   * *

rat_      GGAGGTGTGGGTGCCTCCGTCCTGCGCATGCGCA------------------CTCCGTTC 1856
human_    TGGGGGGGGTGTGTGCCCGCCTTGCGCATGCGTGTTCCCTGGGCATGGCCGGCTCCGTTC 2010
          * ** * * ***   *** * **********   *           ********

rat_      ---------GGGCATAGCATTGTCTTCCCCCACT-----------CTCTTGCCCTGTG-- 1894
human_    CATCCTTCTGCACAGGGTATCGCCTCTCTCCGTTTGGTACATCCCCTCCTCCCCCACGCC 2070
                   *  **  * ** * **  * **  *         *** * ***    *

rat_      ----------TGGTACATGCTGCTTCCGCTTGCGCCGCCCCCTCCCAATTGGTTTCCGCG 1944
human_    CGGACTGGGGTGGTAGACGCCGCCTCCGCT--CATCGCCCC-TCCCCATCGGTTTCCGCG 2127
                    ***** * ** ** ******   *  ****** ** ** ** **********

                                                              Reverse
rat_      CGCGCGAAAAAGCCGGGGT-CTCGTTCAGA-GCTGTCCTGTCGTCTGCAACCTGCAAGAT 2002
human_    CG-----AAAAGCCGGGGCGCCTGCGCTGCCGCCGCCGCGTCTGCTGAAGCCTCCGAGAT 2182
          **     ***********  *  *   * *  * * *  *** ***  *** * *** ****

rat_      GCCAGCACGAACAGCTCCAGCCCGAGTGCCTGCACTTGCCTCCCCGGCAGGCTCGCTCCC 2062
human_    GCCGGCGCGTACCGCCCCAGCCCGGGTGCCCACACTGGCCGTCCCGGCCATCTC------ 2236
          *** ** ** ** ** ******** ***** * *** *** ****** **  ***

rat_      CG 2064
human_    --
```

Figure 5.1. Alignment of rat and human DNMT1 promoter regions. The nucleotide bases in the DNMT1 sequence of two species. The alignment sequence includes the PPARγ putative binding site in the rat DNMT1 promoter region (pink) and the human DNMT1 promoter region (yellow). The primers used to clone the rat Dnmt1 promoter forward, and reverse are shown in blue.

5.2.2 Endogenous DNMT1 mRNA expression is negatively regulated by rosiglitazone

To determine whether PPARγ may regulate endogenous DNMT1 expression, *SK-N-AS* cells were treated with increasing concentrations of the PPARγ ligand, RGZ for 24 and 72 hours. After 24 hours, there was a decrease in DNMT1 mRNA expression at 5, 50 and 100µM RGZ. After 72 hours, although there was an increase in expression at 5µM, however, at 50 and 100µM RGZ, there was a decrease in DNMT1 expression. This suggests that the PPARγ ligand RGZ induces the down regulation of DNMT1 expression (figure 5.2).
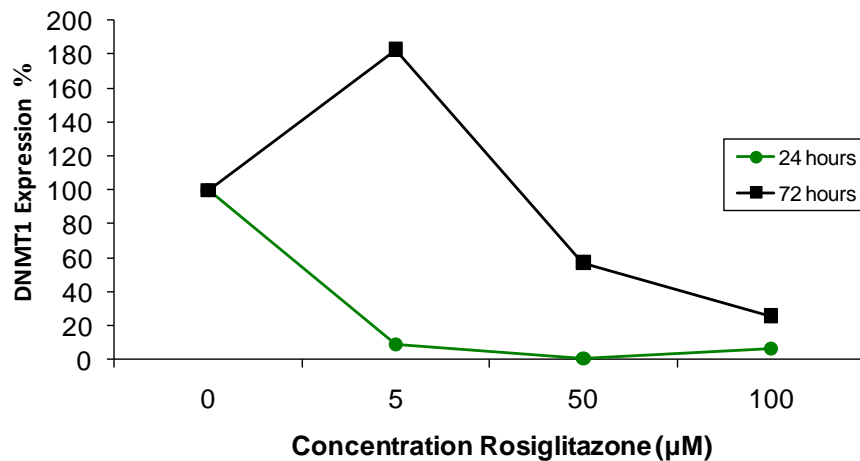
Figure 5.2. The expression of DNA methyltransferase 1 with increasing concentration of rosiglitazone over 24 and 72 hours. The expression of DNMT1 was detected in *SK-N-AS* cells by real-time PCR (n=1). There was an overall decrease in DNMT1 expression with increasing RGZ concentration at both 24 and 72 hours.

5.2.3 PPARγ represses DNMT1 promoter activity at 24 hours and 48 hours

To begin to determine whether PPARγ directly regulates DNMT1 expression, a construct (DNMT1-Luc) containing the promoter region of rat DNMT1 which had been cloned upstream of the luciferase reporter gene in the vector pGL3 basic (Kind gift of Amal Alenad) was transfected into *SK-N-AS* cells with increasing concentrations of an expression vector containing a full length cDNA clone of PPARγ. The rat DNMT1 promoter region included the PPARγ putative binding site, and encompasses the region from -751bp to +15bp (figure 5.3A).

The experiment is designed for trasnfection with the final volume of 300ng plasmid. The amount of PPARγ and PPARγ DN has transfected either 100ng or 200ng. However, the amount of DNMT1 has remained constant at 100ng for the entire experiment. The results showed that the addition of increasing amounts of the PPARγ expression vector (100 and 200ng) into cells transfected with the DNMT1-Luc construct led to a decrease in luciferase activity, suggesting that PPARγ can repress DNMT1 promoter activity (figure 5.3B). Moreover, as we can see in the column of number 5 of figure 5.3B, even though transfection of the DNMT1-Luc construct with increasing amounts of the PPARγ dominant negative expression vector (200ng) led to an small increase in DNMT1 promoter activity, consistent with previous findings, that wild-type PPARγ inhibits DNMT1 promoter activity (figure 5.3B).

A.

Rat DNMT1 promoter region

```
>8 dna:chromosome chromosome:RGSC3.4:8:19926966:19974256:-1

                                         Forward
AGGGTTTCTCTGTATAGCCCTGGCTGTCCTAGAATTCACTGTATAGACTTGGCTAGCCTC
AAATAGTGATCTGTCTGCCTCTGCCTCAGTGCAAGGGATTAAAGGCATGCGCCACTGCTG
CCTGGGTTTTTTTTTTTTTTTTTTTTTTTTGGTTCTTTTTTTTTGGAGCTGGGGACCGAA
CCCAGGGCCTTGCGCTTCCTAGGTAAGCGCTCTACCACTGAGCTAAATCCCCAACCCTTT
TTTTCTTTTTTAAAAAGACTGTTTTTAGACCAGGCTGAACACACAGATCCTCCCACTTCT
                                         #PPARγ binding site
GCCCCCAGAGTGCTGGGATTAAAAACATGGCGCCACAGACTCCACCACCTCTGCCCGACT
CAAAAGATCACTTTTTTTAAAAAAAATTGTGTTTGTGCATGTGAGTGCGGTGCCCATAGA
GACCAGAAGAGGGCGTAGGATCCCCTGGAAGTGGAACTACAAGGGCTTGGAGTGCCTGGA
TGTGGGTGCCCTGTGAAAGGGGAGTACTACCTGCTCTCAAGGGCTGATCCACCTCTTCAG
GCAAGGGGGAGGTGAGTGGCTCCAGTCACAGTGCGGACGAGCCCACTCCAGCCAGGAGGT
GTGGGTGCCTCCGTCCTGCGCATGCGCACTCCGTTCGGGCATAGCATTGTCTTCCCCCAC
TCTCTTGCCCTGTGTGGTACATGCTGCTTCCGCTTGCGCCCCCCCTCCCAATTGGTTTC
                                         +1(Transcription start site)
CGCGCGCGCGAAAAAGCCGGGGTCTCGTTCAGAGCTGTCCTGTCGTCTGCAACCTGCAAG
Translation start site
ATGCCAGCACGAACAGCTGCAGCCCGAGTGCCTGCACTTGCCTCCCCGGCAGGCTCGCTC
        Reverse
```

B.
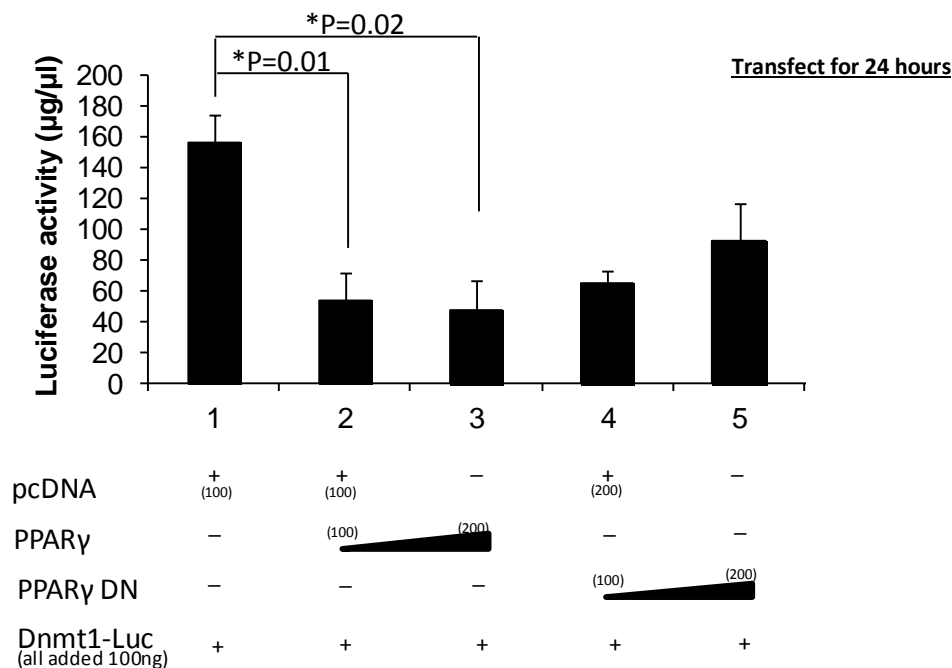
Figure 5.3 PPARγ negatively regulates rat DNMT1 promoter activity at 24 hours. A. Rat DNMT1 promoter region. The primers (forward and reverse (blue)) and PPARγ binding site (pink) are shown. The transcription start site starts from guanine (G) (red). The ATG is shown in bold. **B.** *SK-N-AS* cells were plated out in 24-well dishes at 2.5×10^4 cells per well and transfected with either the empty pcDNA 3.1 expression vector, PPARγ1 expression vector or the PPARγ dominant negative expression plasmid together with the rat DNMT1 promoter reporter plasmid. Cells were harvested after 24 hours and luciferase activity of the rat DNMT1 promoter luciferase reporter in the cells (normalising its activity of concentration protein 1μg/μl) measured. This experiment represents three independent experiments ± s.d. Statistics were calculated using a Student's *t*-test.

5.2.4 Both natural and synthetic PPARγ ligands repress rat DNMT1 promoter activity in *SK-N-AS* cells at 48 hours

Having shown that transfection of a PPARγ expression vector leads to the repression of rat DNMT1 promoter activity at 24 hours, we then examined whether addition of PPARγ ligands would also lead to the repression of DNMT1 promoter activity at 48 hours. To investigate this, cells were transfected with an increasing amount of PPARγ expression vector together with DNMT1 reporter construct DNMT1-Luc, in the presence or absence of one or more of the PPARγ ligand, RGZ or 15dPGJ2. We found that PPARγ at 200μg repressed DNMT1 promoter activity significantly. This repression was further enhanced by the treatment of transfected cells with either 15dPGJ2 (P=0.01) or RGZ (P=0.003).
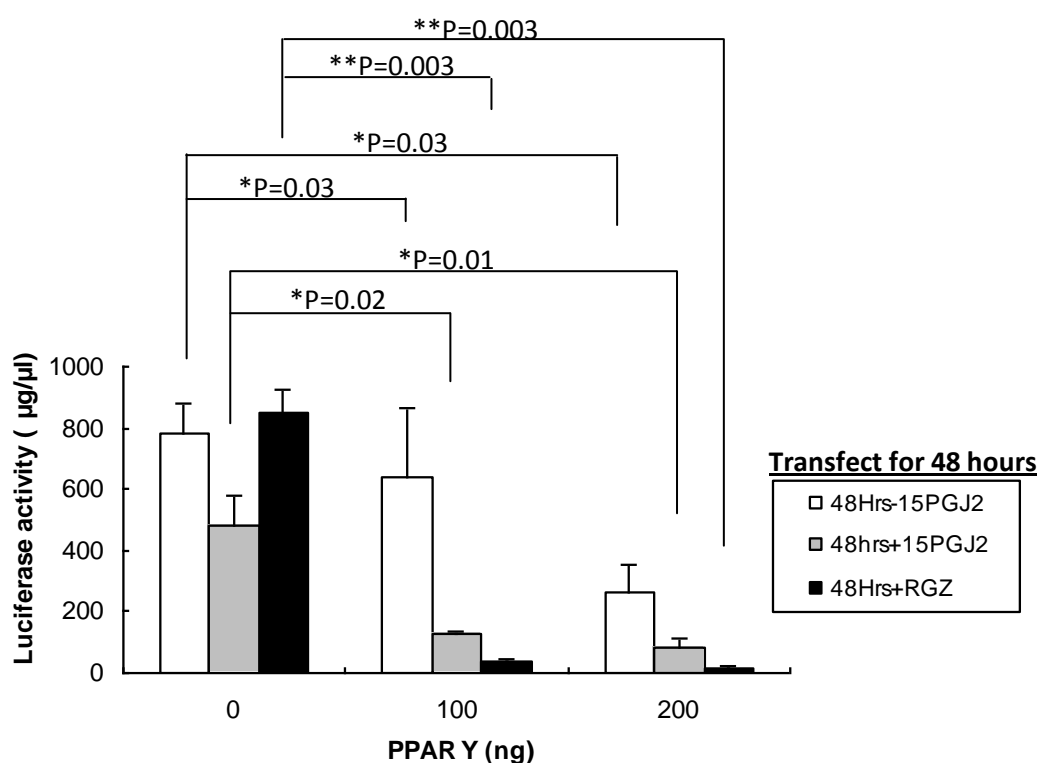
Figure 5.4. The effect of 15dPGJ2 and rosiglitazone on DNMT1 promoter activity at 48 hours. *SK-N-AS* cells were plated out at 2.5×10^4 cell density and transfected with either an empty expression vector or PPARγ expression plasmid together with the rat DNMT1-Luc reporter plasmid. Then after 48 hours, the cells were treated for 24 hours with 10μM 15dPGJ2 or 50μM RGZ and luciferase activity measured by TD-20/20 luminometer and normalised by protein concentration (1μg/μl). This represents three independent experiments ± s.d. Statistics were calculated using a Student's *t*-test and showed significant difference in the level of luciferase activity of the DNMT1 promoter luciferase activity (*P<0.05 and **P<0.01).

5.2.5 Does deletion of the putative PPRE abolish repression by PPARγ?

To determine whether the putative PPRE located at -336 to -359 base pair mediated the repression by PPAR on rat DNMT1 promoter activity, a shorter DNMT1 promoter construct was made, but lacking the PPRE site. The rat DNMT1-Luc reporter plasmid was digested from restriction enzymes BamHI and HindIII to create a DNMT1 promoter fragment of 356 base pair and religated into pGL3basic. Unfortunately, because of time constraints, we were unable to test whether this construct responded to PPARγ (figure 5.5).

A.

```
                              Forward
AGGGTTTCTCTGTATAGCCCTGGCTGTCCTAGAATTCACTGTATAGACTTGGCTAGCCTC
AAATAGTGATCTGTCTGCCTCTGCCTCAGTGCAAGGGATTAAAGGCATGCGCCACTGCTG
CCTGGGTTTTTTTTTTTTTTTTTTTTTTTTGGTTCTTTTTTTTTGGAGCTGGGGACCGAA
CCCAGGGCCTTGCGCTTCCTAGGTAAGCGCTCTACCACTGAGCTAAATCCCCAACCCTTT
TTTTCTTTTTTAAAAAGACTGTTTTTAGACCAGGCTGAACACACAGATCCTCCCACTTCT
                                      #PPARγ binding site
GCCCCCAGAGTGCTGGGATTAAAAACATGGCGCCACAGACTCCACCACCTCTGCCCGACT
CAAAAGATCACTTTTTTTAAAAAAAAATTGTGTTTGTGCATGTGAGTGCGGTGCCCATAGA
```

BamHI

```
GACCAGAAGAGGGCGTAGGA [ TCCCCTGGAAGTGGAACTACAAGGGCTTGGAGTGCCTGGA
TGTGGGTGCCCTGTGAAAGGGGAGTACTACCTGCTCTCAAGGGCTGATCCACCTCTTCAG
GCAAGGGGGAGGTGAGTGGCTCCAGTCACAGTGCGGACGAGCCCACTCCAGCCAGGAGGT
GTGGGTGCCTCCGTCCTGCGCATGCGCACTCCGTTCGGGCATAGCATTGTCTTCCCCCAC
TCTCTTGCCCTGTGTGGTACATGCTGCTTCCGCTTGCGCC CCCCCTCCCAATTGGTTTC
                              +1(Transcription start site)
CGCGCGCGCGAAAAAGCCGGGGTCTCGTTCAGAGCTGTCCTGTCGTCTGCAACCTGCAAG
+83 Translation start site
ATGCCAGCACGAACAGCTC ] HindIII
Reverse
```

356bp

(Cloning into pGL3 vector)

B.
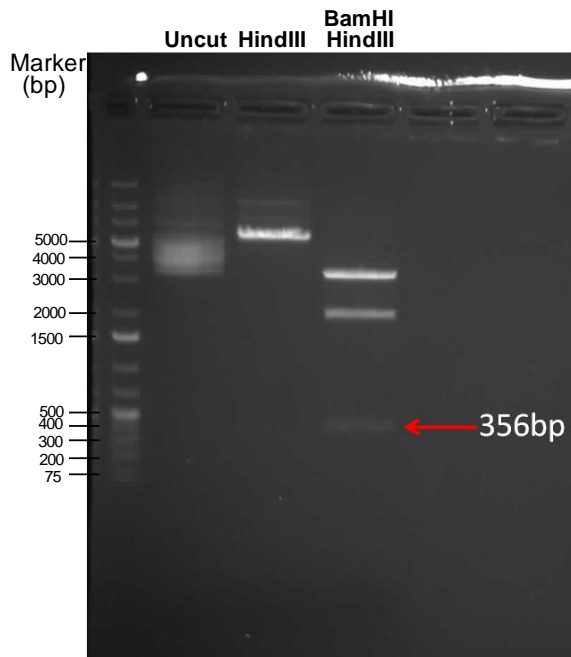
Figure 5.5. Rat DNMT1-Luc reporter plasmid digested with restriction enzymes. A. The sequence of the rat DNMT1 promoter region indicating the location of the PPARγ binding site and restriction enzymes sites used to create a truncated promoter fragment. **B.** Rat DNMT1-Luc reporter plasmid digested with Bam HI with Hind III (lane 3). DNA product is 356 base pairs. Cutting plasmid DNA was extracted from the agarose gel ready to clone the insert to the pGL3 luciferase reporter vector.

5.3 Discussion

There is growing evidence that aberrant methylation plays a key role in cancer initiation and progression (Plass 2002). Hypermethylation of the gene promoter leads to gene inactivation of the corresponding genes, because methylated cytosines are recognised and bound by methyl binding proteins such as MeCP2, which in turns recruits HDACs (Taby and Issa 2010). Methylated-associated gene silencing in various genes has been demonstrated, including tumour suppressor genes (p14^{ARF} and p16$^{INK4\alpha}$). Gene hypermethylation can be a target for therapeutic invention by hypomethylating agents. In neuroblastoma, drug resistance to conventional chemotherapy drugs has also been linked to altered DNA methylation. It has been shown that the expression of DNMT1 is correlated with drug resistance (Qiu et al 2002b). Qiu's (2002) group has reported that in drug-resistant cells, the activity of DNMT1 enzyme has increased 33% compared to the non-drug-resistant cells. Moreover, the protein expression of DNMT1 is significantly increased in drug-resistant cells. However, this may mean that the loss of the function of cell growth control or overexpression of DNMT1 may be silencing the tumour suppressor gene because of gene methylation (Qiu et al 2002b). Therefore, it is important to understand how DNMT1 can be regulated.

In this chapter, we show for the first time that PPARγ can negatively regulate rat DNMT1 promoter activity (figure 5.3). There is no concentration dependent repression of DNMT1 in the presence of increasing concentration of PPARγ as DNMT1 expression was decreased to a similar extent with both 100ng and 200ng PPARγ at 24 hours. To see a concentration dependent decrease in DNMT1 is observed lower concentrations of PPARγ may be needed. Moreover, PPARγ ligands (15dPGJ2 and RGZ) repress DNMT1 promoter activity (figure 5.4). This suggests that PPARγ ligands may, in addition to their anti-growth properties, also affect DNA methylation levels in cancer cells. The average luciferase activity in the experiments where cells were treated for 24hrs as opposed to 48 hours was much higher, which could be due to differences in the treatment period. A decrease in DNMT1 expression in response to 200µg of PPARγ was again observed (figure 5.4). It also suggests that combining PPARγ ligands with conventional chemotherapy agents might be beneficial in terms of reducing drug resistance. For those results, combining epigenetic treatment (5-aza-2'-deoxycytidine) and TZDs (rosiglitazone) might have a synergistic effect on cancer because overexpression DNMT1 has been implicated in drug resistance (Qiu et al 2002b). Therefore,

it may prove possible to combine epigenetic treatments, such as 5-aza-2'-deoxycytidine and TZDs, for a synergistic effect on cancer in the future.

In future studies, our group will focus on how PPARγ inhibits DNMT1 in specific regions; therefore, firstly, we were going to prepare the rat DNMT1 promoter region without PPARγ putative binding site and clone it to the pGL3 reporter plasmid to demonstrate whether the PPARγ putative binding region can affect the transcription of rat DNMT1 in neuroblastoma *SK-N-AS* cells (figure 5.5). Secondly, in order to understand whether PPARγ ligand directly or indirectly inhibits DNMT1 mRNA expression, previous results have shown that RGZ may increase DNMT1 mRNA expression; therefore, we will use cycloheximide which inhibits protein synthesis in cytoplasm.

Chapter 6

Final Conclusions and Discussion

The aim of this study was to investigate the role of PPARγ in neuroblastoma *SK-N-AS* cells to establish whether PPARγ acts as a tumour suppressor gene in neuroblastoma cells. PPARγ is present in neuroblastoma cell lines (Servidei et al 2004) and also in primary neuroblastoma cell cultures (Grommes et al 2004b). In order to understand the action of PPARs on neuroblastoma cells, most studies have investigated the influence of their natural or synthetic ligands on cell proliferation, death and differentiation. It has been shown that the natural PPARγ agonist (15dPGJ2) inhibits cellular growth, decreases cellular viability and induces apoptosis in human neuroblastoma cells *in vitro* (Han et al 2001a, Han et al 2001c, Rodway et al 2004a, Servidei et al 2004). In addition, it has been shown that treatment of neuroblastoma cells with PPARγ ligands leads to the induction of the cyclin-dependent kinase inhibitor (CDKI), involving p21^{CIP}, p27 and p16$^{INK4\alpha}$ (Chang and Szabo 2000, Han et al 2004, Lapillonne et al 2003, Wang et al 2006b, Yang et al 2005, Yoshizawa et al 2002, Yoshizumi et al 2004). However, several papers have demonstrated that the effect is based on the PPARγ independent pathway (Giri et al 2004).

High levels of PPARγ have been reported to be associated with low stage neuroblastoma with a well differentiated phenotype, while low levels of PPARγ have been associated with high stage poorly differentiated neuroblastoma. We have shown that increasing the level of PPARγ expression and activity in neuroblastoma cells leads to a decrease in cell growth, although no effect on cell viability or differentiation was seen. It would have been interesting to have examined the expression of proteins associated with a mature differentiated phenotype, or to have stably transfected cells with the PPARγ expression vector, so that cells could be left for a longer period of time before examining for signs of morphological differentiation.

We did however see an increase in the expression of p14^{ARF} in cells overexpressing PPARγ. Moreover, analysis of the promoter region of p14^{ARF} found a PPRE sequence, increasing the possibility that PPARγ may directly regulate p14^{ARF} expression. Interestingly bioinformatic analysis of the promoter regions of p21^{CIP} and p16$^{INK4\alpha}$ also revealed the presence of putative PPREs, suggesting that these cell cycle inhibitors may also be directly regulated by PPARγ

and their induction may play a role in the decrease in cell growth induced by higher levels of PPARγ and in the inhibition of cell proliferation induced by PPARγ ligands.

To determine whether combining PPARγ ligands with conventional chemotherapy agents may improve potency and allow a lower concentration of the chemotherapy agent to be used, we treated cells with a combination of RGZ and either cisplatin or etoposide. We found that the combination of RGZ with moderate concentrations of either cisplatin or etoposide did enhance the growth inhibitory effects of the chemotherapy agents; although at higher concentrations of cisplatin and etoposide, no additive effect was seen. In our experiments, cisplatin and etoposide at the concentrations used had very little effect on cell viability either alone or in combination with RGZ. It may be that higher concentrations of these agents are required to induce cell death. We used a range of concentrations which were shown in the literature to induce growth inhibition and cell death in other cancer cell lines, such as small cell lung cancer (Jordan and Carmo-Fonseca 2000, Kurup and Hanna 2004, Zamble and Lippard 1995); however, it has been reported that some cells, such as *SH-SY5Y cells,* are more resistance to these agents because endogenous expression of nerve growth factor (TRK-B) and its ligand-brain-derived neurotrophic factor (BDNF) (Ho et al 2002). With a combination of RGZ and etoposide, however, a decrease in cell viability was observed with up to 50% decrease in cell viability observed with 2μM etoposide and 100μM RGZ.

As there is increasing evidence that methylation plays a key role in cancer initiation and progression, we also examined the effect of folic acid supplementation on the response of cells to either RGZ or the conventional chemotherapy agents, cisplatin and etoposide. However, we found that folic acid had little effect alone or in combination with either RGZ, or cisplatin or etoposide. Further experiments are needed to examine the impact methylation has on these agents either by carrying out a dose-response experiment over a larger concentration range in folate-depleted medium or by using anti methylating agents, such as 5-aza-2'-deoxycytidine, to affect levels of methylation within the cells.

We did however find that PPARγ negatively regulates DNMT1 expression. DNA methyltransferase 1 (DNMT1) maintains DNA methylation patterns during replication and is overexpressed in many human cancers (Luczak and Jagodzinski 2006). Increased DNMT1 (mRNA and protein) in various cancer types is correlated with hypermethylation in the CpG island on the cyclin-dependent kinase inhibitors promoter regions, such as p16[INK4α], mismatch repair gene (MLH1), retinoblastoma 1 (Rb1), TIMP metallopeptidase inhibitor 3

(TIMP3) and other tumour suppressor genes (Sato et al 2002). We have found that PPARγ can negatively regulate DNMT1 expression. We have shown that PPARγ ligands down-regulate endogenous DNMT1 expression and that either overexpression of PPARγ or addition of PPARγ ligands represses DNMT1 promoter activity. It would have been interesting to determine whether PPARγ directly affects DNMT1 expression by i) mutation and/or deletion the putative PPREs within the DNMT1 promoter and analysing the effect of PPARγ on the mutated construct, and by ii) treating cells with both a PPAR ligand and cycloheximide to block protein synthesis to determine whether a decrease in DNMT1 expression is still observed.

The ability of PPARγ to potentially regulate DNMT1 is very important and may contribute to the anti-cancer effects of PPARγ and its ligands. DNMT1 has been implicated not only in the progression of cancer but also in the development of drug resistance to conventional chemotherapy agents. Treatment of PPARγ ligands together with conventional chemotherapy agents might therefore lessen the development of drug resistance. This is potentially a very important avenue to follow up. The finding that PPARγ can regulate DNMT1 will also help us to understand the role of PPARγ in the treatment of neuroblastoma and understand the link between methylation and PPARγ.

List of References

Abdelrahman M, Sivarajah A, Thiemermann C (2005). Beneficial effects of PPAR-gamma ligands in ischemia-reperfusion injury, inflammation and shock. *Cardiovasc Res* **65:** 772-781.

Abedin SA, Thorne JL, Battaglia S, Maguire O, Hornung LB, Doherty AP *et al* (2009). Elevated NCOR1 disrupts a network of dietary-sensing nuclear receptors in bladder cancer cells. *Carcinogenesis* **30:** 449-456.

Adamson PC, Matthay KK, O'Brien M, Reaman GH, Sato JK, Balis FM (2007). A phase 2 trial of all-trans-retinoic acid in combination with interferon-alpha2a in children with recurrent neuroblastoma or Wilms tumor: A Pediatric Oncology Branch, NCI and Children's Oncology Group Study. *Pediatr Blood Cancer* **49:** 661-665.

Akiyama TE, Meinke PT, Berger JP (2005). PPAR ligands: potential therapies for metabolic syndrome. *Curr Diab Rep* **5:** 45-52.

Alaminos M, Davalos V, Cheung NK, Gerald WL, Esteller M (2004). Clustering of gene hypermethylation associated with clinical risk groups in neuroblastoma. *J Natl Cancer Inst* **96:** 1208-1219.

Altiok S, Xu M, Spiegelman BM (1997). PPARgamma induces cell cycle withdrawal: inhibition of E2F/DP DNA-binding activity via down-regulation of PP2A. *Genes Dev* **11:** 1987-1998.

Ambros PF, Ambros IM, Strehl S, Bauer S, Luegmayr A, Kovar H *et al* (1995). Regression and progression in neuroblastoma. Does genetics predict tumour behaviour? *Eur J Cancer* **31A:** 510-515.

Auboeuf D, Rieusset J, Fajas L, Vallier P, Frering V, Riou JP *et al* (1997). Tissue distribution and quantification of the expression of mRNAs of peroxisome proliferator-activated receptors and liver X receptor-alpha in humans: no alteration in adipose tissue of obese and NIDDM patients. *Diabetes* **46:** 1319-1327.

Barak Y, Nelson MC, Ong ES, Jones YZ, Ruiz-Lozano P, Chien KR *et al* (1999). PPAR gamma is required for placental, cardiac, and adipose tissue development. *Mol Cell* **4:** 585-595.

Basu-Modak S, Braissant O, Escher P, Desvergne B, Honegger P, Wahli W (1999). Peroxisome proliferator-activated receptor beta regulates acyl-CoA synthetase 2 in reaggregated rat brain cell cultures. *J Biol Chem* **274:** 35881-35888.

Baylin SB (2004). Reversal of gene silencing as a therapeutic target for cancer--roles for DNA methylation and its interdigitation with chromatin. *Novartis Found Symp* **259:** 226-233; discussion 234-227, 285-228.

Bender CM, Pao MM, Jones PA (1998). Inhibition of DNA methylation by 5-aza-2'-deoxycytidine suppresses the growth of human tumor cell lines. *Cancer Res* **58:** 95-101.

Berthold F, Hero B, Kremens B, Handgretinger R, Henze G, Schilling FH *et al* (2003). Long-term results and risk profiles of patients in five consecutive trials (1979-1997) with stage 4 neuroblastoma over 1 year of age. *Cancer Lett* **197:** 11-17.

Biedler JL, Spengler BA (1976). A novel chromosome abnormality in human neuroblastoma and antifolate-resistant Chinese hamster cell lives in culture. *J Natl Cancer Inst* **57:** 683-695.

Bigner SH, Mark J, Bigner DD (1990). Cytogenetics of human brain tumors. *Cancer Genet Cytogenet* **47:** 141-154.

Bigner SH, Vogelstein B (1990). Cytogenetics and molecular genetics of malignant gliomas and medulloblastoma. *Brain Pathol* **1:** 12-18.

Bird A (2002). DNA methylation patterns and epigenetic memory. *Genes Dev* **16:** 6-21.

Bolden JE, Peart MJ, Johnstone RW (2006). Anticancer activities of histone deacetylase inhibitors. *Nat Rev Drug Discov* **5:** 769-784.

Brodeur GM, Green AA, Hayes FA, Williams KJ, Williams DL, Tsiatis AA (1981). Cytogenetic features of human neuroblastomas and cell lines. *Cancer Res* **41:** 4678-4686.

Brodeur GM, Seeger RC, Schwab M, Varmus HE, Bishop JM (1984). Amplification of N-myc in untreated human neuroblastomas correlates with advanced disease stage. *Science* **224:** 1121-1124.

Brodeur GM (2003). Neuroblastoma: biological insights into a clinical enigma. *Nat Rev Cancer* **3:** 203-216.

Burdge GC, Rodway H, Kohler JA, Lillycrop KA (2000). Effect of fatty acid supplementation on growth and differentiation of human IMR-32 neuroblastoma cells in vitro. *J Cell Biochem* **80:** 266-273.

Burdick AD, Kim DJ, Peraza MA, Gonzalez FJ, Peters JM (2006). The role of peroxisome proliferator-activated receptor-beta/delta in epithelial cell growth and differentiation. *Cell Signal* **18:** 9-20.

Burstein HJ, Demetri GD, Mueller E, Sarraf P, Spiegelman BM, Winer EP (2003). Use of the peroxisome proliferator-activated receptor (PPAR) gamma ligand troglitazone as treatment for refractory breast cancer: a phase II study. *Breast Cancer Res Treat* **79:** 391-397.

Cerbone A, Toaldo C, Laurora S, Briatore F, Pizzimenti S, Dianzani MU *et al* (2007). 4-Hydroxynonenal and PPARgamma ligands affect proliferation, differentiation, and apoptosis in colon cancer cells. *Free Radic Biol Med* **42:** 1661-1670.

Chan HS, Gallie BL, DeBoer G, Haddad G, Ikegaki N, Dimitroulakos J *et al* (1997). MYCN protein expression as a predictor of neuroblastoma prognosis. *Clin Cancer Res* **3:** 1699-1706.

Chang TH, Szabo E (2000). Induction of differentiation and apoptosis by ligands of peroxisome proliferator-activated receptor gamma in non-small cell lung cancer. *Cancer Res* **60:** 1129-1138.

Chawla A, Schwarz EJ, Dimaculangan DD, Lazar MA (1994). Peroxisome proliferator-activated receptor (PPAR) gamma: adipose-predominant expression and induction early in adipocyte differentiation. *Endocrinology* **135:** 798-800.

Chellappan SP, Giordano A, Fisher PB (1998). Role of cyclin-dependent kinases and their inhibitors in cellular differentiation and development. *Curr Top Microbiol Immunol* **227:** 57-103.

Chen A, Xu J (2005). Activation of PPAR{gamma} by curcumin inhibits Moser cell growth and mediates suppression of gene expression of cyclin D1 and EGFR. *Am J Physiol Gastrointest Liver Physiol* **288:** G447-456.

Cheng JC, Weisenberger DJ, Gonzales FA, Liang G, Xu GL, Hu YG *et al* (2004). Continuous zebularine treatment effectively sustains demethylation in human bladder cancer cells. *Mol Cell Biol* **24:** 1270-1278.

Choi SW, Mason JB (2000). Folate and carcinogenesis: an integrated scheme. *J Nutr* **130:** 129-132.

Choi SW, Mason JB (2002). Folate status: effects on pathways of colorectal carcinogenesis. *J Nutr* **132:** 2413S-2418S.

Clay CE, Namen AM, Fonteh AN, Atsumi G, High KP, Chilton FH (2000). 15-deoxy-Delta(12,14)PGJ(2) induces diverse biological responses via PPARgamma activation in cancer cells. *Prostaglandins Other Lipid Mediat* **62:** 23-32.

Cox D, Yuncken C, Spriggs AI (1965). Minute Chromatin Bodies in Malignant Tumours of Childhood. *Lancet* **1:** 55-58.

Cross SH, Meehan RR, Nan X, Bird A (1997). A component of the transcriptional repressor MeCP1 shares a motif with DNA methyltransferase and HRX proteins. *Nat Genet* **16:** 256-259.

D'Arpa P, Liu LF (1989). Topoisomerase-targeting antitumor drugs. *Biochim Biophys Acta* **989:** 163-177.

Das S, Foley N, Bryan K, Watters KM, Bray I, Murphy DM *et al* (2010). MicroRNA mediates DNA demethylation events triggered by retinoic acid during neuroblastoma cell differentiation. *Cancer Res* **70:** 7874-7881.

Day TW, Wu CH, Safa AR (2009). Etoposide induces protein kinase Cdelta- and caspase-3-dependent apoptosis in neuroblastoma cancer cells. *Mol Pharmacol* **76:** 632-640.

Dean W, Santos F, Reik W (2003). Epigenetic reprogramming in early mammalian development and following somatic nuclear transfer. *Semin Cell Dev Biol* **14:** 93-100.

Debrock G, Vanhentenrijk V, Sciot R, Debiec-Rychter M, Oyen R, Van Oosterom A (2003). A phase II trial with rosiglitazone in liposarcoma patients. *Br J Cancer* **89:** 1409-1412.

Demetri GD, Fletcher CD, Mueller E, Sarraf P, Naujoks R, Campbell N *et al* (1999). Induction of solid tumor differentiation by the peroxisome proliferator-activated receptor-gamma ligand troglitazone in patients with liposarcoma. *Proc Natl Acad Sci U S A* **96:** 3951-3956.

Desvergne B, Wahli W (1999). Peroxisome proliferator-activated receptors: nuclear control of metabolism. *Endocr Rev* **20:** 649-688.

Di Loreto S, D'Angelo B, D'Amico MA, Benedetti E, Cristiano L, Cinque B *et al* (2007). PPARbeta agonists trigger neuronal differentiation in the human neuroblastoma cell line SH-SY5Y. *J Cell Physiol* **211:** 837-847.

Dulloo AG, Gubler M, Montani JP, Seydoux J, Solinas G (2004). Substrate cycling between de novo lipogenesis and lipid oxidation: a thermogenic mechanism against skeletal muscle lipotoxicity and glucolipotoxicity. *Int J Obes Relat Metab Disord* **28 Suppl 4:** S29-37.

Duthie SJ (1999). Folic acid deficiency and cancer: mechanisms of DNA instability. *Br Med Bull* **55:** 578-592.

Edelman SV (2003). The role of the thiazolidinediones in the practical management of patients with type 2 diabetes and cardiovascular risk factors. *Rev Cardiovasc Med* **4 Suppl 6:** S29-37.

Ehrlich M (2002). DNA methylation in cancer: too much, but also too little. *Oncogene* **21:** 5400-5413.

Elbrecht A, Chen Y, Cullinan CA, Hayes N, Leibowitz MD, Moller DE *et al* (1996). Molecular Cloning, Expression and Characterization of Human Peroxisome Proliferator Activated Receptors γ1 and γ2. Biochem Biophys Res Commun. **224(2):**431-7.

Elnemr A, Ohta T, Iwata K, Ninomia I, Fushida S, Nishimura G *et al* (2000). PPARgamma ligand (thiazolidinedione) induces growth arrest and differentiation markers of human pancreatic cancer cells. *Int J Oncol* **17:** 1157-1164.

Elstner E, Muller C, Koshizuka K, Williamson EA, Park D, Asou H *et al* (1998). Ligands for peroxisome proliferator-activated receptorgamma and retinoic acid receptor inhibit growth and induce apoptosis of human breast cancer cells in vitro and in BNX mice. *Proc Natl Acad Sci U S A* **95:** 8806-8811.

Escher P, Wahli W (2000). Peroxisome proliferator-activated receptors: insight into multiple cellular functions. *Mutat Res* **448:** 121-138.

Esteller M (2002). CpG island hypermethylation and tumor suppressor genes: a booming present, a brighter future. *Oncogene* **21:** 5427-5440.

Evans AE, D'Angio GJ, Randolph J (1971). A proposed staging for children with neuroblastoma. Children's cancer study group A. *Cancer* **27:** 374-378.

Evans AE, Baum E, Chard R (1981). Do infants with stage IV-S neuroblastoma need treatment? *Arch Dis Child* **56:** 271-274.

Fajas L, Fruchart JC, Auwerx J (1998). PPARgamma3 mRNA: a distinct PPARgamma mRNA subtype transcribed from an independent promoter. *FEBS Lett* **438:** 55-60.

Fang JY, Lu YY (2002). Effects of histone acetylation and DNA methylation on p21(WAF1) regulation. *World J Gastroenterol* **8:** 400-405.

Farrow B, O'Connor KL, Hashimoto K, Iwamura T, Evers BM (2003). Selective activation of PPARgamma inhibits pancreatic cancer invasion and decreases expression of tissue plasminogen activator. *Surgery* **134:** 206-212.

Ferruzzi P, Ceni E, Tarocchi M, Grappone C, Milani S, Galli A *et al* (2005). Thiazolidinediones inhibit growth and invasiveness of the human adrenocortical cancer cell line H295R. *J Clin Endocrinol Metab* **90:** 1332-1339.

Finklestein JZ, Krailo MD, Lenarsky C, Ladisch S, Blair GK, Reynolds CP *et al* (1992). 13-cis-retinoic acid (NSC 122758) in the treatment of children with metastatic neuroblastoma unresponsive to conventional chemotherapy: report from the Childrens Cancer Study Group. *Med Pediatr Oncol* **20:** 307-311.

Fitzpatrick FA, Wynalda MA (1983). Albumin-catalyzed metabolism of prostaglandin D2. Identification of products formed in vitro. *J Biol Chem* **258:** 11713-11718.

Formelli F, Cleris L (2000). Therapeutic effects of the combination of fenretinide and all-trans-retinoic acid and of the two retinoids with cisplatin in a human ovarian carcinoma xenograft and in a cisplatin-resistant sub-line. *Eur J Cancer* **36:** 2411-2419.

French AE, Grant R, Weitzman S, Ray JG, Vermeulen MJ, Sung L *et al* (2003a). Folic acid food fortification is associated with a decline in neuroblastoma. *Clin Pharmacol Ther* **74:** 288-294.

French AE, Grant R, Weitzman S, Ray JG, Vermeulen MJ, Sung L *et al* (2003b). Folic acid food fortification is associated with a decline in neuroblastoma. *Clin Pharmacol Ther* **74:** 288-294.

Galli A, Ceni E, Crabb DW, Mello T, Salzano R, Grappone C *et al* (2004). Antidiabetic thiazolidinediones inhibit invasiveness of pancreatic cancer cells via PPARgamma independent mechanisms. *Gut* **53:** 1688-1697.

Gan Q, Huang J, Zhou R, Niu J, Zhu X, Wang J *et al* (2008). PPAR{gamma} accelerates cellular senescence by inducing p16INK4{alpha} expression in human diploid fibroblasts. *J Cell Sci* **121:** 2235-2245.

Garattini E, Gianni M, Terao M (2007). Retinoids as differentiating agents in oncology: a network of interactions with intracellular pathways as the basis for rational therapeutic combinations. *Curr Pharm Des* **13:** 1375-1400.

Gatsinzi T, Iverfeldt K (2011). Sensitization to TRAIL-induced apoptosis in human neuroblastoma SK-N-AS cells by NF-kappaB inhibitors is dependent on reactive oxygen species (ROS). *J Neurooncol*.

Gilbert F, Balaban G, Moorhead P, Bianchi D, Schlesinger H (1982). Abnormalities of chromosome 1p in human neuroblastoma tumors and cell lines. *Cancer Genet Cytogenet* **7:** 33-42.

Gilbert SF (2009). Ageing and cancer as diseases of epigenesis. *J Biosci* **34:** 601-604.

Giles H, Leff P (1988). The biology and pharmacology of PGD2. *Prostaglandins* **35:** 277-300.

Giri S, Rattan R, Singh AK, Singh I (2004). The 15-deoxy-delta12,14-prostaglandin J2 inhibits the inflammatory response in primary rat astrocytes via down-regulating multiple steps in phosphatidylinositol 3-kinase-Akt-NF-kappaB-p300 pathway independent of peroxisome proliferator-activated receptor gamma. *J Immunol* **173:** 5196-5208.

Glover AB, Leyland-Jones B (1987). Biochemistry of azacitidine: a review. *Cancer Treat Rep* **71:** 959-964.

Goto S, Umehara S, Gerbing RB, Stram DO, Brodeur GM, Seeger RC *et al* (2001). Histopathology (International Neuroblastoma Pathology Classification) and MYCN status in patients with peripheral neuroblastic tumors: a report from the Children's Cancer Group. *Cancer* **92:** 2699-2708.

Grau E, Martinez F, Orellana C, Canete A, Yanez Y, Oltra S *et al* (2010). Epigenetic alterations in disseminated neuroblastoma tumour cells: influence of TMS1 gene hypermethylation in relapse risk in NB patients. *J Cancer Res Clin Oncol* **136:** 1415-1421.

Greene ME, Blumberg B, McBride OW, Yi HF, Kronquist K, Kwan K *et al* (1995). Isolation of the human peroxisome proliferator activated receptor gamma cDNA: expression in hematopoietic cells and chromosomal mapping. *Gene Expr* **4:** 281-299.

Grommes C, Landreth GE, Heneka MT (2004a). Antineoplastic effects of peroxisome proliferator-activated receptor gamma agonists. *Lancet Oncol* **5:** 419-429.

Grommes C, Landreth GE, Heneka MT (2004b). Antineoplastic effects of peroxisome proliferator-activated receptor gamma agonists. *Lancet Oncol* **5:** 419-429.

Gurnell M, Wentworth JM, Agostini M, Adams M, Collingwood TN, Provenzano C *et al* (2000). A dominant-negative peroxisome proliferator-activated receptor gamma (PPARgamma) mutant is a constitutive repressor and inhibits PPARgamma-mediated adipogenesis. *J Biol Chem* **275:** 5754-5759.

Hamaguchi N, Hamada H, Miyoshi S, Irifune K, Ito R, Miyazaki T *et al* (2010). In vitro and in vivo therapeutic efficacy of the PPAR-gamma agonist troglitazone in combination with cisplatin against malignant pleural mesothelioma cell growth. *Cancer Sci* **101:** 1955-1964.

Han S, Wada RK, Sidell N (2001a). Differentiation of human neuroblastoma by phenylacetate is mediated by peroxisome proliferator-activated receptor gamma. *Cancer Res* **61:** 3998-4002.

Han S, Sidell N, Fisher PB, Roman J (2004). Up-regulation of p21 gene expression by peroxisome proliferator-activated receptor gamma in human lung carcinoma cells. *Clin Cancer Res* **10:** 1911-1919.

Han SW, Greene ME, Pitts J, Wada RK, Sidell N (2001b). Novel expression and function of peroxisome proliferator-activated receptor gamma (PPARgamma) in human neuroblastoma cells. *Clin Cancer Res* **7:** 98-104.

Han SW, Greene ME, Pitts J, Wada RK, Sidell N (2001c). Novel expression and function of peroxisome proliferator-activated receptor gamma (PPARgamma) in human neuroblastoma cells. *Clin Cancer Res* **7:** 98-104.

Harper JW, Elledge SJ (1996). Cdk inhibitors in development and cancer. *Curr Opin Genet Dev* **6:** 56-64.

Heldin CH, Ostman A (1996). Ligand-induced dimerization of growth factor receptors: variations on the theme. *Cytokine Growth Factor Rev* **7:** 3-10.

Herman JG, Umar A, Polyak K, Graff JR, Ahuja N, Issa JP *et al* (1998). Incidence and functional consequences of hMLH1 promoter hypermethylation in colorectal carcinoma. *Proc Natl Acad Sci U S A* **95:** 6870-6875.

Hermann A, Gowher H, Jeltsch A (2004). Biochemistry and biology of mammalian DNA methyltransferases. *Cell Mol Life Sci* **61:** 2571-2587.

Hernandez-Blazquez FJ, Habib M, Dumollard JM, Barthelemy C, Benchaib M, de Capoa A *et al* (2000). Evaluation of global DNA hypomethylation in human colon cancer tissues by immunohistochemistry and image analysis. *Gut* **47:** 689-693.

Hihi AK, Michalik L, Wahli W (2002). PPARs: transcriptional effectors of fatty acids and their derivatives. *Cell Mol Life Sci* **59:** 790-798.

Hirata M, Kakizuka A, Aizawa M, Ushikubi F, Narumiya S (1994). Molecular characterization of a mouse prostaglandin D receptor and functional expression of the cloned gene. *Proc Natl Acad Sci U S A* **91:** 11192-11196.

Hisatake JI, Ikezoe T, Carey M, Holden S, Tomoyasu S, Koeffler HP (2000). Down-Regulation of prostate-specific antigen expression by ligands for peroxisome proliferator-activated receptor gamma in human prostate cancer. *Cancer Res* **60:** 5494-5498.

Ho R, Eggert A, Hishiki T, Minturn JE, Ikegaki N, Foster P *et al* (2002). Resistance to chemotherapy mediated by TrkB in neuroblastomas. *Cancer Res* **62:** 6462-6466.

Ishola TA, Chung DH (2007). Neuroblastoma. *Surg Oncol* **16:** 149-156.

Jones PA, Taylor SM (1980). Cellular differentiation, cytidine analogs and DNA methylation. *Cell* **20:** 85-93.

Jones PL, Veenstra GJ, Wade PA, Vermaak D, Kass SU, Landsberger N *et al* (1998). Methylated DNA and MeCP2 recruit histone deacetylase to repress transcription. *Nat Genet* **19:** 187-191.

Jordan P, Carmo-Fonseca M (2000). Molecular mechanisms involved in cisplatin cytotoxicity. *Cell Mol Life Sci* **57:** 1229-1235.

Keyes MK, Jang H, Mason JB, Liu Z, Crott JW, Smith DE *et al* (2007). Older age and dietary folate are determinants of genomic and p16-specific DNA methylation in mouse colon. *J Nutr* **137:** 1713-1717.

Kikawa Y, Narumiya S, Fukushima M, Wakatsuka H, Hayaishi O (1984). 9-Deoxy-delta 9, delta 12-13,14-dihydroprostaglandin D2, a metabolite of prostaglandin D2 formed in human plasma. *Proc Natl Acad Sci U S A* **81:** 1317-1321.

Kim YI (1999a). Folate and cancer prevention: a new medical application of folate beyond hyperhomocysteinemia and neural tube defects. *Nutr Rev* **57:** 314-321.

Kim YI (1999b). Folate and cancer prevention: a new medical application of folate beyond hyperhomocysteinemia and neural tube defects. *Nutr Rev* **57:** 314-321.

Kliewer SA, Forman BM, Blumberg B, Ong ES, Borgmeyer U, Mangelsdorf DJ *et al* (1994). Differential expression and activation of a family of murine peroxisome proliferator-activated receptors. *Proc Natl Acad Sci U S A* **91:** 7355-7359.

Koga H, Sakisaka S, Harada M, Takagi T, Hanada S, Taniguchi E *et al* (2001). Involvement of p21(WAF1/Cip1), p27(Kip1), and p18(INK4c) in troglitazone-induced cell-cycle arrest in human hepatoma cell lines. *Hepatology* **33:** 1087-1097.

Kouzarides T (2007). Chromatin modifications and their function. *Cell* **128:** 693-705.

Krieger-Hinck N, Schumacher U, Muller A, Valentiner U (2010). The effect of the PPAR-gamma agonist rosiglitazone on neuroblastoma SK-N-SH cells in a metastatic xenograft mouse model. *Oncol Res* **18:** 387-393.

Krishnan A, Nair SA, Pillai MR (2007). Biology of PPAR gamma in cancer: a critical review on existing lacunae. *Current molecular medicine* **7:** 532-540.

Kubota N, Terauchi Y, Miki H, Tamemoto H, Yamauchi T, Komeda K *et al* (1999). PPAR gamma mediates high-fat diet-induced adipocyte hypertrophy and insulin resistance. *Mol Cell* **4:** 597-609.

Kulke MH, Demetri GD, Sharpless NE, Ryan DP, Shivdasani R, Clark JS *et al* (2002). A phase II study of troglitazone, an activator of the PPARgamma receptor, in patients with chemotherapy-resistant metastatic colorectal cancer. *Cancer J* **8:** 395-399.

Kurup A, Hanna NH (2004). Treatment of small cell lung cancer. *Crit Rev Oncol Hematol* **52:** 117-126.

Lapillonne H, Konopleva M, Tsao T, Gold D, McQueen T, Sutherland RL *et al* (2003). Activation of peroxisome proliferator-activated receptor gamma by a novel synthetic triterpenoid 2-cyano-3,12-dioxooleana-1,9-dien-28-oic acid induces growth arrest and apoptosis in breast cancer cells. *Cancer Res* **63:** 5926-5939.

Lee CH, Olson P, Evans RM (2003). Minireview: lipid metabolism, metabolic diseases, and peroxisome proliferator-activated receptors. *Endocrinology* **144:** 2201-2207.

Lemberger T, Braissant O, Juge-Aubry C, Keller H, Saladin R, Staels B *et al* (1996). PPAR tissue distribution and interactions with other hormone-signaling pathways. *Ann N Y Acad Sci* **804:** 231-251.

Lengauer C (2003). Cancer. An unstable liaison. *Science* **300:** 442-443.

Li MY, Lee TW, Yim AP, Chen GG (2006). Function of PPARgamma and its ligands in lung cancer. *Crit Rev Clin Lab Sci* **43:** 183-202.

Lin X, Asgari K, Putzi MJ, Gage WR, Yu X, Cornblatt BS *et al* (2001). Reversal of GSTP1 CpG island hypermethylation and reactivation of pi-class glutathione S-transferase (GSTP1) expression in human prostate cancer cells by treatment with procainamide. *Cancer Res* **61:** 8611-8616.

Lindskog M, Spenger C, Jarvet J, Graslund A, Kogner P (2004). Predicting resistance or response to chemotherapy by proton magnetic resonance spectroscopy in neuroblastoma. *J Natl Cancer Inst* **96:** 1457-1466.

Livera G, Rouiller-Fabre V, Pairault C, Levacher C, Habert R (2002). Regulation and perturbation of testicular functions by vitamin A. *Reproduction* **124:** 173-180.

Lopatina N, Haskell JF, Andrews LG, Poole JC, Saldanha S, Tollefsbol T (2002). Differential maintenance and de novo methylating activity by three DNA methyltransferases in aging and immortalized fibroblasts. *J Cell Biochem* **84:** 324-334.

Lu Y, Low PS (2002). Folate-mediated delivery of macromolecular anticancer therapeutic agents. *Adv Drug Deliv Rev* **54:** 675-693.

Luczak MW, Jagodzinski PP (2006). The role of DNA methylation in cancer development. *Folia Histochem Cytobiol* **44:** 143-154.

MacLeod AR, Szyf M (1995). Expression of antisense to DNA methyltransferase mRNA induces DNA demethylation and inhibits tumorigenesis. *J Biol Chem* **270:** 8037-8043.

Mandard S, Muller M, Kersten S (2004). Peroxisome proliferator-activated receptor alpha target genes. *Cell Mol Life Sci* **61:** 393-416.

Mansure JJ, Nassim R, Kassouf W (2009a). Peroxisome proliferator-activated receptor gamma in bladder cancer: a promising therapeutic target. *Cancer Biol Ther* **8:** 6-15.

Mansure JJ, Nassim R, Kassouf W (2009b). Peroxisome proliferator-activated receptor gamma in bladder cancer: a promising therapeutic target. *Cancer Biol Ther* **8:** 6-15.

Maris JM, Hogarty MD, Bagatell R, Cohn SL (2007). Neuroblastoma. *Lancet* **369:** 2106-2120.

Mathers JC (2003). Nutrition and cancer prevention: diet-gene interactions. *Proc Nutr Soc* **62:** 605-610.

Michalik L, Desvergne B, Wahli W (2004). Peroxisome-proliferator-activated receptors and cancers: complex stories. *Nat Rev Cancer* **4:** 61-70.

Miles PD, Barak Y, He W, Evans RM, Olefsky JM (2000). Improved insulin-sensitivity in mice heterozygous for PPAR-gamma deficiency. *J Clin Invest* **105:** 287-292.

Morgenstern BZ, Krivoshik AP, Rodriguez V, Anderson PM (2004). Wilms' tumor and neuroblastoma. *Acta Paediatr Suppl* **93:** 78-84; discussion 84-75.

Morrison RF, Farmer SR (1999). Role of PPARgamma in regulating a cascade expression of cyclin-dependent kinase inhibitors, p18(INK4c) and p21(Waf1/Cip1), during adipogenesis. *J Biol Chem* **274:** 17088-17097.

Mueller E, Smith M, Sarraf P, Kroll T, Aiyer A, Kaufman DS *et al* (2000). Effects of ligand activation of peroxisome proliferator-activated receptor gamma in human prostate cancer. *Proc Natl Acad Sci U S A* **97:** 10990-10995.

Mukherjee R, Jow L, Croston GE, Paterniti JR, Jr. (1997). Identification, characterization, and tissue distribution of human peroxisome proliferator-activated receptor (PPAR) isoforms PPARgamma2 versus PPARgamma1 and activation with retinoid X receptor agonists and antagonists. *J Biol Chem* **272:** 8071-8076.

Murakami T, Li X, Gong J, Bhatia U, Traganos F, Darzynkiewicz Z (1995). Induction of apoptosis by 5-azacytidine: drug concentration-dependent differences in cell cycle specificity. *Cancer Res* **55:** 3093-3098.

Nakagawara A, Arima-Nakagawara M, Scavarda NJ, Azar CG, Cantor AB, Brodeur GM (1993). Association between high levels of expression of the TRK gene and favorable outcome in human neuroblastoma. *N Engl J Med* **328:** 847-854.

Nan X, Campoy FJ, Bird A (1997). MeCP2 is a transcriptional repressor with abundant binding sites in genomic chromatin. *Cell* **88:** 471-481.

Nickerson HJ, Matthay KK, Seeger RC, Brodeur GM, Shimada H, Perez C *et al* (2000). Favorable biology and outcome of stage IV-S neuroblastoma with supportive care or minimal therapy: a Children's Cancer Group study. *J Clin Oncol* **18:** 477-486.

Nwankwo JO, Robbins ME (2001). Peroxisome proliferator-activated receptor- gamma expression in human malignant and normal brain, breast and prostate-derived cells. *Prostaglandins Leukot Essent Fatty Acids* **64:** 241-245.

Pabla N, Huang S, Mi QS, Daniel R, Dong Z (2008). ATR-Chk2 signaling in p53 activation and DNA damage response during cisplatin-induced apoptosis. *J Biol Chem* **283:** 6572-6583.

Palmer CN, Hsu MH, Griffin HJ, Johnson EF (1995). Novel sequence determinants in peroxisome proliferator signaling. *J Biol Chem* **270:** 16114-16121.

Panigrahy D, Shen LQ, Kieran MW, Kaipainen A (2003). Therapeutic potential of thiazolidinediones as anticancer agents. *Expert Opin Investig Drugs* **12:** 1925-1937.

Perez CA, Matthay KK, Atkinson JB, Seeger RC, Shimada H, Haase GM *et al* (2000). Biologic variables in the outcome of stages I and II neuroblastoma treated with surgery as primary therapy: a children's cancer group study. *J Clin Oncol* **18:** 18-26.

Picard F, Auwerx J (2002). PPAR(gamma) and glucose homeostasis. *Annu Rev Nutr* **22:** 167-197.

Plass C (2002). Cancer epigenomics. *Hum Mol Genet* **11:** 2479-2488.

Ponthan F, Johnsen JI, Klevenvall L, Castro J, Kogner P (2003a). The synthetic retinoid RO 13-6307 induces neuroblastoma differentiation in vitro and inhibits neuroblastoma tumour growth in vivo. *Int J Cancer* **104:** 418-424.

Ponthan F, Lindskog M, Karnehed N, Castro J, Kogner P (2003b). Evaluation of anti-tumour effects of oral fenretinide (4-HPR) in rats with human neuroblastoma xenografts. *Oncol Rep* **10:** 1587-1592.

Qiu YY, Mirkin BL, Dwivedi RS (2002a). Differential expression of DNA-methyltransferases in drug resistant murine neuroblastoma cells. *Cancer Detect Prev* **26:** 444-453.

Qiu YY, Mirkin BL, Dwivedi RS (2002b). Differential expression of DNA-methyltransferases in drug resistant murine neuroblastoma cells. *Cancer Detect Prev* **26:** 444-453.

Quelle DE, Zindy F, Ashmun RA, Sherr CJ (1995). Alternative reading frames of the INK4a tumor suppressor gene encode two unrelated proteins capable of inducing cell cycle arrest. *Cell* **83:** 993-1000.

Rasheed WK, Johnstone RW, Prince HM (2007). Histone deacetylase inhibitors in cancer therapy. *Expert Opin Investig Drugs* **16:** 659-678.

Reddy RC, Srirangam A, Reddy K, Chen J, Gangireddy S, Kalemkerian GP *et al* (2008). Chemotherapeutic drugs induce PPAR-gamma expression and show sequence-specific synergy with PPAR-gamma ligands in inhibition of non-small cell lung cancer. *Neoplasia* **10:** 597-603.

Reik W, Dean W, Walter J (2001). Epigenetic reprogramming in mammalian development. *Science* **293:** 1089-1093.

Ricote M, Li AC, Willson TM, Kelly CJ, Glass CK (1998). The peroxisome proliferator-activated receptor-gamma is a negative regulator of macrophage activation. *Nature* **391:** 79-82.

Rodway HA, Hunt AN, Kohler JA, Postle AD, Lillycrop KA (2004a). Lysophosphatidic acid attenuates the cytotoxic effects and degree of peroxisome proliferator-activated receptor gamma activation induced by 15-deoxyDelta12,14-prostaglandin J2 in neuroblastoma cells. *Biochem J* **382:** 83-91.

Rodway HA, Hunt AN, Kohler JA, Postle AD, Lillycrop KA (2004b). Lysophosphatidic acid attenuates the cytotoxic effects and degree of peroxisome proliferator-activated receptor gamma activation induced by 15-deoxyDelta12,14-prostaglandin J2 in neuroblastoma cells. *Biochem J* **382:** 83-91.

Sarraf P, Mueller E, Jones D, King FJ, DeAngelo DJ, Partridge JB *et al* (1998). Differentiation and reversal of malignant changes in colon cancer through PPARgamma. *Nat Med* **4:** 1046-1052.

Sarraf P, Mueller E, Smith WM, Wright HM, Kum JB, Aaltonen LA *et al* (1999). Loss-of-function mutations in PPAR gamma associated with human colon cancer. *Mol Cell* **3:** 799-804.

Sato M, Horio Y, Sekido Y, Minna JD, Shimokata K, Hasegawa Y (2002). The expression of DNA methyltransferases and methyl-CpG-binding proteins is not associated with the methylation status of p14(ARF), p16(INK4a) and RASSF1A in human lung cancer cell lines. *Oncogene* **21:** 4822-4829.

Schoonjans K, Peinado-Onsurbe J, Lefebvre AM, Heyman RA, Briggs M, Deeb S *et al* (1996). PPARalpha and PPARgamma activators direct a distinct tissue-specific transcriptional response via a PPRE in the lipoprotein lipase gene. *Embo J* **15:** 5336-5348.

Schramm A, Schulte JH, Astrahantseff K, Apostolov O, Limpt V, Sieverts H *et al* (2005). Biological effects of TrkA and TrkB receptor signaling in neuroblastoma. *Cancer Lett* **228:** 143-153.

Schwartz AD, Dadash-Zadeh M, Lee H, Swaney JJ (1974). Spontaneous regression of disseminated neuroblastoma. *J Pediatr* **85:** 760-763.

Servidei T, Morosetti R, Ferlini C, Cusano G, Scambia G, Mastrangelo R *et al* (2004). The cellular response to PPARgamma ligands is related to the phenotype of neuroblastoma cell lines. *Oncol Res* **14:** 345-354.

Seufert J, Lubben G, Dietrich K, Bates PC (2004). A comparison of the effects of thiazolidinediones and metformin on metabolic control in patients with type 2 diabetes mellitus. *Clin Ther* **26:** 805-818.

Sher T, Yi HF, McBride OW, Gonzalez FJ (1993). cDNA cloning, chromosomal mapping, and functional characterization of the human peroxisome proliferator activated receptor. *Biochemistry* **32:** 5598-5604.

Shimada H, Ambros IM, Dehner LP, Hata J, Joshi VV, Roald B *et al* (1999). The International Neuroblastoma Pathology Classification (the Shimada system). *Cancer* **86:** 364-372.

Siddik ZH (2003). Cisplatin: mode of cytotoxic action and molecular basis of resistance. *Oncogene* **22:** 7265-7279.

Skogsberg J, Kannisto K, Roshani L, Gagne E, Hamsten A, Larsson C *et al* (2000). Characterization of the human peroxisome proliferator activated receptor delta gene and its expression. *Int J Mol Med* **6:** 73-81.

Smith MR, Manola J, Kaufman DS, George D, Oh WK, Mueller E *et al* (2004). Rosiglitazone versus placebo for men with prostate carcinoma and a rising serum prostate-specific antigen level after radical prostatectomy and/or radiation therapy. *Cancer* **101:** 1569-1574.

Steinmetz KL, Pogribny IP, James SJ, Pitot HC (1998). Hypomethylation of the rat glutathione S-transferase pi (GSTP) promoter region isolated from methyl-deficient livers and GSTP-positive liver neoplasms. *Carcinogenesis* **19:** 1487-1494.

Stienstra R, Duval C, Muller M, Kersten S (2007). PPARs, Obesity, and Inflammation. *PPAR Res* **2007:** 95974.

Strakova N, Ehrmann J, Dzubak P, Bouchal J, Kolar Z (2004). The synthetic ligand of peroxisome proliferator-activated receptor-gamma ciglitazone affects human glioblastoma cell lines. *J Pharmacol Exp Ther* **309:** 1239-1247.

Sumanasekera WK, Tien ES, Davis JW, 2nd, Turpey R, Perdew GH, Vanden Heuvel JP (2003). Heat shock protein-90 (Hsp90) acts as a repressor of peroxisome proliferator-activated receptor-alpha (PPARalpha) and PPARbeta activity. *Biochemistry* **42:** 10726-10735.

Suzuki T, Bogenmann E, Shimada H, Stram D, Seeger RC (1993). Lack of high-affinity nerve growth factor receptors in aggressive neuroblastomas. *J Natl Cancer Inst* **85:** 377-384.

Szyf M, Avraham-Haetzni K, Reifman A, Shlomai J, Kaplan F, Oppenheim A *et al* (1984). DNA methylation pattern is determined by the intracellular level of the methylase. *Proc Natl Acad Sci U S A* **81:** 3278-3282.

Taby R, Issa JP (2010). Cancer epigenetics. *CA Cancer J Clin* **60:** 376-392.

Takai D, Jones PA (2002). Comprehensive analysis of CpG islands in human chromosomes 21 and 22. *Proc Natl Acad Sci U S A* **99:** 3740-3745.

Takita J, Hayashi Y, Nakajima T, Adachi J, Tanaka T, Yamaguchi N *et al* (1998). The p16 (CDKN2A) gene is involved in the growth of neuroblastoma cells and its expression is associated with prognosis of neuroblastoma patients. *Oncogene* **17:** 3137-3143.

Thomas MC, Chiang CM (2006). The general transcription machinery and general cofactors. Crit Rev Biochem Mol Biol. **41(3):**105-78.

Tontonoz P, Hu E, Spiegelman BM (1994). Stimulation of adipogenesis in fibroblasts by PPAR gamma 2, a lipid-activated transcription factor. *Cell* **79:** 1147-1156.

Tugwood JD, Issemann I, Anderson RG, Bundell KR, McPheat WL, Green S (1992). The mouse peroxisome proliferator activated receptor recognizes a response element in the 5' flanking sequence of the rat acyl CoA oxidase gene. *EMBO J* **11:** 433-439.

Valentiner U, Carlsson M, Erttmann R, Hildebrandt H, Schumacher U (2005). Ligands for the peroxisome proliferator-activated receptor-gamma have inhibitory effects on growth of human neuroblastoma cells in vitro. *Toxicology* **213:** 157-168.

Viktorsson K, Lewensohn R, Zhivotovsky B (2005). Apoptotic pathways and therapy resistance in human malignancies. *Adv Cancer Res* **94:** 143-196.

Voutsadakis IA (2007). Peroxisome proliferator-activated receptor gamma (PPARgamma) and colorectal carcinogenesis. *J Cancer Res Clin Oncol* **133:** 917-928.

Wainfan E, Dizik M, Stender M, Christman JK (1989). Rapid appearance of hypomethylated DNA in livers of rats fed cancer-promoting, methyl-deficient diets. *Cancer research* **49:** 4094-4097.

Wainfan E, Poirier LA (1992). Methyl groups in carcinogenesis: effects on DNA methylation and gene expression. *Cancer research* **52:** 2071s-2077s.

Wang T, Xu J, Yu X, Yang R, Han ZC (2006a). Peroxisome proliferator-activated receptor gamma in malignant diseases. *Crit Rev Oncol Hematol* **58:** 1-14.

Wang T, Xu J, Yu X, Yang R, Han ZC (2006b). Peroxisome proliferator-activated receptor gamma in malignant diseases. *Crit Rev Oncol Hematol* **58:** 1-14.

Welch C, Chen Y, Stallings RL (2007). MicroRNA-34a functions as a potential tumor suppressor by inducing apoptosis in neuroblastoma cells. *Oncogene* **26:** 5017-5022.

Xu HE, Lambert MH, Montana VG, Parks DJ, Blanchard SG, Brown PJ *et al* (1999a). Molecular recognition of fatty acids by peroxisome proliferator-activated receptors. *Mol Cell* **3:** 397-403.

Xu HE, Lambert MH, Montana VG, Parks DJ, Blanchard SG, Brown PJ *et al* (1999b). Molecular recognition of fatty acids by peroxisome proliferator-activated receptors. *Mol Cell* **3:** 397-403.

Yang FG, Zhang ZW, Xin DQ, Shi CJ, Wu JP, Guo YL *et al* (2005). Peroxisome proliferator-activated receptor gamma ligands induce cell cycle arrest and apoptosis in human renal carcinoma cell lines. *Acta Pharmacol Sin* **26:** 753-761.

Yoder JA, Yen RW, Vertino PM, Bestor TH, Baylin SB (1996). New 5' regions of the murine and human genes for DNA (cytosine-5)-methyltransferase. *J Biol Chem* **271:** 31092-31097.

Yoshizawa K, Cioca DP, Kawa S, Tanaka E, Kiyosawa K (2002). Peroxisome proliferator-activated receptor gamma ligand troglitazone induces cell cycle arrest and apoptosis of hepatocellular carcinoma cell lines. *Cancer* **95:** 2243-2251.

Yoshizumi T, Ohta T, Ninomiya I, Terada I, Fushida S, Fujimura T *et al* (2004). Thiazolidinedione, a peroxisome proliferator-activated receptor-gamma ligand, inhibits growth and metastasis of HT-29 human colon cancer cells through differentiation-promoting effects. *Int J Oncol* **25:** 631-639.

Zamble DB, Lippard SJ (1995). Cisplatin and DNA repair in cancer chemotherapy. *Trends Biochem Sci* **20:** 435-439.

Zhang F, Lavan B, Gregoire FM (2004). Peroxisome proliferator-activated receptors as attractive antiobesity targets. *Drug News Perspect* **17:** 661-669.

Zhang S, Hunter DJ, Hankinson SE, Giovannucci EL, Rosner BA, Colditz GA *et al* (1999). A prospective study of folate intake and the risk of breast cancer. *Jama* **281:** 1632-1637.

Zhu WG, Lakshmanan RR, Beal MD, Otterson GA (2001). DNA methyltransferase inhibition enhances apoptosis induced by histone deacetylase inhibitors. *Cancer Res* **61:** 1327-1333.

Zhu Y, Qi C, Korenberg JR, Chen XN, Noya D, Rao MS *et al* (1995). Structural organization of mouse peroxisome proliferator-activated receptor gamma (mPPAR gamma) gene: alternative promoter use and different splicing yield two mPPAR gamma isoforms. *Proc Natl Acad Sci U S A* **92:** 7921-7925.

Zhu Y, Qi C, Calandra C, Rao MS, Reddy JK (1996). Cloning and identification of mouse steroid receptor coactivator-1 (mSRC-1), as a coactivator of peroxisome proliferator-activated receptor gamma. *Gene Expr* **6:** 185-195.

Books

King, J.B. (2000). *Cancer Biology.* Person education.

Lodish, P., Berk, A., Matsudaira, P., Kaiser, C.A., Krieger, M., Scott, M.P. et al., (2003). *Molecular Cell Biology.* Sara Tenney.

Pecorino, L. (2005). *Molecular Biology of Cancer.* Published in the United States by Oxford University Press Inc., New York.

Pinkerton, C.R., Cushing, P. and Sepion, B. (1994). *Childhood Cancer Management.* Copublished in the USA by Oxford University Press, Inc., New York.

Rang, P.H., Dale, M. M, Ritter, J.M. and Moore, P.K. (2003). *Pharmacology.* Elsevier Science.